

UNIVERSITY OF CALIFORNIA  
RIVERSIDE

Computational Chemistry, Drug Design, and Drug Re-Discovery Aimed at Theory-Directed Synthesis of Cannabinoids and Computational Methods to Predict Bioactivity from Ligand Structure

A Dissertation submitted in partial satisfaction  
of the requirements for the degree of

Doctor of Philosophy

in

Chemistry

by

Angie Garcia

June 2012

Dissertation Committee:

Dr. Michael J. Marsella, Chairperson

Dr. Christopher Y. Switzer

Dr. Catharine H. Larsen

Copyright by  
Angie Garcia  
2012

The Dissertation of Angie Garcia is approved:

---

---

---

Committee Chairperson

University of California, Riverside

## Acknowledgments

It has been an honor for me to work under the advisement of Prof. Michael Marsella. I will forever be indebted to him for his help and guidance. He has been an extraordinary advisor who has allowed me the freedom to explore any project I wanted and has always been extremely supportive and encouraging. Thank you.

I would like to give a special thanks to my undergraduate lab advisor, Dr. Steve Angle for allowing me to work in his lab and introducing me to a career in research. His continued support throughout my graduate career has been greatly appreciated. I would also like to thank my committee members, Prof. Christopher Switzer and Prof. Catharine Larsen.

Thank you to the Marsella group, past and present graduate students and undergrads. Thank you to Dr. Shohreh Rahbarnia for mentoring me as an undergrad and for her continued support throughout my graduate career. I would also like to give a very special thank you to future doctor Jenifer Nalbandian and Dr. Katherine Hawkins for allowing me to vent my frustrations, and for always taking my side; you truly are great friends. I also want to give a special thanks to Mrs. Maria Franco-Aguilar for her help, warmth, and kindness all these years. As well as anyone else who has helped bring me to this point. Thank you very much!

I would like to thank Prof. Chia-En Chang for CB<sub>1</sub>/THC(an) docking studies and Drs. O. Salo-Ahen and A. Gonzalez for providing the CB<sub>1</sub> homology model used in these studies. I am also thankful to Dr. Dan Borchardt for the complete NMR analysis of the THCan-C5 isomers, help with NMR interpretation and with running NMR experiments, as well as Dr. Yi Meng, Dr. Rich Kondrat, Ron New, and Baback Bastin for mass spec samples.

Above all else I would like to thank my family, especially my mom, Josefina Garcia and my dad, Jose Garcia. Your faith in me has given me the strength and courage to follow my dreams. None of this would have been possible without you. Thank you for believing in me, even when I found it hard to believe in myself. Thank you for showing me that with hard work, sacrifice, and dedication great things can happen. Thank you to my aunt, Maria (Bola) Macias who has been like a second mom to my siblings and me. Thank you to my sisters, Maria Salazar and Alicia Cataudella, for being great role models. Thank you to my brothers, Jose (Junier) Garcia, and Ricardo Garcia, for being great big brothers. Thank you to Santo Cataudella, Roberto Salazar, Norma Garcia and families Cataudella, Salazar, and Garcia. And thank you to my incredible nieces and nephews, Robert Salazar, Brittany Cataudella, Kaylee Garcia, Brandon Salazar, Giuliana Cataudella, Olivia Salazar, Dominic Cataudella, and Vanessa Garcia. Thank you all for making me laugh and bringing great joy to my life. I love you very much.

Dedicated to my mom for her unconditional love and support,  
and my dad, the greatest man I've ever known.

## ABSTRACT OF THE DISSERTATION

Computational Chemistry, Drug Design, and Drug Re-Discovery Aimed at Theory-Directed Synthesis of Cannabinoids and Computational Methods to Predict Bioactivity from Ligand Structure

by

Angie Garcia

Doctor of Philosophy, Graduate Program in Chemistry  
University of California, Riverside, June 2012  
Prof. Michael J. Marsella, Chairperson

The aim of this thesis is the discovery or re-discovery of drug-like compounds having therapeutic value; although two distinct strategies are reported, both share a strong dependence on computational chemistry.

The first project to be reported describes synthetic strategies applied to the synthesis of cannabinoids; successful strategies evolved from computational analysis of cannabinoid isomerization via pericyclic reactions. This project exemplifies a strategy designed to predict the best ligand for a specific receptor protein.

The second project reports our strategy to classify drugs according to their predicted indication. Here, structure of a drug-like compound is the only required input. The output will then report the indication class that is predicted to best describe the compound's drug-activity.

## Table of Contents

Chapter 1: The Synthesis and Therapeutic Effects of Cannabinoids and their Analogues	
1.1 Introduction.....	2
1.2 Cannabinoid Receptors.....	2
1.3 Cannabinoids and their Biological Activity.....	3
1.4 Cannabinoid-Based Drugs.....	8
1.5 The Biosynthetic Pathway of Cannabinoids.....	9
1.6 Previous Olivetol-Based Syntheses to $\Delta^1$ -THC.....	11
1.7 Synthesis of Olivetol and Potential Derivatives.....	16
1.8 Alternatives to Olivetol.....	16
1.9 Modifications to the Side Chain.....	18
References.....	21
Chapter 2: The Design, Synthesis, Computational Analysis, and <i>in silico</i> and Biological Screening of Cannabinoids and their Analogues	
2.1 Introduction.....	25
2.2 Isomerization of Cannabinoids and its Effects.....	25
2.3 Thermal Isomerization of Cannabinoid Analogues.....	27
2.4 Cannabinoid Analogues.....	32
2.5 Computational Docking Studies.....	36
2.6 Aromatic Cannabinoid Analogues.....	40
2.7 ALS Studies.....	44
2.8 Conclusion.....	46



References.....	48
Chapter 3: Molecular Docking: A CADD Approach for Known Targets	
3.1 Introduction.....	50
3.2 Molecular Docking Overview.....	50
3.3 The Search Algorithms.....	52
3.4 Scoring.....	53
3.5 Docking Procedure.....	54
3.5.1 Preparing the Protein.....	54
3.5.2 The Ligand Set.....	54
3.5.3 The Binding Box.....	55
3.5.4 The Results.....	55
3.6 Error in CADD.....	56
References.....	58
Chapter 4: CADD Approaches for Unknown Targets	
4.1 Introduction.....	60
4.2 Predicting Intestinal Absorption: Lipinski's 'Rule of Five'.....	60
4.3 Similarity and Substructure Searching.....	61
4.4 Pharmacophore Models.....	61
4.5 QSAR.....	65
4.6 Group Additivity.....	68
4.7 Neural networks.....	68
4.8 Hologram QSAR.....	68

4.9 3D-QSAR.....	69
References.....	73
Chapter 5: A New Approach to Computational Drug Design and Drug Re-discovery	
5.1 Introduction.....	75
5.2 The UBANTR Approach.....	76
5.3 The Process.....	79
5.4 Results and Discussion.....	80
5.5 Conclusion.....	94
References.....	96
Appendix A: Experimental Procedures and Spectroscopic Data .....	98
Appendix B: NMR Spectra for THC <sub>an</sub> with C <sub>5</sub> alkyl chain and NMR analysis .....	108
Appendix C: Ground State and TS Coordinates .....	114
Appendix D: Proteins and Ligands used in UBANTR approach.....	162

## List of Figures

<b>Figure 1.1</b>	$\Delta^1$ -THC: a) different numbering schemes b) biologically active active isomer.	5
<b>Figure 2.1</b>	Isomerization Effects.	26
<b>Figure 2.2</b>	Spartan calculations (B3LYP/6-31G*) for starting material, products, and transition states for the aromatic version of compounds found in Scheme 2.1.	28
<b>Figure 2.3</b>	Spartan calculations (B3LYP/6-31G*) for starting material, products, and transition states of compounds found in Scheme 2.1.	32
<b>Figure 2.4</b>	Alignment of $\Delta^1$ -THC <sub>an</sub> stereoisomers, showing pentyl side-chain in extended conformation for all isomers. Blue, <i>trans</i> -( <i>R,R</i> ); cyan, <i>trans</i> -( <i>S,S</i> ); yellow, <i>cis</i> -( <i>R,S</i> ); red, <i>cis</i> -( <i>S,R</i> ).	37
<b>Figure 2.5</b>	<i>(R,R)</i> - $\Delta^1$ -THC <sub>an</sub> docked into a modeled CB <sub>1</sub> receptor. The receptor is represented by the gray tube while residues interacting with the ligand (cyan) are represented by thin line.	38
<b>Figure 2.6</b>	<i>(R,R)</i> - $\Delta^1$ -THC docked into a modeled CB <sub>1</sub> receptor. The receptor is represented by gray tube while interacting residues are represented by thin line. Ligand shown in cyan.	39
<b>Figure 2.7</b>	<i>Trans</i> -( <i>R,R</i> )-THC <sub>an</sub> (blue), <i>cis</i> -( <i>R,S</i> )-THC <sub>an</sub> (yellow), and <i>trans</i> -( <i>R,R</i> )-THC (orange) docked to the modeled CB1 receptor.	40
<b>Figure 2.8</b>	ALS macrophages treated with stimulated superoxide dismutase 1 (SOD-1). <b>a</b> ) negative control (not treated with stimulated SOD-1); <b>b</b> ) positive control (treated with stimulated SOD-1); <b>c</b> ) treated with SOD-1 then CBC <sub>an</sub> (R=C <sub>5</sub> H <sub>11</sub> ).	46
<b>Figure 3.1</b>	<b>a</b> ) Ball and stick representation of 17-beta-hydroxysteroid-dehydrogenase (PDB 1A27) complexed with estradiol (cyan) <b>b</b> ) ribbon representation of the same protein with estradiol (mint green).	51
<b>Figure 4.1</b>	<b>a</b> ) Chemical structures of Paclitaxel and Epothilone A <b>b</b> ) alignment of the lowest energy conformers of Paclitaxel (tan) and Epothilone A (cyan), as bound to tubulin receptors 1TUB and 1TVK, respectively	63

(receptor omitted for clarity). The yellow circles show the similarities in pharmacophore (i.e., overlapping of aromatic or hydrophobic regions and hydrogen bond donors and acceptors).

<b>Figure 4.2</b>	3D-QSAR process: i) starting with a training set ii) the lowest energy conformer is determined iii) which then establishes the pharmacophore iv) that is placed in a lattice to determine the interactions via a probe atom.	71
<b>Figure 5.1</b>	Docking FDA-approved library to receptors produces unique fingerprint.	78
<b>Figure 5.2</b>	Hierarchical clustering produced from Orange.	81
<b>Figure 5.3</b>	Clustered group of anti-histaminic drugs.	82
<b>Figure 5.4</b>	Clustered group of anti-histaminic drugs with one antidepressant.	82
<b>Figure 5.5</b>	STITCH output for clustered drugs from Figure 5.4	83
<b>Figure 5.6</b>	Drug cluster dividing into two major indications.	84
<b>Figure 5.7</b>	Two different drug clusters.	85
<b>Figure 5.8</b>	Drug cluster with its STITCH output.	86
<b>Figure 5.9</b>	Orange outputs for clustered SSRIs and TCA. Unless otherwise specified, all drugs are anti-depressants.	88
<b>Figure 5.10</b>	a) fluoxetine b) luvox	89
<b>Figure 5.11</b>	a) <i>R</i> -fluoxetine bound into one of the 15 receptors. b) all SSRIs: cyan: ( <i>R</i> )- fluoxetine (cyan), yellow: ( <i>S</i> )- fluoxetine magenta (yellow), and luvox (magenta) bound into the same random receptor.	90
<b>Figure 5.12</b>	Representation of lowest binding conformers for all clustered SSRIs to most of the 15 random receptors.	91
<b>Figure 5.13</b>	Control results showing random groupings of drugs.	93

## List of Schemes

<b>Scheme 1.1</b>	Cannabinoids and their biosynthetic pathway.	10
<b>Scheme 1.2</b>	The first synthesis to <i>rac</i> - $\Delta^1$ -THC.	11
<b>Scheme 1.3</b>	BF <sub>3</sub> route to ( $\pm$ ) $\Delta^1$ -THC and isomers.	12
<b>Scheme 1.4</b>	Synthesis of (-) $\Delta^1$ -THC.	12
<b>Scheme 1.5</b>	Evans synthesis to ( <i>S,S</i> )- $\Delta^1$ -THC.	13
<b>Scheme 1.6</b>	Trost's ( <i>R,R</i> )- $\Delta^1$ -THC synthesis.	15
<b>Scheme 1.7</b>	Focella's synthesis to olivetol.	16
<b>Scheme 1.8</b>	Tietze's synthesis to aromatic THC analogues.	17
<b>Scheme 2.1</b>	The oxo-6 $\pi$ electrocyclization reaction versus the Diels-Alder.	27
<b>Scheme 2.2</b>	Thermal isomerization.	29
<b>Scheme 2.3</b>	Synthesis of $\Delta^1$ -THC analogue.	29
<b>Scheme 2.4</b>	Aromatization of $\Delta^1$ -THC <sub>an</sub> to $\Delta^1$ -THC.	31
<b>Scheme 2.5</b>	Synthesis of THC- <i>gem</i> -dimethyl analogues.	35
<b>Scheme 2.6</b>	LAH reduction.	36
<b>Scheme 2.7</b>	Proposed synthetic route towards $\Delta^1$ -THC.	41
<b>Scheme 2.8</b>	New synthetic plan towards $\Delta^1$ -THC.	42
<b>Scheme 2.9</b>	Synthesis of THC <sub>est</sub> and Spartan calculation results.	43
<b>Scheme 2.10</b>	Synthesis of aromatic analogue.	44

## List of Tables

<b>Table 1.1</b>	Cannabinoids and their known receptor activity.	3
<b>Table 1.2</b>	$\Delta^6$ -THC side chain modification $K_i$ values. Shown in parenthesis in nM.	19
<b>Table 2.1.</b>	Thermal isomerization comparison reactions: the affects of EDDA.	30
<b>Table 2.2</b>	CB <sub>1</sub> receptor binding affinity for $\Delta^1$ -THC and other cannabinoid analogues.	33
<b>Table 5.1</b>	Drugs Undergoing Testing for New Uses.	76
<b>Table 5.2</b>	Inputted data for trimipramine using the UBANTR (U) approach versus the control (C).	92

## **Chapter 1**

### **The Synthesis and Therapeutic Effects of Cannabinoids and their Analogues**

## **1.1 Introduction**

The discovery of cannabinoid receptors in the 1980's caused an increasing interest in cannabinoid synthesis.<sup>1</sup> This is largely due to the cannabinoids great therapeutic potential in areas like anxiety disorders, Parkinson's and Huntington's disease, multiple sclerosis, cancer, stroke, myocardial infarction, hypertension, and glaucoma.<sup>2</sup> Therapy for these diseases or conditions is achieved by developing a type of agonist or antagonist that targets one or both of the two main cannabinoid receptors. The following sections will focus on cannabinoid ligands, their therapeutic activity, and biosynthetic pathways. An emphasis will also be placed on  $\Delta^1$ -THC and previous synthetic methods to this cannabinoid. The impact of side-chain modifications on biological activity will also be discussed.

## **1.2 Cannabinoid Receptors**

There are two main types of cannabinoid receptors. Cannabinoid receptor 1 (CB<sub>1</sub>) is found predominantly in the central nervous system and cannabinoid receptor 2 (CB<sub>2</sub>) is found more peripherally and seems to play a role in the immune system. They are G protein-coupled receptors and it has been predicted that both receptors have 44% similarity in amino acid sequence.<sup>3,4</sup> Evidence has shown that when activated, CB<sub>1</sub> receptors can mobilize arachidonic acid and close 5-HT<sub>3</sub> receptor ion channels.

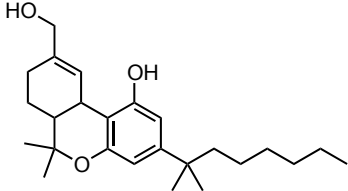
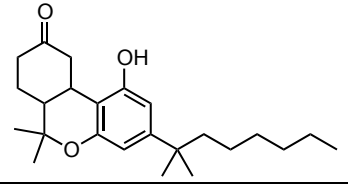
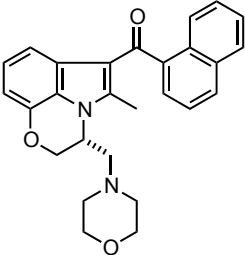
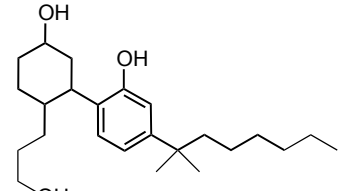
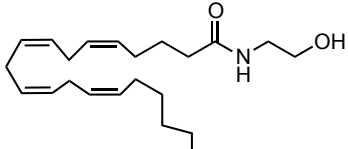
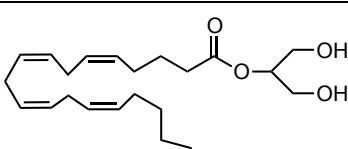


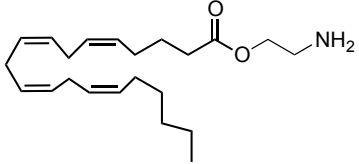
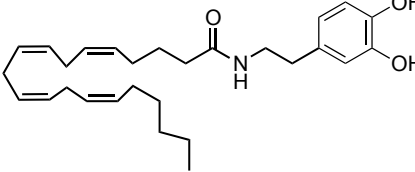
### 1.3 Cannabinoids and their Biological Activity

There are over 60 different types of cannabinoids that can be derived from the plant *Cannabis sativa*. These types of cannabinoids are considered the phytocannabinoids. Some examples can be found in Table 1.1<sup>2</sup> along with any activity towards a cannabinoid receptor. There are also the synthetic cannabinoids, some of which are modeled after the phytocannabinoids, and the endogenous cannabinoids, which are produced within the body.

**Table 1.1** Cannabinoids and their known receptor activity.<sup>2</sup>

<b>Phytocannabinoids</b>			
<b>Entry</b>	<b>Structure</b>	<b>Name</b>	<b>Activity</b>
1		$\Delta^1$ - tetrahydrocannabinol	CB <sub>1</sub> and CB <sub>2</sub> agonist
2		cannabivarin	CB <sub>1</sub> and CB <sub>2</sub> antagonist
3		cannabidiol	no activity
4		cannabichromene	no activity

<b>Synthetic Cannabinoids</b>			
5		(-) HU-210	activity at both CB <sub>1</sub> and CB <sub>2</sub>
6		nabilone	activity at both CB <sub>1</sub> and CB <sub>2</sub>
7		WIN 55,212-2	CB <sub>1</sub> and CB <sub>2</sub> agonist
8		(-) CP55940	CB <sub>1</sub> and CB <sub>2</sub> agonist
<b>Endogenous Cannabinoids</b>			
9		anandamide	CB <sub>1</sub> and CB <sub>2</sub> agonist
10		2-arachidonoyl	CB <sub>1</sub> and CB <sub>2</sub> agonist

11		<i>O</i> -arachidonoyl ethanolamine	CB <sub>1</sub> and CB <sub>2</sub> agonist
12		<i>N</i> -arachidonoyl dopamine	CB <sub>1</sub> and CB <sub>2</sub> agonist

$\Delta^1$ -Tetrahydrocannabinol ( $\Delta^1$ -THC) is the most highly recognized cannabinoid. It is also known as  $\Delta^9$ -THC, depending on the numbering scheme that is used (Fig. 1.1a). This review will use the numbering of the structure found on the left side of Fig. 1.1a. It is the cannabinoid found most abundantly in the cannabis plant. Its bioactivity is found in the (*R,R*)-*trans*-isomer of THC and is psychoactive (Fig. 1.1b). It behaves as both a CB<sub>1</sub> and CB<sub>2</sub> agonist.<sup>2</sup>

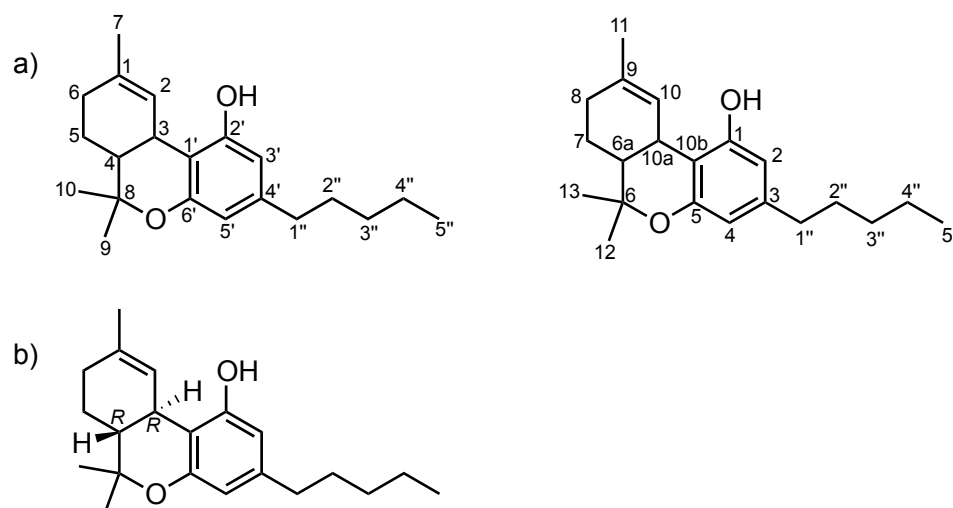


**Figure 1.1**  $\Delta^1$ -THC: a) different numbering schemes b) biologically active isomer.

Cannabivarin is found to be a cannabinoid receptor antagonist. (-)-Cannabidiol (CBD) is also a major component of the cannabis plant. While it does not show any cannabinoid receptor activity, analogues of this cannabinoid possess therapeutic effects as seen in some animal and human studies.<sup>5</sup> It is being investigated for its potential biological activity towards epilepsy and for its anti-inflammatory properties. In a mouse study, CBD was actually shown to antagonize two other cannabinoid agonists (WIN 55,212, CP 55,940) and one antagonist (SR 141716A).<sup>5</sup> Cannabichromene also lacks cannabinoid receptor activity, but appears to have antimicrobial effects.<sup>6</sup>

Cannabinoids have been shown to have an effect on disorders of the central nervous system (CNS). The high abundance of CB<sub>1</sub> receptors in the brain, in particular, its location in the cortex, cerebellum, hippocampus, and basal ganglia, have targeted conditions that affect movement as well as mood and anxiety disorders.<sup>2</sup> For example, cannabinoid HU-211, which is similar to HU-210 (Table **1.1**, entry 5), but has the double bond at position 6 instead of 1 (Fig. **1.1a**), has been shown to possess a protective effect in traumatic brain injury. In a rat model study, the cannabinoid was able to reduce brain damage as well as improve motor and cognitive function.<sup>7,8</sup> In another example, the brain levels of mice with closed head injury showed an increase in the endogenous cannabinoid, 2-arachidonoyl or 2-AG, (Table **1.1**, entry 10). An hour after the injury, administration of exogenous 2-AG, showed an infarct size reduction and ameliorated the neurological outcome.<sup>9</sup>

Anandamide (Table 1.1, entry 9), 2-AG, and WIN 55,212-2 (Table 1.1, entry 7) showed signs of protecting against ischemic strokes. Its major cause is the disruption of blood that is allocated to the brain due to the thrombotic occlusion of blood vessels. It can cause death and permanent disability to its victims. These cannabinoids guard against hypoxia and glucose deprivation which helps protect against the effects of the stroke.<sup>10,11,12</sup>

There has also been some therapeutic effects in multiple sclerosis (MS). MS is an inflammatory disease that affects the brain and spinal cord by slowing down or stopping nerve signals.<sup>13</sup> It affects about 2 to 5 million people worldwide<sup>14</sup> and symptoms often include tremor, cognitive and visual impairment, paralysis, difficulties in speech, loss of bladder control, and painful muscle spasms.<sup>15</sup> Based on an MS laboratory model in rats, THC was shown to lower CNS inflammation and improve survival rates against those that were administered the placebo.<sup>16</sup> HU-211 was also shown to stop inflammation in the brain and spinal cord of rats, leading to less objectionable symptoms.<sup>17</sup> In a separate mouse model, THC, WIN 55,212-2, and another cannabinoid (JWH-133) were found to diminish tremor and spasticity.<sup>18</sup>

Human studies for treating MS have also yielded promising results. There is a report that marijuana smoking can alleviate some of the symptoms of MS.<sup>19,20</sup> And when nabilone (Table 1.1, entry 6) was administered to a single MS patient, there was an improvement in muscle spasms.<sup>21</sup> Furthermore, in a study containing almost 20 MS patients, subjects

reported a decline in spasticity and better bladder control when administered THC and CBD (Table 1.1, entry 3).<sup>22</sup>

Amyotrophic lateral sclerosis (ALS), also known as Lou Gehrig's disease, is a neurodegenerative disease that targets the brain and spinal cord. It eventually results in escalating weakness, paralysis, and early death.<sup>23</sup> However, based on a mouse model, THC appears to delay the progression of ALS if administered before or after visible signs of the disease. Mice that were treated with THC showed slowed motor impairment and an increase in their survival rate.<sup>24</sup>

Clinical studies on cannabinoid targets are ongoing as there is great therapeutic potential in a wide pool of compounds.

#### **1.4 Cannabinoid-Based Drugs**

There are currently several cannabinoid-based drugs on the market. As previously mentioned, the combination of THC and CBD showed therapeutic effects towards MS. This combination is actually marketed as Sativex® and is composed of marijuana extracts of THC and CBD in a 1:1 ratio. It is designed as a mouth spray for MS to deal with neuropathic pain and spasticity.

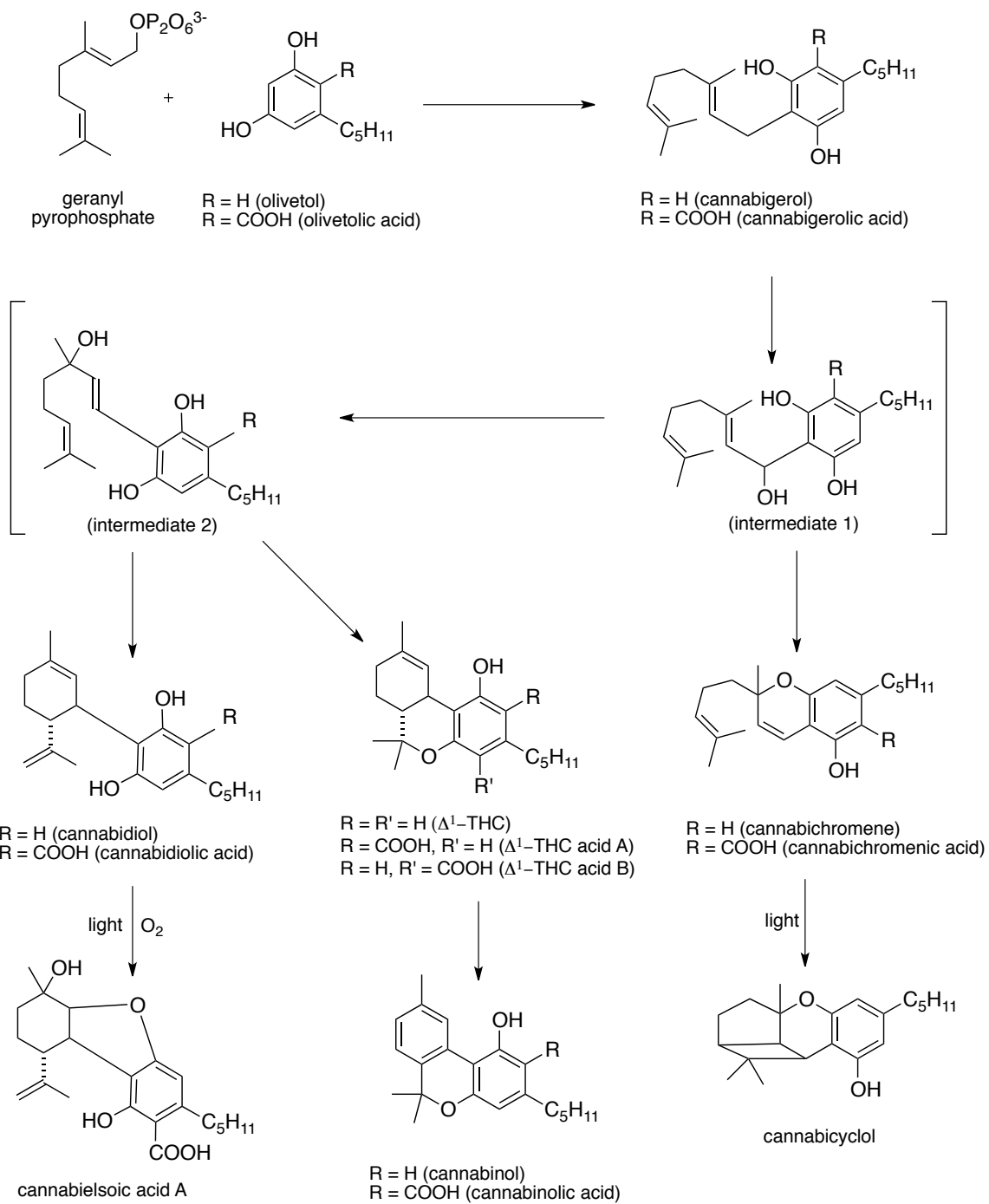
Marinol,® also known as dronabinol, is probably the most well known cannabinoid-based drug. It is made up of a synthetic version of the active isomer of THC and is found

in capsule form. Its main purpose is to relieve nausea and vomiting due to chemotherapy. It also helps to deal with the loss of weight and appetite in AIDS patients.

Another cannabinoid-based drug that also works as an antiemetic is Cesamet.<sup>®</sup> It is also found in capsule form and is composed of racemic nabilone, which is a synthetic cannabinoid that is structurally similar to THC.

### **1.5 The Biosynthetic Pathway of Cannabinoids**

The actual biosynthetic pathway for the formation of cannabinoids in the cannabis plant is still under study. However, Scheme 1.1 gives a good idea of this process.<sup>25</sup> It is suggested that geranyl pyrophosphate and olivetolic acid form cannabigerolic acid. It then goes through the proposed intermediate 1, undergoes an allylic rearrangement to the proposed intermediate 2 to yield cannabidiolic acid, and can then form cannabielsoic acid.  $\Delta^1$ -THC acid A can then be directly obtained from cannabigerolic acid (through the same proposed intermediates), bypassing the formation of cannabidiolic acid, via an enzymatic oxidation-cyclization process.<sup>26</sup> It can then produce cannabinolic acid. Lastly, cannabichromenic acid can be obtained from the proposed intermediate 1, which can then produce cannabicyclol.<sup>25</sup>

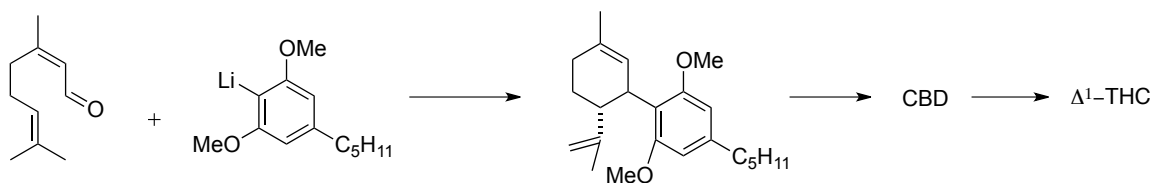


**Scheme 1.1** Cannabinoids and their biosynthetic pathway.



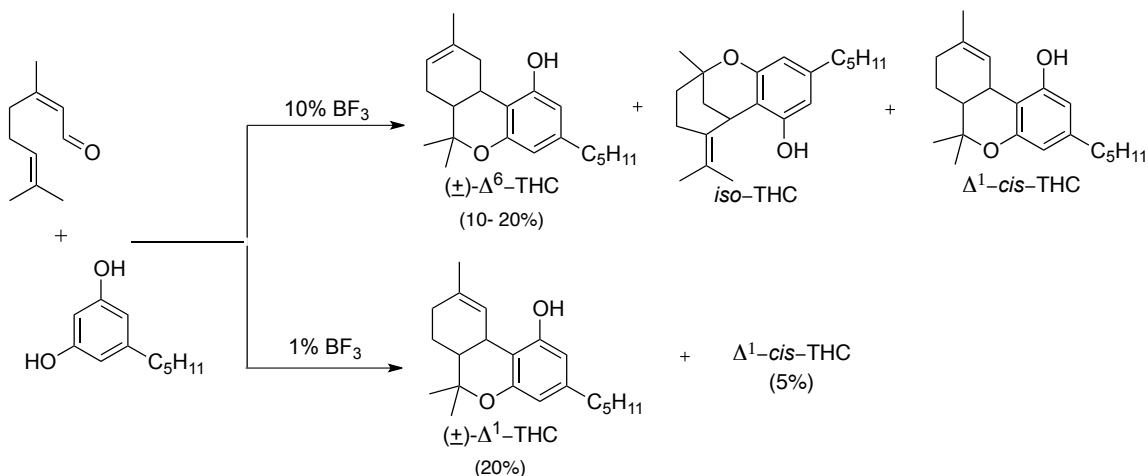
## 1.6 Previous Olivetol-Based Syntheses to $\Delta^1$ -Tetrahydrocannabinol ( $\Delta^1$ -THC)

Previous syntheses to  $\Delta^1$ -THC involve the use of olivetol at some point during the synthesis. The first synthesis was developed in 1965 (Scheme 1.2). Reaction of citral with the lithium olivetol derivative produced the methoxy-protected cannabidiol compound. Then heating with methylmagnesium iodide gave racemic cannabidiol. Then continued heating with hydrochloric acid produced a mixture of starting material and racemic  $\Delta^1$ -THC in a 2% overall yield.<sup>27</sup>



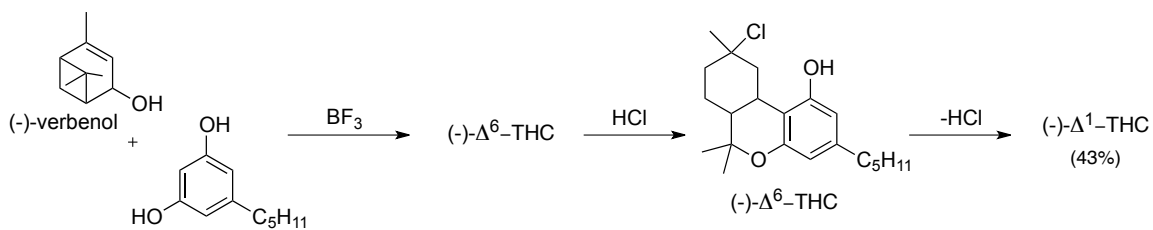
**Scheme 1.2** The first synthesis to *rac*- $\Delta^1$ -THC.

Another synthesis by Mechoulam and co-workers leading to *dl*- $\Delta^1$ -THC used olivetol and a catalytic amount of boron trifluoride ( $\text{BF}_3$ ). The amount of  $\text{BF}_3$  that was used had an affect on the number and types of products (Scheme 1.3). Using 10%  $\text{BF}_3$  produced a racemic mixture of  $\Delta^6$ -THC with trace amounts of  $\Delta^1$ -THC that was not easy to isolate, as well as *iso*-THC and the *cis*-isomer of  $\Delta^1$ -THC. However, decreasing the amount of  $\text{BF}_3$  to just 1%, produced  $\Delta^1$ -THC as a racemic mixture in 20% yield, along with some of the *cis*-isomer.<sup>28</sup>



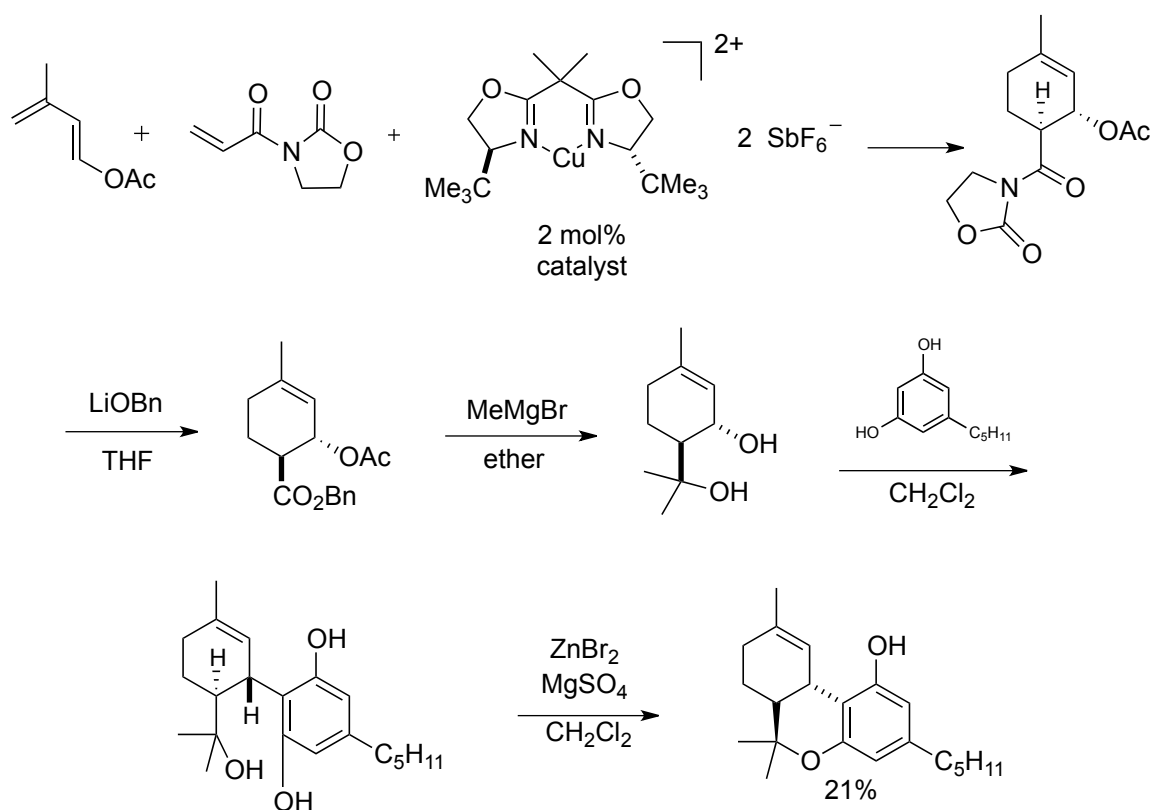
**Scheme 1.3**  $\text{BF}_3$  route to  $(\pm)$   $\Delta^1$ -THC and isomers.

Eventually, an attempt was made to synthesize only the naturally occurring isomer of  $\Delta^1$ -THC (Scheme 1.4). Using (-)-verbenol, instead of citral, produces (-)- $\Delta^6$ -THC, which is then treated with acid to produce the chloro-hexahydrocannabinol. Dehydrochlorination will then produce (-)- $\Delta^1$ -THC in a 43% overall yield. In a similar fashion, use of (+)-verbenol will result in (+)- $\Delta^1$ -THC.<sup>28</sup>



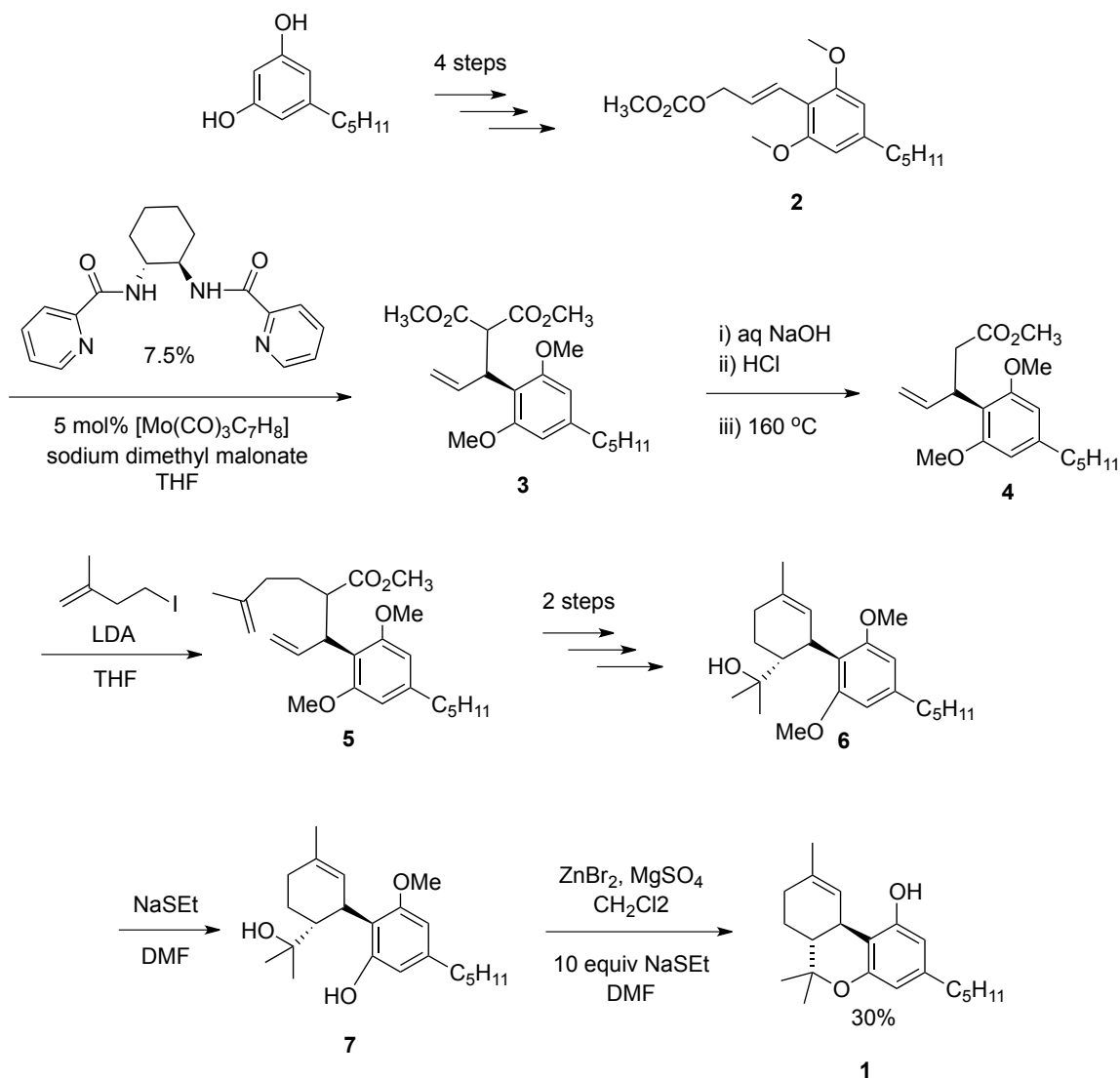
**Scheme 1.4** Synthesis of (-)  $\Delta^1$ -THC.

Evans and Trost have also designed olivetol-based syntheses. In 1997, Evans and co-workers used a cationic bis(oxazoline)copper (II) catalyst, to synthesize the non-active (*S,S*)-isomer of  $\Delta^1$ -THC (Scheme 1.5).<sup>29</sup> This was the first asymmetric synthesis that utilized an enantioselective Diels-Alder reaction. This was achieved by reacting the diene and acrylamide, along with the selected Cu(II) catalyst, resulting in the shown cycloadduct. LiOBn was then used to cleave the imide, which was then treated with methylmagnesium bromide to give the diol. At that point, reaction with olivetol and *p*-TSA produces the triol, which is then cyclized to give (*S,S*)- $\Delta^1$ -THC in an overall yield of 21%.<sup>29</sup>



**Scheme 1.5** Evans synthesis to (*S,S*)- $\Delta^1$ -THC.

Then in 2007, Trost introduced his synthesis of enantioselective  $\Delta^1$ -THC with an overall yield of 30% via a molybdenum-catalyzed asymmetric allylic alkylation reaction (Scheme 1.6).<sup>30</sup> This synthesis also allows for creation of THC analogues by substituting compound **2** for other aromatic derivatives as well as the alkylating reagent that results in compound **5**. The synthesis starts with olivetol to make the desired aromatic compound in four steps. Then, along with the chiral ligand, the molybdenum catalyst is added to afford compound **3**. Treatment with aqueous sodium hydroxide and hydrochloric acid then yields compound **4**. Alkylation then proceeds using the selected iodide and lithium diisopropylamide to yield compound **5**, which is eventually converted to the alcohol over two steps. Next, NaSEt is used to selectively deprotect one of the hydroxyl groups. The reaction then proceeds to yield (*R,R*)- $\Delta^1$ -THC synthesis when treated with zinc bromide, magnesium sulfate, and NaSEt one last time.<sup>30</sup>

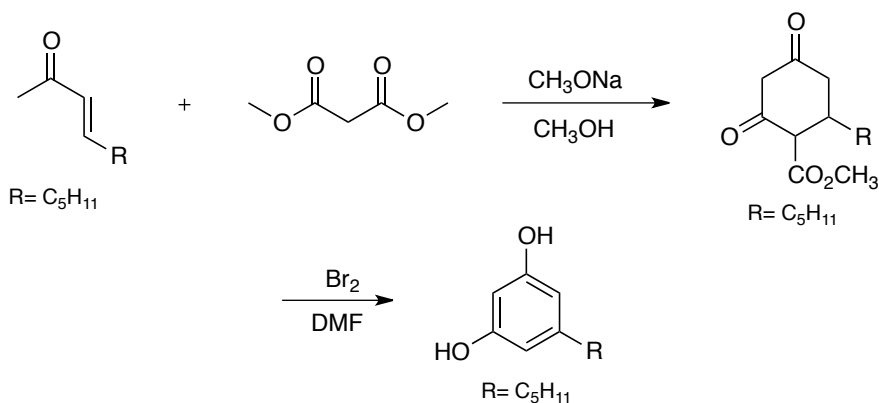


**Scheme 1.6** Trost's (*R,R*)- $\Delta^1$ -THC synthesis.

These syntheses make it difficult to design analogues of  $\Delta^1$ -THC that include facile substitution of the bioactive R-group, a pentyl sidechain attached to the aromatic ring. This is mainly due to the fact that analogues are usually made via resorcinol derivatives.

## 1.7 Synthesis of Olivetol and Potential Derivatives

Focella and co-workers synthesize olivetol by taking 3-nonen-2-one and reacting it with dimethyl malonate using sodium methoxide in methanol (Scheme 1.7).<sup>31</sup> The synthesis allows for the development of analogues through substitution of the  $\alpha$ ,  $\beta$ -unsaturated ketone. However, one of the major drawbacks of this synthesis involves aromatization of the 1,3-cyclohexanedione. The purification process can take days and small amounts of impurities often remain. Also, most of the desired  $\alpha$ ,  $\beta$ -unsaturated ketone are not commercially available; therefore the synthesis may need to proceed with additional steps.



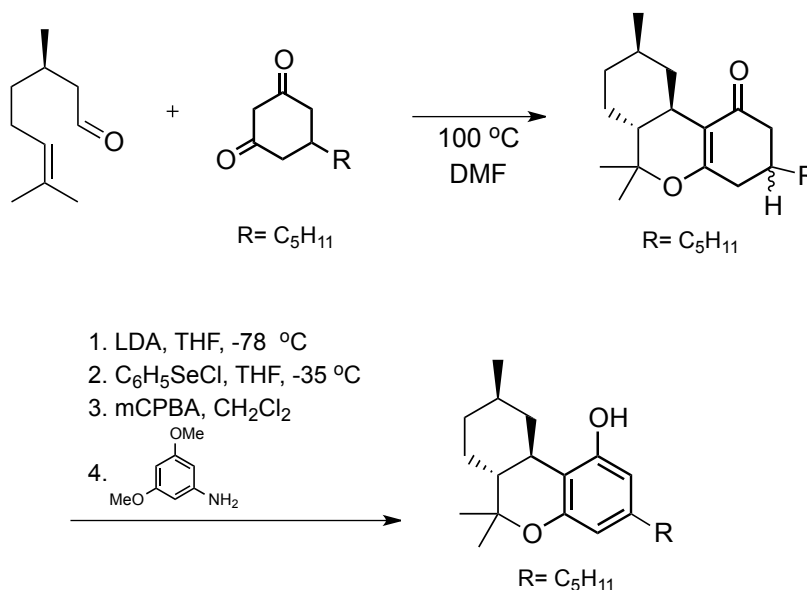
**Scheme 1.7** Focella's synthesis to olivetol.

## 1.8 Alternatives to Olivetol

Alternatives to olivetol are highly desired, not only because of the difficulty with purification after aromatization, but because the scope of potential analogues is

dependent on the commercial availability of the desired  $\alpha$ ,  $\beta$ -unsaturated ketone or the degree of difficulty in synthesizing the starting material. It would also be difficult to start off with 1,3-dihydroxybenzene. Since the starting material would be ortho/para directing, it would be difficult to target the meta position with a different R group.

Tietze has shown that you can use analogues of the 1,3-cyclohexanedione to synthesize analogues of THC and then aromatize as a last step (Scheme 1.8).<sup>32</sup> (*R*)-citronellal and 5-*n*-pentyl-1,3-cyclohexanedione are heated in DMF at 100 °C to yield the non-aromatic THC analogue. Then deprotonation with LDA and reaction with phenylselenium chloride provides a selenide intermediate (not shown). Upon oxidation with *m*-chloroperbenzoic acid the selenium oxide is obtained (not shown) and lastly, a *syn*-elimination yields the aromatic THC analogue.



**Scheme 1.8** Tietze's synthesis to aromatic THC analogues.

## 1.9 Modifications to the Side Chain

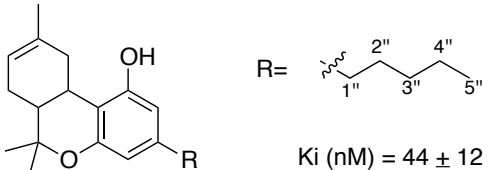
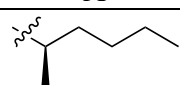
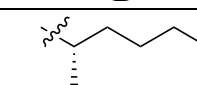
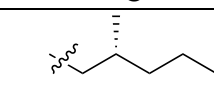
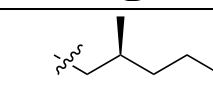
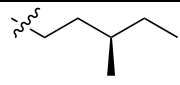
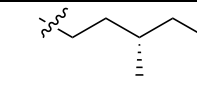
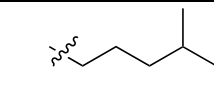
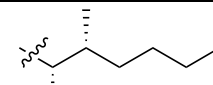
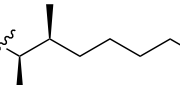
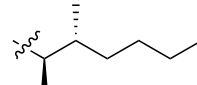
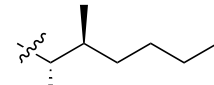
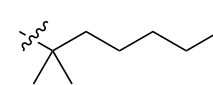
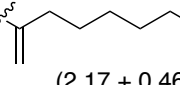
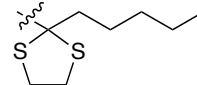
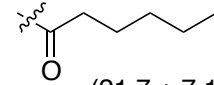
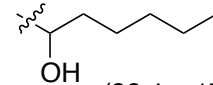
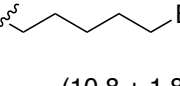
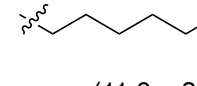
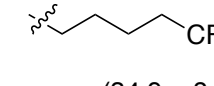
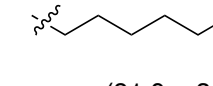
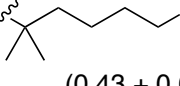
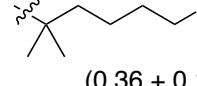
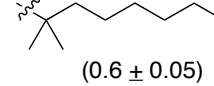
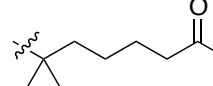
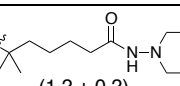
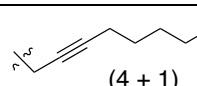
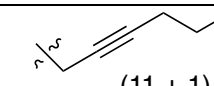
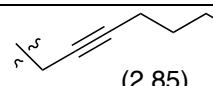
The most desired analogues model after  $\Delta^1$ -THC and simply differ at the alkyl side-chain. Looking at Table 1.1, it is evident that the cannabinoids have different types of side-chains at position 4', whether it be length of the chain or any substituent branching off of it (Fig. 1.1a). It is known that the type of side-chain can have a definite impact on a cannabinoid compound's biological activity and a better representation of the types of modifications can be found in Table 1.2.

It has been found that in order to produce any type of activity the chain must be at least three carbon atoms long, with the optimal length being between five to seven carbon atoms long.<sup>5</sup> Branching of the side chain at the 1'' position (Fig. 1.1a) with two methyl groups has been shown to increase activity. A 1'',2''- dimethylheptyl side chain has also shown high affinity for the receptor. Most of these SAR studies have been performed using  $\Delta^6$ -THC since it has been found easier to synthesize and its potency and activity is still similar to  $\Delta^1$ -THC.<sup>5</sup>

Table 1.2 compared binding affinity data for some  $\Delta^6$ -THC analogues, modified at the R group side-chain. The analogues were bound to the CB<sub>1</sub> receptor preparation of a rat cortex. The binding affinity for  $\Delta^6$ -THC ( $K_i$ ) was found to be  $44 \pm 12$  nM.<sup>33</sup> By looking at Table 1.2, the ones with a lower  $K_i$  value than  $\Delta^6$ -THC possess better binding affinity.



**Table 1.2**  $\Delta^6$ -THC side chain modification  $K_i$  values. Shown in parenthesis in nM.<sup>33-43</sup>

 $K_i$ (nM) = $44 \pm 12$				
	A	B	C	D
1	 ( $7.6 \pm 0.6$ )	 ( $20 \pm 4$ )	 ( $19 \pm 5$ )	 ( $11 \pm 1$ )
2	 ( $38 \pm 3$ )	 ( $53 \pm 1$ )	 ( $141 \pm 52$ )	 ( $0.46 \pm 0.04$ )
3	 ( $0.60 \pm 0.15$ )	 ( $0.84 \pm 0.21$ )	 ( $0.81 \pm 0.08$ )	 ( $0.77 \pm 0.11$ )
4	 ( $2.17 \pm 0.46$ )	 ( $0.32 \pm 0.08$ )	 ( $21.7 \pm 7.1$ )	 ( $86.4 \pm 17.9$ )
5	 ( $10.8 \pm 1.8$ )	 ( $11.0 \pm 3.4$ )	 ( $34.9 \pm 8.1$ )	 ( $81.0 \pm 3.5$ )
6	 ( $0.43 \pm 0.09$ )	 ( $0.36 \pm 0.14$ )	 ( $0.6 \pm 0.05$ )	 ( $0.86 \pm 0.06$ )
7	 ( $1.2 \pm 0.2$ )	 ( $4 \pm 1$ )	 ( $11 \pm 1$ )	 (2.85)

As previously mentioned, branching the alkyl chain was shown to improve affinity, as represented by the lower  $K_i$  values (Table 1.2, examples 1A- 1D). However, once the branching starts at the 3'' of the side chain, affinity starts to decrease (higher  $K_i$ ). Although analogue 2A is still somewhat more active than  $\Delta^6$ -THC, its isomer, analogue

**2B**, is actually worse than  $\Delta^6$ -THC. Further extending into the 4'' position (example **2C**) makes the analogue's affinity three times as bad as that of  $\Delta^6$ -THC. The addition of an extra methyl group (examples **3A-4A**) greatly improves affinity and seems to produce the optimal analogue. With the exception of fluorine (**5D**), halogens (**5A** and **5B**) seem to improve affinity and when combined with a gem dimethyl (**6A**), the analogues further increase in affinity. Amides (**6D** and **7A**) and some acetylenes (**7B** and **7D**) show good affinity, while ketones (**4C**), and hydroxyl groups (**4D**) do not. However, the best affinities were seen with the addition of a dithiolane (**4B**) and the cyano- *gem*-dimethyl (**6B**) and are found to be potent CB<sub>1</sub> agonists.<sup>41</sup> Therefore, optimal affinity is reached with a seven-carbon atom chain and a bulky group at the 1'' position.<sup>33</sup>

Based on these SAR studies, the ideal analogue contains a side-chain that allows itself to loop back towards the phenolic ring it is attached to. This will allow for optimal receptor affinity and potency.<sup>5</sup>

## REFERENCES:

1. Felder, C.C.; Glass, M., *Annu. Rev. Pharmacol. Toxicol.*, 1998, 38, 179-200.
2. Pacher, P.; Batkai, S.; Kunos, G., *Pharmacol. Rev.*, **2006**, 58, 389-462.
3. Matsuda, L.A., *Crit Revs Neurobiol*, **1997**, 11, 143.
4. Pertwee, R.G., *Current Medicinal Chemistry*, **1999**, 6 (8), 635-664.
5. Razdan, R.K., *The Cannabinoid Receptors*, (The Receptors Series), pp. 3-19, ed. Reggio, P.H., Humana Press, New York, 2009.
6. ElSohly, H.N.; Turner, C.E.; Clark, A.M.; ElSohly, M.A., *J Pharm Sci*, **1982**, 71, 1319-1323.
7. Shohami, E.; Novikov, M.; Mechoulam, R., *J. Neurotrauma*, **1993**, 10, 109-119.
8. Shohami, E.; Novikov, M.; Bass, R., *Brain Res.*, **1995**, 674, 55-62.
9. Panikashvili, D.; Simeonidou, C.; Ben-Shabat, S.; Hanus, L.; Breuer, A.; Mechoulam, R.; Shohami, E., *Nature (Lond)*, **2001**, 413, 527-531.
10. Klijjn, C.J.; Hankey, G.J., *Lancet Neurol*, **2003**, 2, 698-701.
11. Nagayama, T.; Sinor, A.D.; Simon, R.P.; Chen, J.; Graham, S.H.; Jin, K.; Greenberg, D.A., *J Neurosci*, **1999**, 19, 2987-2995.
12. Sinor, A.D.; Irvin, S.M.; Greenberg, D.A., *Neurosci Lett*, **2000**, 278, 157-160.
13. Sospedra, M.; Martin, R., *Annu Rev Immunol*, **2005**, 23, 683-747.
14. Compston, A.; Coles, A., *Lancet*, **2002**, 359, 1221-1231.
15. Killestein, J.; Polman, C.H., *Curr Opin Neurol*, **2005**, 18, 253-260.
16. Wirguin, I.; Mechoulam, R.; Breuer, A.; Schezen, E.; Weidenfeld, J.; Brenner, T., *Immunopharmacology*, **1994**, 28, 209-214.
17. Achiron, A.; Miron, S.; Lavie, V.; Margalit, R.; Biegon, A., *J Neuroimmunol*, **2000**, 102, 26-31.
18. Baker, D.; Pryce, G.; Croxford, J.L.; Brown, P.; Pertwee, R.G.; Huffman, J.W.; Layward, L., *Nature (Lond)*, **2000**, 404, 84-87.

19. Grinspoon, L.; Bakalar, J.B.; *The history of cannabis, in Marihuana: The Forbidden Medicine*, Yale University Press, New Haven, CT. **1993**.
20. Grinspoon, L.; Bakalar, J.B., *J Psychoact Drugs*, **1998**, 30, 171-177.
21. Martyn, C.N.; *Lancet*, **1995**, 345, 579.
22. Wade, D.T.; Robson, P.; House, H.; Makela, P.; Aram, J., *Clin Rehabil*, **2003**, 17, 21-29.
23. Rowland, L.P.; Shneider, N.A.; *N Engl J Med*, **2001**, 344, 1688- 1700.
24. Raman, C.; McAllister, S.D.; Gulrukh, R.; Patel, S.G.; Moore, D.H.; Abood, M.E., *ALS and other motor neuron disorders*, **2004**, 5, 33-39.
25. Mechoulam, R., *Current Pharmaceutical Design*, **2000**, 6, 1313-1322.
26. Taura, F.; Morimoto, S; Shoyama, Y.; Mechoulam, R., *J Amer Chem Soc*, **1995**, 117, 9766.
27. Mechoulam, R.; Gaoni, Y., *J Amer Chem Soc*, **1965**, 87, 3273- 3275.
28. Mechoulam, R.; Braun, P.; Gaoni, Y., *J Amer Chem Soc*, **1972**, 6159-6165.
29. Evans, D.A., et al. *Tetrahedron Letters*, 1997, 3193-3194.
30. Trost, B. et al. *Organic Letters*, 2007, 861-863
31. Focella, A.; Teitel, S.; Brossi, A., *J. Org. Chem.*, **1977**, 42, 3456-3457.
32. Tietze, L.F. *Chem. Rev.* **1996**, 96, 115-136
33. Seltzman, H.H., *Current Medicinal Chemistry*, **1999**, 6, 685-704.
34. Martin, B.R.; Compton, D.R.; Prescott, W.R.; Barrett, R.L.; Razdan, R.K., *Drug Alcohol Depend*, **1995**, 37, 231.
35. Huffman, J.W.; Lainton, J.A.H.; Banner, W.K.; Duncan, J.S.G.; Jordan, R.D.; Yu, S.; Dai, D.; Martin, B.R.; Wiley, J.L.; Compton, D.R., *Tetrahedron*, **1997**, 53, 1557.
36. Huffman, J.W.; Duncan, S.G.; Wiley, J.L.; Martin, B.R., *Bioorganic & Med Chem Lett*, **1997**, 7, 2799.

37. Papahatjis, D.P.; Kourouli, T.; Abadji, V.; Goutopoulos, A.; Makriyannis, A., *J Med Chem*, **1998**, 41, 1195.
38. Mavromoustakos, T.; Theodoropoulou, E.; Zervou, M.; Kourouli, T.; Papahatjis, D., *J Pharm Biomed Anal*, **1999**, 18, 947.
39. Charalambous, A.; Lin, S.; Marciniak, G.; Banijamali, A.; Friend, F.L.; Compton, D.R.; Martin, B.R.; Makriyannis, A., *Pharmacol Biochem Behav*, **1991**, 40, 509.
40. Martin, B.R.; Compton, D.R.; Semus, S.F.; Lin, S.; Marciniak, G.; Grzybowska, J.; Charalambous, A.; Makriyannis, A., *Pharmacol Biochem Behav*, **1993**, 46, 295.
41. Singer, M.; Ryan, W.J.; Saha, B.; Martin, B.R.; Razdan, R.K., *J Med Chem*, **1998**, 41, 4400.
42. Ryan, W.; Singer, M.; Razdan, R.K.; Compton, D.R.; Martin, B.R., *Life Sci*, **1995**, 56, 2013.
43. Ross, R.A.; Brockie, H.C.; Fernando, S.R.; Saha, B.; Razdan, R.K.; Pertwee, R.G., *Br J Pharmacol*, **1998**, 125, 1345.

## **Chapter 2**

**The Design, Synthesis, Computational Analysis, and *in silico* and Biological**

**Screening of Cannabinoids and their Analogues**

## 2.1 Introduction

The great therapeutic potential of cannabinoids and their analogues has caused much interest in finding more efficient methods that allow facile development of these analogues. Focusing on the thermal isomerization of cannabinoid analogues and using the most well known cannabinoid,  $\Delta^1$ -THC, as a starting point, we built off of the seminal work of Tietze. Then, based on computational docking studies, we later discovered that aromaticity was not essential for CB<sub>1</sub> receptor affinity and that all isomers of  $\Delta^1$ -THC showed a similar affinity for the receptor. Besides *in silico* screening, our cannabinoid analogues were also biologically screened and preliminary studies showed they possessed therapeutic potential towards ALS.

## 2.2 Isomerization of Cannabinoids and its Effects

Our interest in thermal isomerization of cannabinoid analogues stems from a N.Y. State Psychiatric Institute report that compared behavioral effects between cannabis smokers and those who were orally administered equivalent dosages of  $\Delta^1$ -THC after they abruptly quit. It was found that there was a significantly higher observation of withdrawal symptoms in the cannabis smokers versus those of oral intake.<sup>1</sup>

As mentioned in the previous chapter, marijuana is composed of a mixture of several cannabinoids including  $\Delta^1$ -THC, CBD, and CBC. Currently, there are few studies on the thermolysis product resulting from smoking marijuana. If marijuana were heated along with tobacco, we would see an increase in THC at the expense of CBD, as CBD is known

to convert to THC. A representation of this can be found in Figure 2.1. Based on results to be discussed, it is also proposed that if  $\Delta^1$ -THC were heated by itself, as in the process of smoking marijuana, there will be an increase in the amount of  $\Delta^1$ -THC at the expense of CBC in the form of all stereoisomers (Fig. 2.1). However, if  $\Delta^1$ -THC is taken orally, for example as in the form of Marinol®, only the *trans*-(*R,R*) isomer of  $\Delta^1$ -THC is consumed since this form of intake does not require heating.

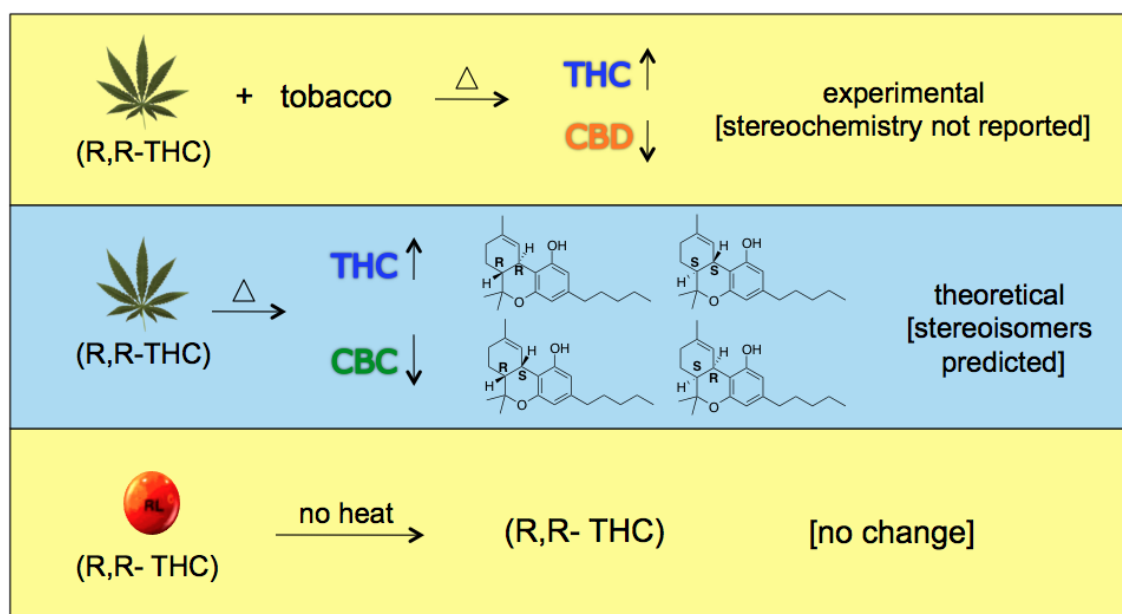


**Figure 2.1** Isomerization Effects.

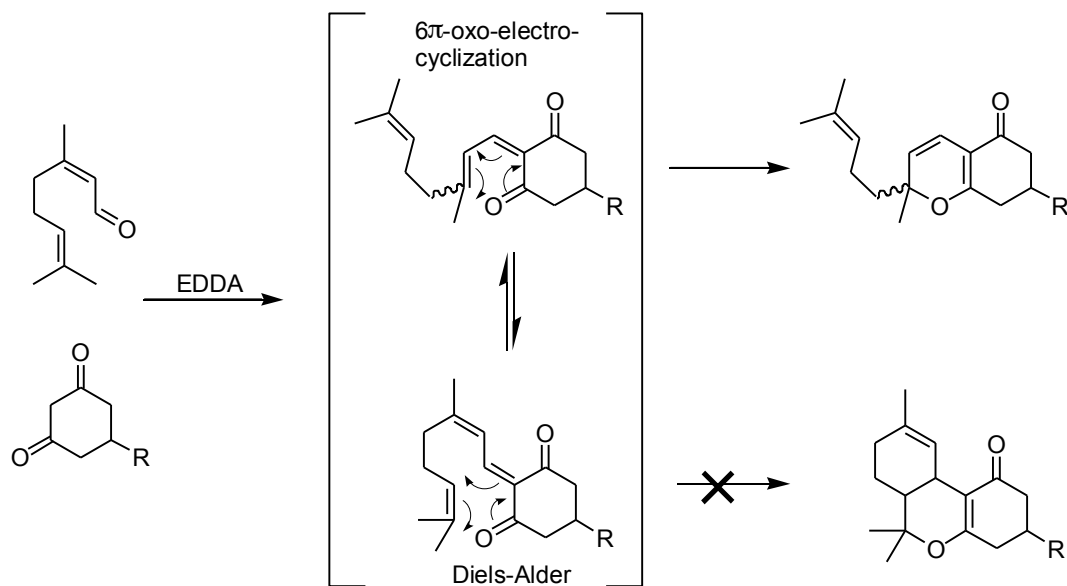
Therefore, we are predicting that the formation of the unnatural isomers of  $\Delta^1$ -THC during the process of smoking marijuana could be the cause of the withdrawal symptoms. While no human studies reported on the effects of these unnatural isomers of  $\Delta^1$ -THC



currently exist, there is evidence for the isolation of the unnatural, *cis*- isomer of  $\Delta^1$ -THC from confiscated marijuana, based on routine analysis.<sup>2</sup>

### 2.3 Thermal Isomerization of Cannabinoid Analogues.

In synthesizing these cannabinoid analogues, we have built off of Tietze's work and adopted the concept of a tandem Knoevenagel – Diels-Alder cascade reaction.<sup>3</sup> In our synthetic plan, non-aromatic analogues of CBC and THC ( $\text{CBC}_{\text{an}}$  and  $\text{THC}_{\text{an}}$ ) share the same intermediate Knoevenagel product. The product depends on the competition between a Diels-Alder reaction and an oxo-6 $\pi$  electrocyclization (Scheme 2.1).



**Scheme 2.1** The oxo-6 $\pi$  electrocyclization reaction versus the Diels-Alder.

Trauner provides evidence that EDDA catalyzes both the Knoevenagel reaction and the oxo-6 $\pi$ -cyclization.<sup>5</sup> To investigate this further, we performed a computational analysis using Spartan, a molecular modeling and computational program, at B3LYP/6-31G\* level of theory.<sup>6</sup> Starting materials, products, and transition states associated with Scheme 2.1 were studied and predict the transition state for the oxo-6 $\pi$ -electrocyclization (no EDDA) to be lower in energy than both the *cis*- and *trans*- Diels-Alder transition states. However, THC<sub>an</sub> product is thermodynamically favored over CBC<sub>an</sub> by ca. 13 kcal/mol (Fig. 2.2). Given this prediction, we targeted thermodynamic control of this reaction.

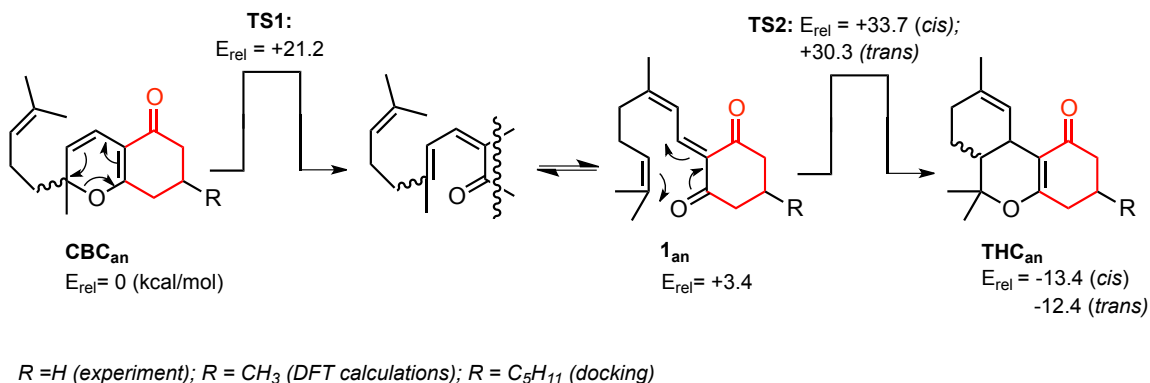
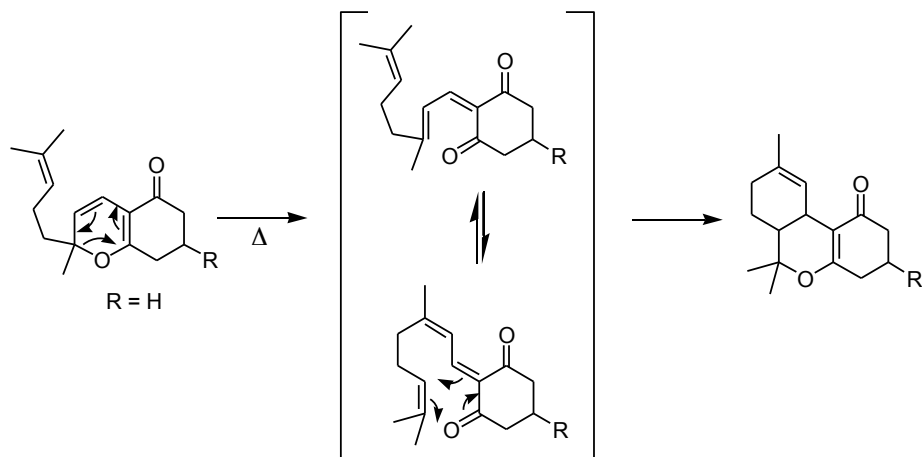


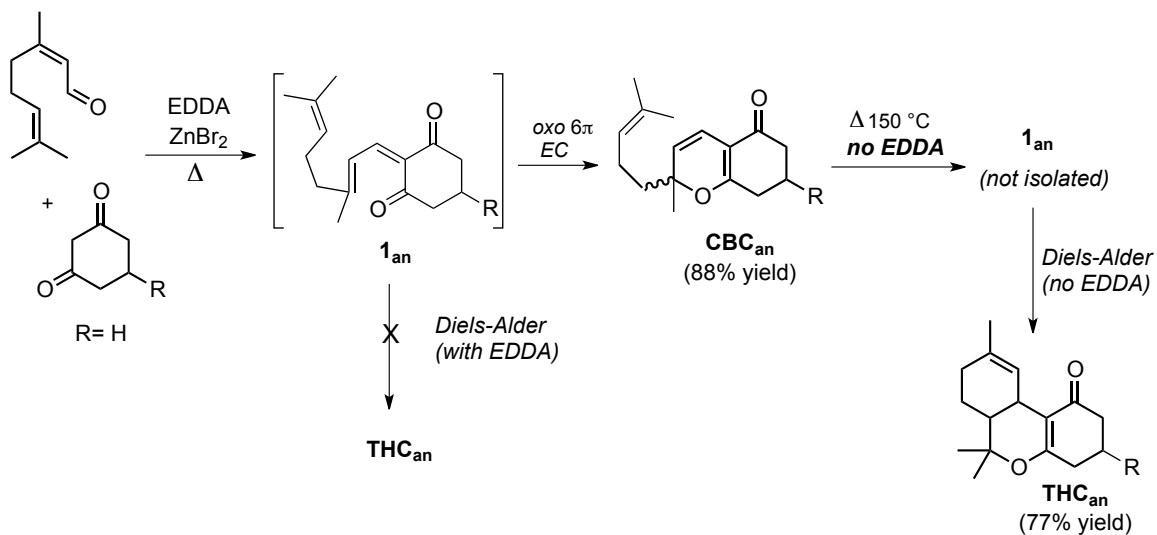
**Figure 2.2** Spartan calculations (B3LYP/6-31G\*) for starting material, products, and transition states of compounds found in Scheme 2.1.

By adsorbing CBC<sub>an</sub> onto silica and heating to 150 °C, CBC<sub>an</sub> was cleanly converted to a mixture of *cis*- and *trans*-  $\Delta^1$ -THC<sub>an</sub> (Scheme 2.2). This result established a previously unknown thermal conversion between two phytocannabinoid analogues, CBC<sub>an</sub> to THC<sub>an</sub>.



**Scheme 2.2** Thermal isomerization.

Scheme 2.3 then shows the complete  $\text{THC}_{\text{an}}$  synthesis. Reaction of citral and a 1,3-cyclohexanedione, catalyzed by  $\text{ZnBr}_2$  and ethylenediamine diacetate (EDDA) results exclusively in a tandem Knoevenagel – oxo- $6\pi$ -electrocyclization to afford  $\text{CBC}_{\text{an}}$  in excellent yield.  $\text{CBC}_{\text{an}}$  is then isomerized to  $\Delta^1\text{-THC}_{\text{an}}$  at  $150\text{ }^\circ\text{C}$ .<sup>4</sup>



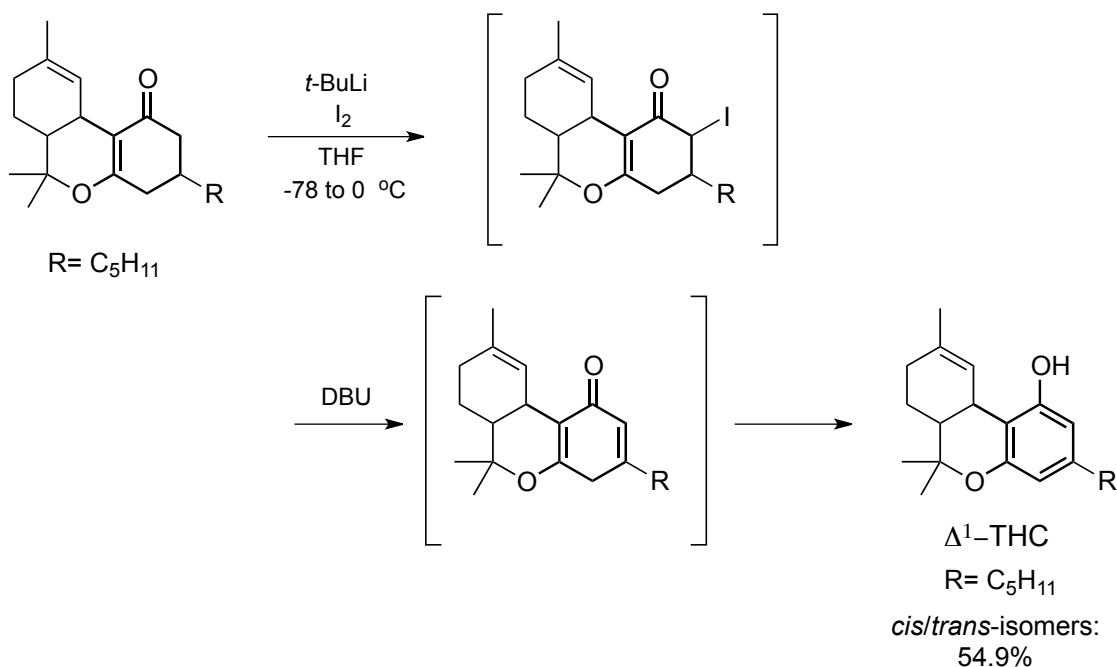
**Scheme 2.3** Synthesis of  $\Delta^1\text{-THC}$  analogue.

When looking at the synthesis, it is important to note that we cannot directly heat the reaction to 150 °C and obtain  $\text{THC}_{\text{an}}$  without first isolating  $\text{CBC}_{\text{an}}$  and to prove that, we ran two thermal isomerization reactions (Table 2.1). The first followed the standard procedure of adsorbing CBC onto silica and the second was adsorbed onto an admixture of silica and EDDA. Both reactions were heated side-by-side at 150 °C for 40 minutes. Reaction one showed full conversion of  $\text{CBC}_{\text{an}}$  to  $\text{THC}_{\text{an}}$ . In reaction 2, when you adsorb  $\text{CBC}_{\text{an}}$  onto an admixture of silica and EDDA, you get a mixture of  $\text{CBC}_{\text{an}}$  and  $\text{THC}_{\text{an}}$  in a 1:2 ratio. Even continued heating of reaction 2 for another 40 minutes, will not result in full conversion to  $\text{THC}_{\text{an}}$ . Therefore, EDDA lowers the reaction rate. We also cannot completely eliminate EDDA from the reaction. Repeating the reaction in the absence of EDDA does not produce  $\text{CBC}_{\text{an}}$  in any amount; only starting materials are obtained.

**Table 2.1.** Thermal isomerization comparison reactions: the affects of EDDA.

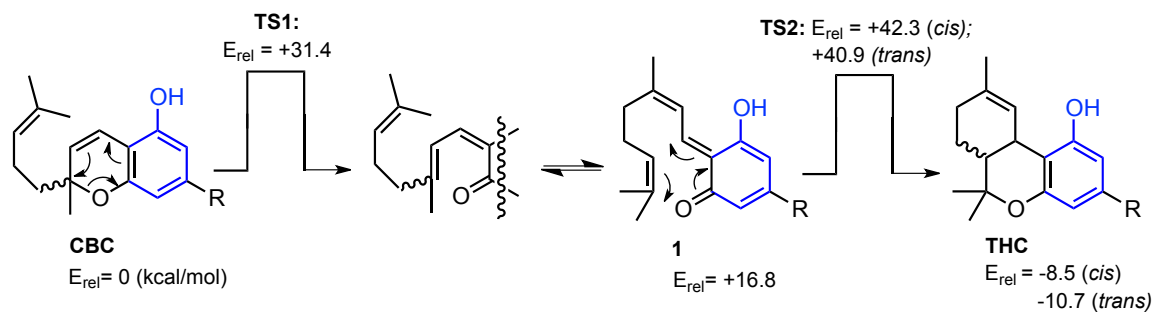
<b>Reaction</b>	<b>Adsorbent</b>	<b>Time (minutes)</b>	<b>Temperature (°C)</b>	<b><math>\text{CBC}_{\text{an}}</math>: <math>\text{THC}_{\text{an}}</math> ratio</b>
1	silica	40	150	0:1
2	admix mass ratio: silica (98): EDDA (2)	40	150	1:2

Aromatization of  $\text{THC}_{\text{an}}$  was then achieved by using *t*-BuLi and iodine to iodinate alpha to the carbonyl. Elimination with 1,8-Diazabicycloundec-7-ene (DBU) then allows the compound to tautomerize to  $\Delta^1$ -THC in a mixture of *cis* and *trans*- isomers (Scheme 2.4).



**Scheme 2.4** Aromatization of  $\Delta^1$ - $\text{THC}_{\text{an}}$  to  $\Delta^1$ -THC.

Similar energy calculations were also performed for CBC and  $\Delta^1$ -THC (Fig. 2.3). The results followed a similar trend, favoring  $\Delta^1$ -THC as the thermodynamic product and leading to our proposition that CBC can thermally isomerize to  $\Delta^1$ -THC during the process of marijuana smoking.



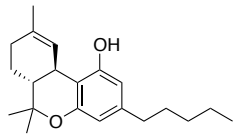
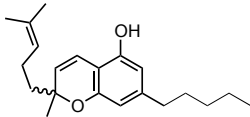
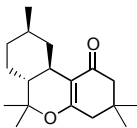
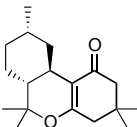
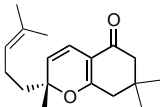
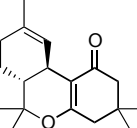
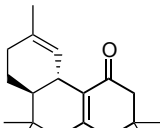
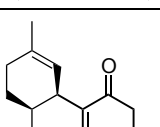
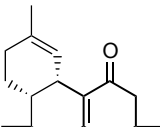
$R = C_5H_{11}$  (phytocannabinoid, docking);  $R = CH_3$  (DFT calculations)

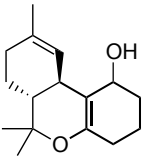
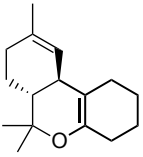
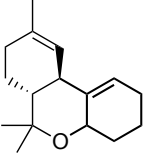
**Figure 2.3** Spartan calculations (B3LYP/6-31G\*) for starting material, products, and transition states for the aromatic version of compounds found in Scheme 2.1.

## 2.4 Cannabinoid Analogues

Computational docking using the molecular modeling program PyRx,<sup>7</sup> was used to establish different cannabinoid analogues. Using an X-ray crystal structure or homology model of a protein, in this case CB<sub>1</sub>, we can test the potential of the ligand to bind to the protein.<sup>8</sup> Table 2.2 shows the CB<sub>1</sub> receptor affinity of these analogues and compares them to that of  $\Delta^1$ -THC (entry 1), which has known therapeutic activity for the CB<sub>1</sub> receptor. Any score that is equal or lower (higher negative number) in value to that of  $\Delta^1$ -THC is considered to have good affinity for the CB<sub>1</sub> receptor.

**Table 2.2** CB<sub>1</sub> receptor binding affinity for  $\Delta^1$ -THC and other cannabinoid analogues.

Entry	Compound	Binding Affinity (kcal/mol)
1		-7.0
2		-6.0
3		-7.4
4		-7.3
5		-6.2
6		-7.6
7		-7.3
8		-7.8
9		-7.6

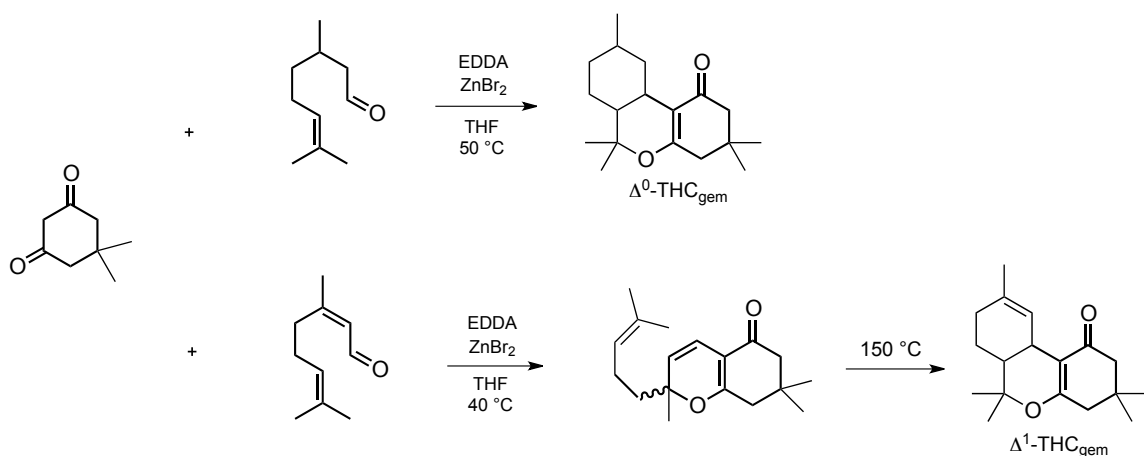
<b>10</b>		-6.9
<b>11</b>		-7.3
<b>12</b>		-6.6

Entries **3** and **4** (Table **1**) show the binding affinity for isomers of the same compound to be -7.4 and -7.3 kcal/mol, respectively, and higher than that of  $\Delta^1$ -THC (-7.0 kcal/mol). Entries **6-9** show the binding affinities for the  $\Delta^1$ -version of this analogue and most show a significantly higher affinity for the CB<sub>1</sub> receptor, with entry **8** showing the greatest affinity (-7.8 kcal/mol).

The syntheses of these analogues follow similar synthetic methods. Substitution of 1,3-cyclohexanedione with 5,5-dimethyl-1,3-cyclohexanedione, and reaction with citronellal produces the THC-*gem*-dimethyl analogue ( $\Delta^0$ -THC<sub>gem</sub>), shown in Scheme **2.5**. Synthesis of  $\Delta^1$ -THC<sub>gem</sub> follows a similar pathway as THC<sub>an</sub>, which also proceeds via a CBC analogue (Scheme **2.5**). A previous synthesis to this CBC intermediate analogue (CBC<sub>gem</sub>) currently exists, however it involves the use of a synthetically prepared phosphoric acid and reaction in methylene chloride to yield the chromene in 95% yield.<sup>9</sup>

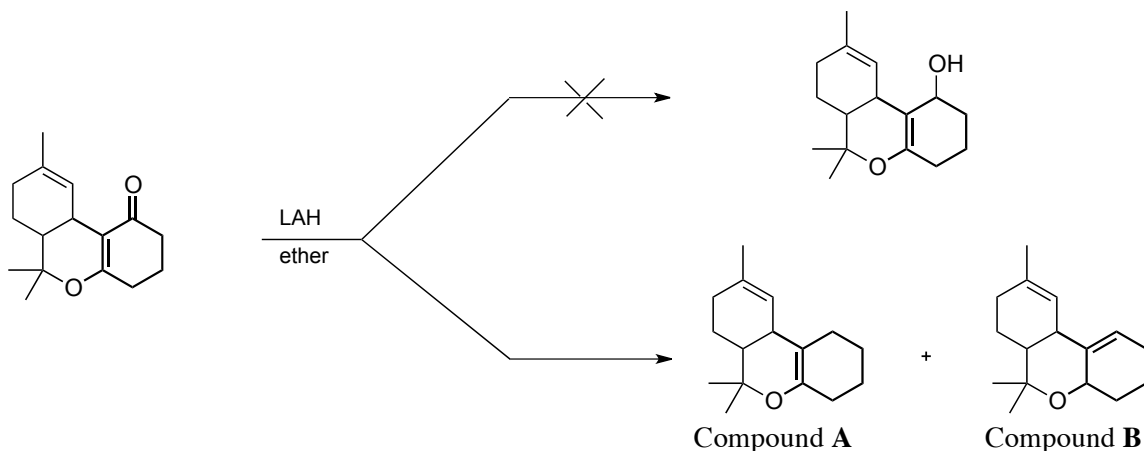


The previously known chromene was then adsorbed onto silica, following our established procedure, and isomerized to the  $\Delta^1$ -THC analogue in quantitative yield as a mixture of *cis* and *trans*- isomers.



**Scheme 2.5** Synthesis of THC-*gem*-dimethyl analogues.

Another interesting reaction involves reducing  $\Delta^1$ -THC<sub>an</sub> with an excess amount of lithium aluminum hydride (LAH) to produce a mixture of the tricyclic compounds (Scheme 2.6). The initial target was the alcohol shown as entry **10** (table 1) with an estimated binding affinity of -6.9 kcal/mol, still relatively close to that of  $\Delta^1$ -THC.



**Scheme 2.6** LAH reduction.

However, this did not undergo the expected reduction. The excess LAH causes complete removal of the oxygen atom to produce compounds **A** and **B** in a ratio of 4:1, with the major of these two products showing higher CB<sub>1</sub> affinity than the initial alcohol target and Δ<sup>1</sup>-THC.

## 2.5 Computational Docking Studies

Our previously mentioned hypothesis targeting unnatural cannabinoid isomers as the origin of withdrawal symptoms contributed to our collaboration with Dr. Chia-En Chang at UCR. Computational docking analysis found little difference in CB<sub>1</sub> receptor affinity among natural and unnatural THC isomers.<sup>4</sup> By looking at Fig. **2.4** we can see that, when aligning the global minimum-energy conformers of all isomers of Δ<sup>1</sup>-THC<sub>an</sub> (where R=C<sub>5</sub>H<sub>11</sub>), the pentyl side-chain is extended outward for all isomers.

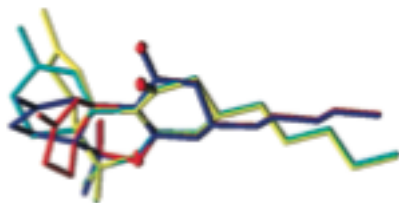


**Figure 2.4** Alignment of  $\Delta^1$ -THC<sub>an</sub> stereoisomers, showing pentyl side-chain in extended conformation for all isomers. Blue, *trans*-(*R,R*); cyan, *trans*-(*S,S*); yellow, *cis*-(*R,S*); red, *cis*-(*S,R*).

Using a modeled CB<sub>1</sub> receptor, the minimum-energy conformers for all stereoisomers of  $\Delta^1$ -THC and  $\Delta^1$ -THC<sub>an</sub> were docked to compare their interaction energies. The best ranked conformer of the naturally occurring (*R,R*)-  $\Delta^1$ -THC stereoisomer is shown docked to the CB<sub>1</sub> receptor in Fig. 2.5. The ligand interacts with both aromatic and hydrophobic residues and the binding is predominantly motivated by attractive van der Waals interactions. The interaction energies of (*R,R*)-  $\Delta^1$ -THC and (*R,R*)-  $\Delta^1$ -THC<sub>an</sub> were then compared and found to be similar with a  $\Delta E$  of approximately -34 kcal/mol.<sup>4</sup>

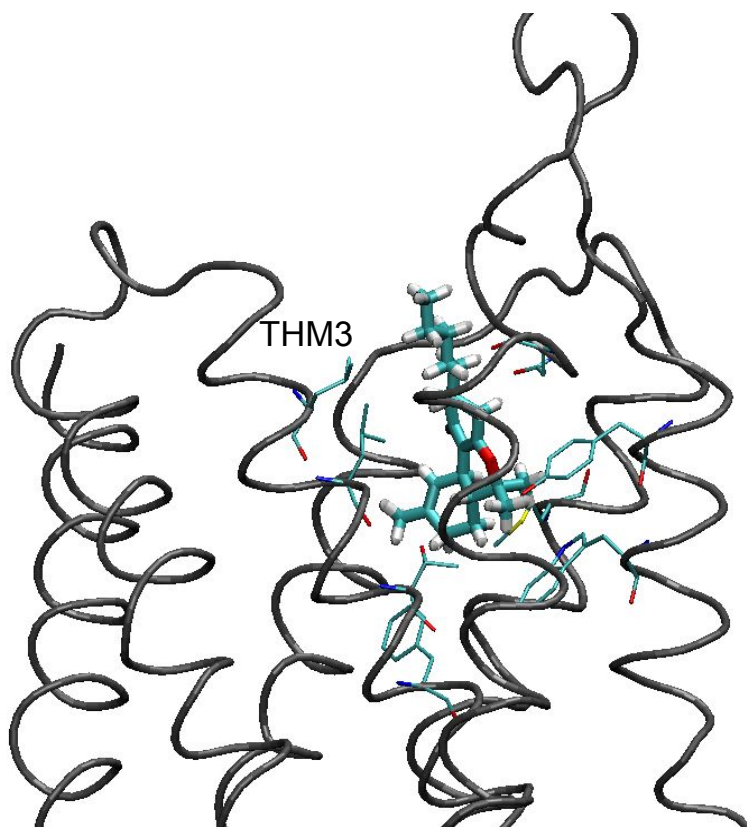


**Figure 2.5** (*R,R*)- $\Delta^1$ -THC<sub>an</sub> docked into a modeled CB<sub>1</sub> receptor. The receptor is represented by the gray tube while residues interacting with the ligand (cyan) are represented by thin line.

The high negative value is due to the fact that our calculations did not include entropy losses and the electrostatic desolvation penalty. However, since the structures of both  $\Delta^1$ -THC and  $\Delta^1$ -THC<sub>an</sub> are similar it suggests that the entropy and desolvation are alike.<sup>4</sup>

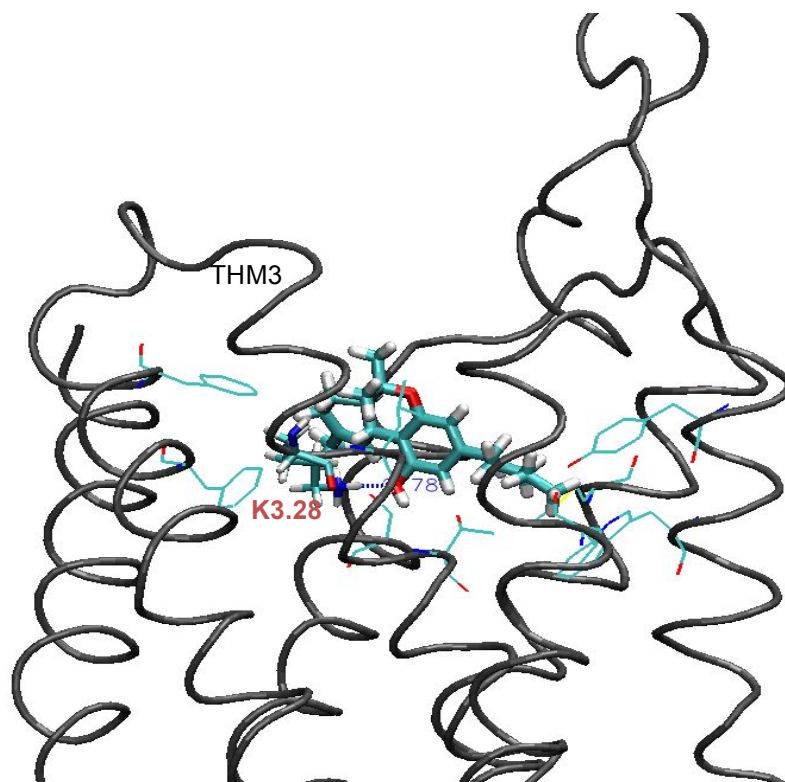


**Figure 2.6** (*R,R*)- $\Delta^1$ -THC docked into a modeled CB<sub>1</sub> receptor. The receptor is represented by gray tube while interacting residues are represented by thin line. Ligand shown in cyan.

Figure 2.6 shows the phytocannabinoid, (*R,R*)- $\Delta^1$ -THC docked to the same modeled CB<sub>1</sub> receptor. The docking results were found to be similar to earlier findings.<sup>8</sup> There is a predicted hydrogen bond between the phenolic hydrogen of (*R,R*)- $\Delta^1$ -THC and residue K3.28 (192), containing an N-O distance of approximately 2.78 Å. Figure 2.7 then shows how the pentyl side-chains of the most stable conformers face opposing directions when docked to the receptor, while the ring part of the compounds interact with the residues, T3.33 (197), Y5.39 (275), W5.43 (279), and M6.55 (363).<sup>4</sup>

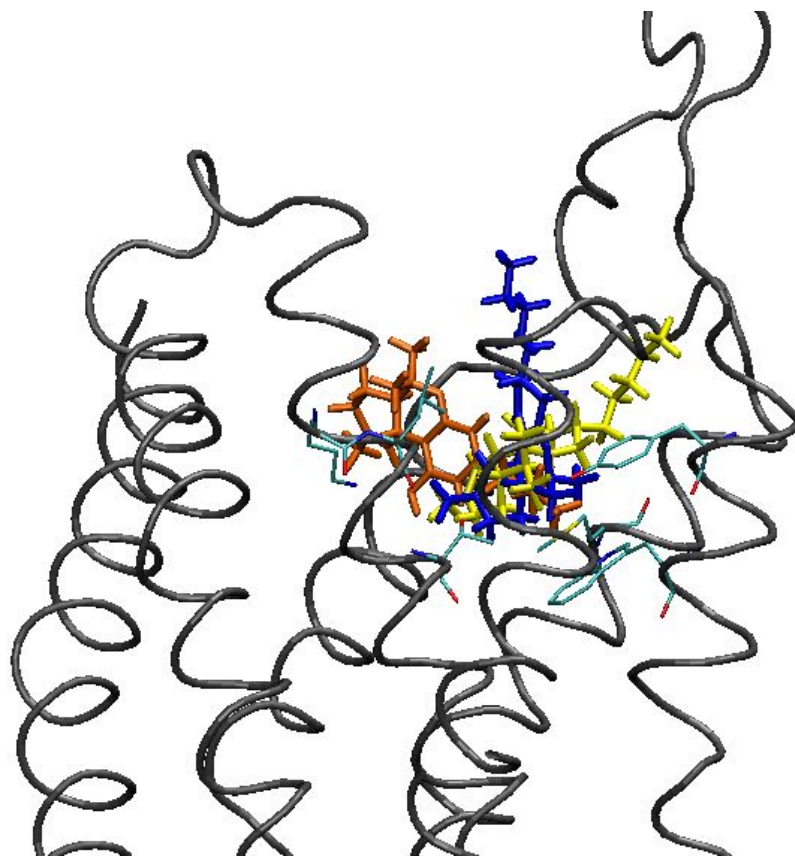


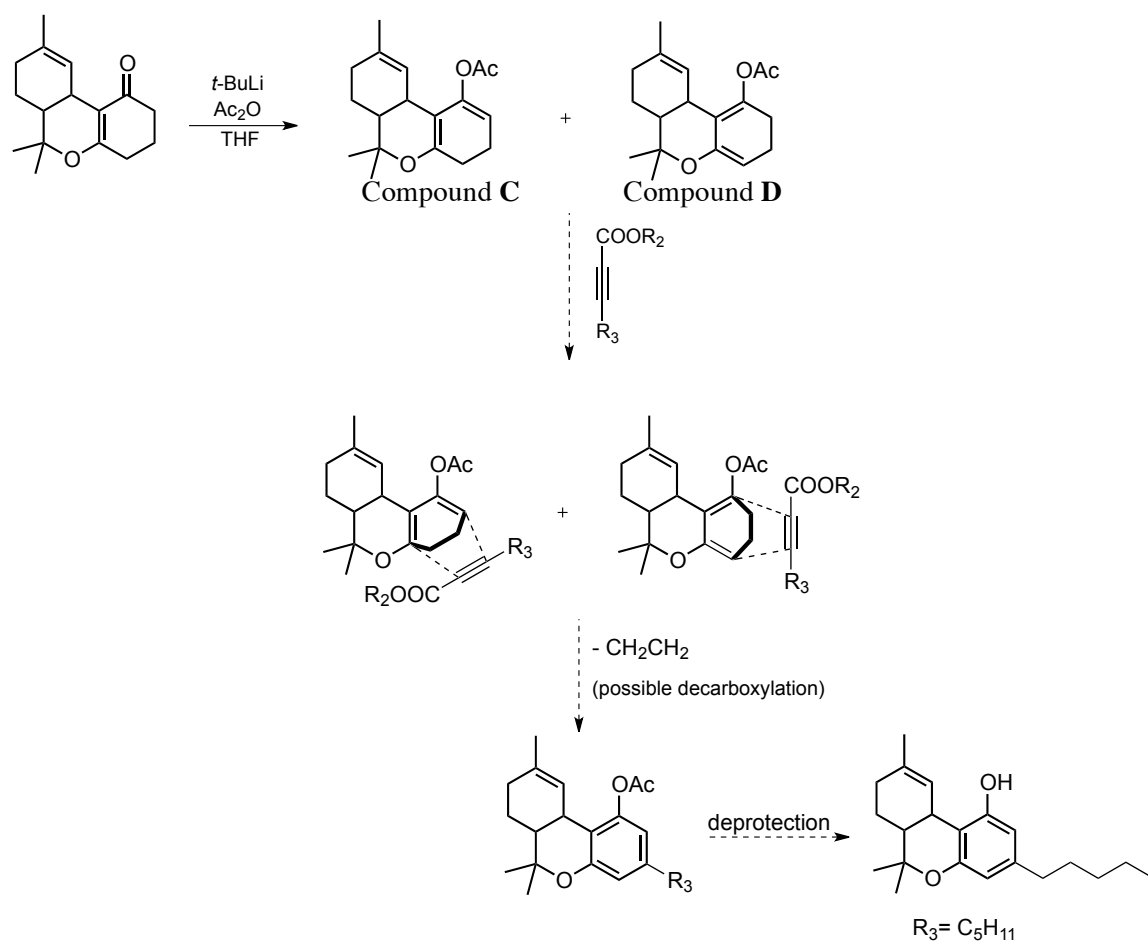
**Figure 2.7** *Trans*-(R,R)-THC<sub>an</sub> (blue), *cis*-(R,S)-THC<sub>an</sub> (yellow), and *trans*-(R,R)-THC (orange) docked to the modeled CB<sub>1</sub> receptor.

The *cis*-(R,S)-  $\Delta^1$ THC<sub>an</sub> and *cis*-(S,R)-  $\Delta^1$ -THC<sub>an</sub> isomers also showed strong interactions to the modeled CB<sub>1</sub> receptor with a  $\Delta E$  of approximately -33 kcal/mol.<sup>4</sup>

## 2.6 Aromatic Cannabinoid Analogues

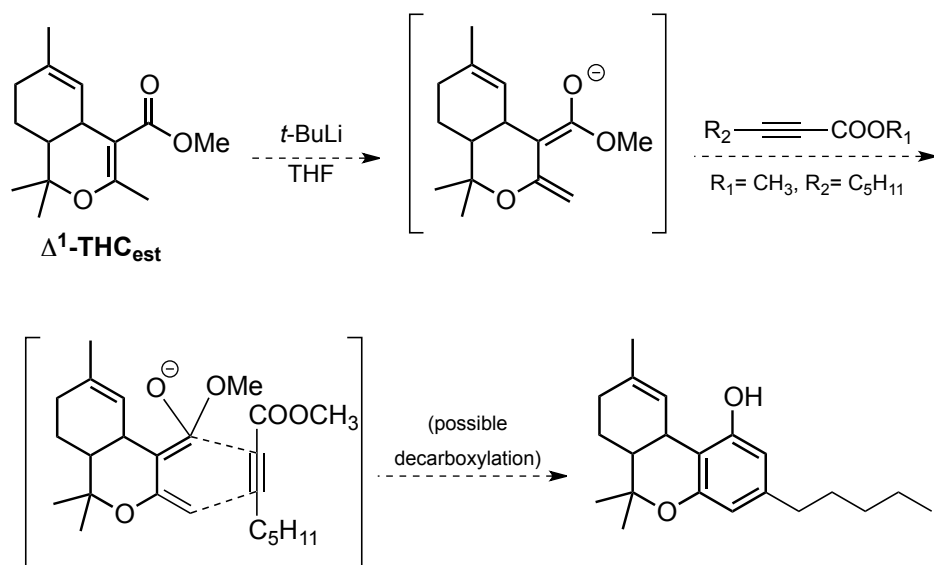
Despite the evidence showing that aromaticity was not essential for CB<sub>1</sub> receptor affinity, efforts were put into developing a facile synthesis toward aromatic cannabinoid analogues in order to expand the pool of available drug candidates. Initial studies focused on using THC<sub>an</sub> (R=H) as starting material and creating a diene that can undergo a Diels-

Alder reaction with various different acetylenes (varying at  $R_3$ ). A retro-Diels-Alder reaction would then cause elimination of ethylene. A possible decarboxylation, followed by deprotection of the hydroxyl group would yield an aromatic ring. Assuming commercially available methyl 2-octynoate ( $R_2 = \text{CH}_3$ ,  $R_3 = \text{C}_5\text{H}_{11}$ ) was used as the acetylene, the resulting product would be *rac*- $\Delta^1$ -THC. (Scheme 2.7).



**Scheme 2.7** Proposed synthetic route towards  $\Delta^1$ -THC.

Formation of the acetate-diene, compounds **C** and **D** (Scheme 2.7), with LDA or *t*-BuLi predominantly results in recovered starting material (THC<sub>an</sub>). Therefore the approach shown in Scheme 2.8 was taken to ensure the formation of one diene product (*cis/trans* isomers) and the opening of the ring would allow for quicker formation of the Diels-Alder adduct, not requiring the elimination of ethylene.

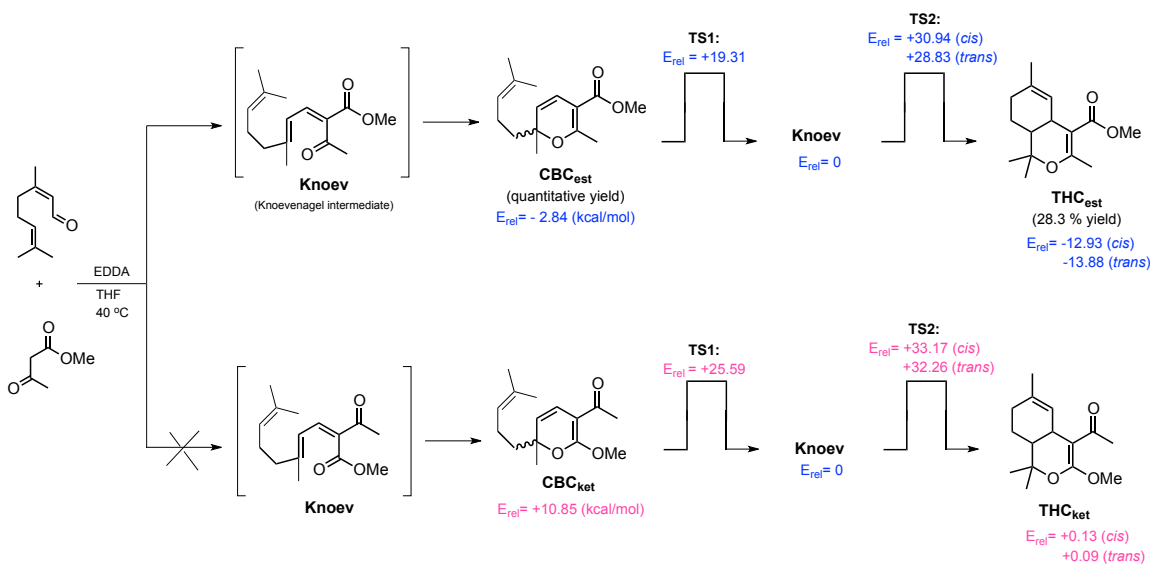


**Scheme 2.8** New synthetic plan towards  $\Delta^1$ -THC.

The THC<sub>ester</sub> was prepared in a somewhat similar fashion as THC<sub>an</sub> (Scheme 2.9), excluding the use of zinc bromide, which was found to inhibit the reaction. Even with the use of an asymmetric 1,3-dione, the product results exclusively in the desired CBC-ester analogue (CBC<sub>est</sub>). Spartan<sup>6</sup> calculations at the B3LYP 6-31G\* level of theory were performed on the products and transition states for both the ester and ketone products of CBC and THC (CBC<sub>est</sub>, CBC<sub>ket</sub>, THC<sub>est</sub>, and THC<sub>ket</sub>) and it was found that the reaction

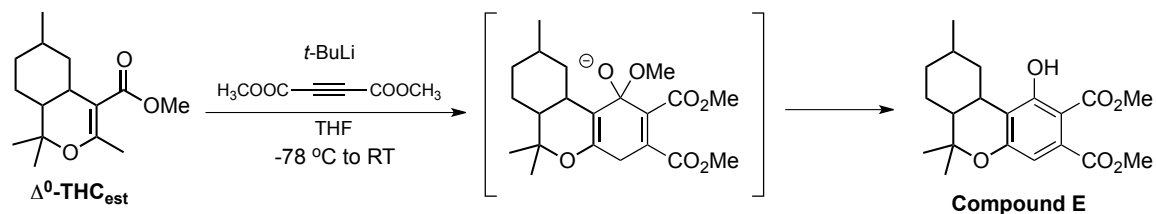


favors the formation of the ester products ( $\text{CBC}_{\text{est}}$  and  $\text{THC}_{\text{est}}$ ), which is consistent with experimental results (Scheme 2.9).



**Scheme 2.9** Synthesis of  $\text{THC}_{\text{est}}$  and Spartan calculation results.

Initial work on the synthesis involved the use of dimethyl acetylenedicarboxylate as the acetylene and the  $\Delta^0\text{-THC}_{\text{est}}$  to test out the Diels-Alder chemistry (Scheme 2.10). Previous synthetic methods to  $\Delta^0\text{-THC}_{\text{est}}$  have reported the THC-ester analogue (versus the ketone) as the major product, with only trace amounts of the ketone present.<sup>10</sup> Reaction with *t*-BuLi then resulted in the aromatic compound **E**. Recovered  $\Delta^0\text{-THC}_{\text{est}}$  is the major result of the reaction with only trace amounts of the target aromatic species obtained. While optimization is still required, the reaction showed the potential of this route to aromatic THC analogues and the delta-one version of  $\text{THC}_{\text{est}}$  can easily be obtained and used (Scheme 2.9) to yield  $\Delta^1\text{-THC}$  analogues as well.



**Scheme 2.10** Synthesis of aromatic analogue.

## 2.7 ALS Studies

In collaboration with Dr. Milan Fiala at UCLA's department of Medicine, some of the cannabinoid analogues were tested as pharmaceutical targets for amyotrophic lateral sclerosis (ALS). ALS is a neurodegenerative disease that affects the brain and spinal cord, having poor effective treatment.<sup>11,12</sup> And, as mentioned in the previous chapter, a link has already been found between ALS and cannabinoids, with THC showing some biological activity towards it.<sup>13</sup>

The tests were based on the compounds' inhibition of Interleukin-17, IL-17, (a cytokine) in macrophages of ALS patients.<sup>14</sup> IL-17 is known to have a role in inflammatory processes and a hypothesized role in ALS so inhibition or regulation of these proteins might be therapeutically beneficial. Therefore, targeting inhibition of IL-17 in ALS patients could lead to potential ALS therapy.

Figure **2.8** shows some of the results of this collaboration. One of our compounds,  $\text{CBC}_{\text{an}}$  (Scheme **2.3**), where  $\text{R} = \text{C}_5\text{H}_{11}$ , was tested for its potential inhibition of IL-17. This process entails using macrophages of ALS patients that are treated with stimulated superoxide dismutase 1 (SOD-1). Fig. **2.8a** is the negative control; therefore it is not treated with stimulated SOD-1. It is considered healthy as represented by the green coloring. The predominantly red coloring shown in Fig. **2.8b** is representative of a macrophage that is treated with stimulated SOD-1 and therefore the positive control. Fig **2.8c** then shows the results of the test compound. The macrophage was treated with SOD-1, followed by  $\text{CBC}_{\text{an}}$  ( $\text{R} = \text{C}_5\text{H}_{11}$ ). While there is some red coloring, the macrophage shows that it is primarily green. This would imply that the cannabinoid analogue was in fact found to partially inhibited IL-17.

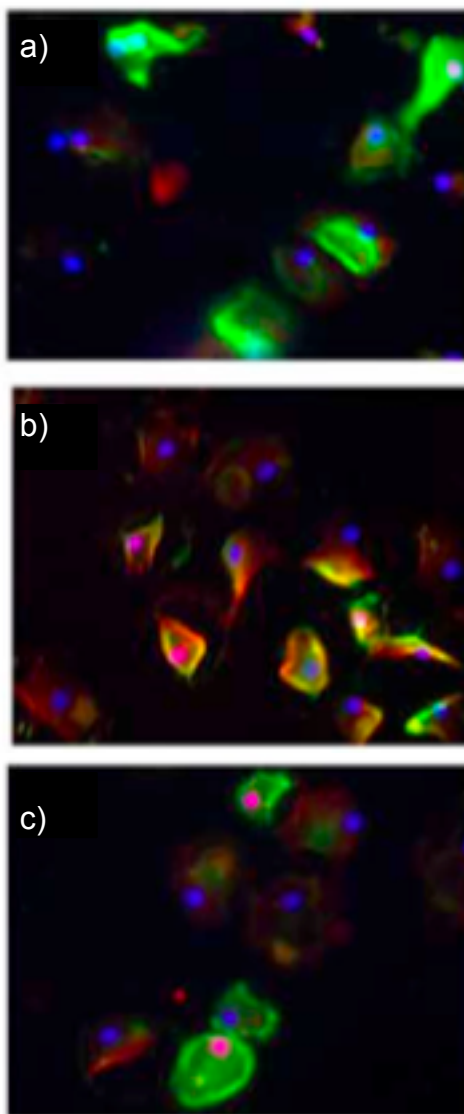


**Figure 2.8** ALS macrophages treated with stimulated superoxide dismutase 1 (SOD-1). **a)** negative control (not treated with stimulated SOD-1); **b)** positive control (treated with stimulated SOD-1); **c)** treated with SOD-1 then  $\text{CBC}_{\text{an}}$  ( $\text{R}=\text{C}_5\text{H}_{11}$ ).

## 2.8 Conclusion

The great therapeutic potential of cannabinoids and their analogues has increased the need to find more efficient methods towards these compounds. In an effort to design a

facile synthesis, we investigated the thermal isomerization of cannabinoid analogues, involving a tandem Knoevenagel-Diels-Alder cascade reaction. This allowed us to produce several cannabinoid analogues and by looking at *in silico* screening results, some have the potential to possess some therapeutic benefit. Biological screening showed that CBC<sub>an</sub> served as a partial inhibitor of IL-17 and therefore could be useful as ALS therapy. Our collaborative docking studies then led us to hypothesize that unnatural THC isomers might be the cause of marijuana withdrawal symptoms and showed us that these unnatural isomers have a similar CB<sub>1</sub> receptor affinity to the natural THC isomer.

## REFERENCES:

1. Hart, C.L.; Ward, A.S.; Haney, M.; Comer, S.D.; Foltin, R.W.; Fischman, M.W., *Psychopharmacology*, **2002**, 164, 407-415.
2. Kempfert, K.D.; Smith, R.M, *Phytochemistry*, **1977**, 1088-1089.
3. Tietze, L. F., *Chem. Rev.* **1996**, 96, 115–136.
4. Garcia, A.; Borchardt, D.; Chang, C.E.; Marsella, M.J. *J. Am. Chem. Soc.*, **2009**, 131, 16640-16641.
5. Malerich, J.P.; Maimone, T.J; Elliott, G.I., Trauner D. *J. Am. Chem. Soc.*, **2005**, 127, 6276-6283.
6. Spartan' 06; Ver. 1.1.0; Wavefunction Inc., 18401 Von Karman Avenue, Suite 370 Irvine, CA 92612, USA.
7. PyRx: Trott, O.; Olson, A.J., *J. Comput. Chem.* 2010, 31, 455-461.
8. CB<sub>1</sub> homology model provided by Drs. O. Salo-Ahen and A. Gonzalez.
9. Moreau, J.; Hubert, C.; Batany, J.; Toupet, L.; Roisnel, T.; Hurvois, J.P.; Renaud, J. L., *J. Org. Chem.* **2009**, 8963-8973.
10. Tietze, L. F.; Beifuss, U.; Ruther, M., *J. Org. Chem.* **1989**, 54, 3120-3129.
11. ALS Association. <  
<http://www.alsa.org/als/what.cfm?CFID=6918435&CFTOKEN=1ecadca021698a69--357EE929-188B-2E62-8061EBC64B924404>>
12. Raman, C.; McAllister, S.D.; Rizvi, G.; Patel, S.G.; Moore, D.H.; Abood, M.E., *ALS and other motor neuron disorders*, **2004**, 5, 33-39.
13. Picone, R.P.; Khanolkar, A. D.; Xu, W.; Ayotte, L. A.; Thakur, G. A.; Hurst, D. P.; Abood, M. E.; Reggio, P. H.; Fournier, D. J.; Makriyannis, A. *Mol. Pharmacol.* **2005**, 68, 1623-1635.
14. Aggarwal, S.; Gurney, A., *J. Leukocyte Biol.*, **2002**, 71, 1-8.

## **Chapter 3**

### **Molecular Docking: A CADD Approach for Known Targets**

### **3.1 Introduction**

Computer-aided drug design (CADD) covers a range of different techniques that predominantly incorporate use of known data as a means of establishing new leads or hits for the development of new drugs. It typically involves the use of some type of software that can allow the screening of multiple structures. The selected approach to drug design will typically depend on whether the target is known or not. This chapter will focus on the method most commonly used when the target protein is known.

### **3.2 Molecular Docking Overview**

The overall best approach to CADD involves molecular docking. It is a process that can save time and efforts by giving some insight into the potential biological activity of compounds without the necessity of their synthesis. It is computationally based and involves the binding of drug candidates to the actual protein that is known to trigger the therapeutic effects via that binding interaction. Figure **3.1** gives an idea of what would typically be displayed on a computer screen if working with a docking program. The first image is the ball and stick representation of the residues that make up the protein (Fig **3.1a**). This example uses 17-beta-hydroxysteroid-dehydrogenase as the protein and estradiol as the bound ligand (shown in cyan). The red dots around the protein illustrate water (Fig **3.1a**). Figure **3.1b** is then the ribbon representation of the same protein and makes the estradiol ligand easier to see (mint green).<sup>1</sup> The potential biological activity is determined by comparing its binding affinity to the targeted protein with that of a reference drug (a compound that is already known to be active towards that protein). Any



candidates that score well (by displaying the lowest energy binding affinity) pass on to the next phase of drug design, which includes their synthesis to allow for biological screening.

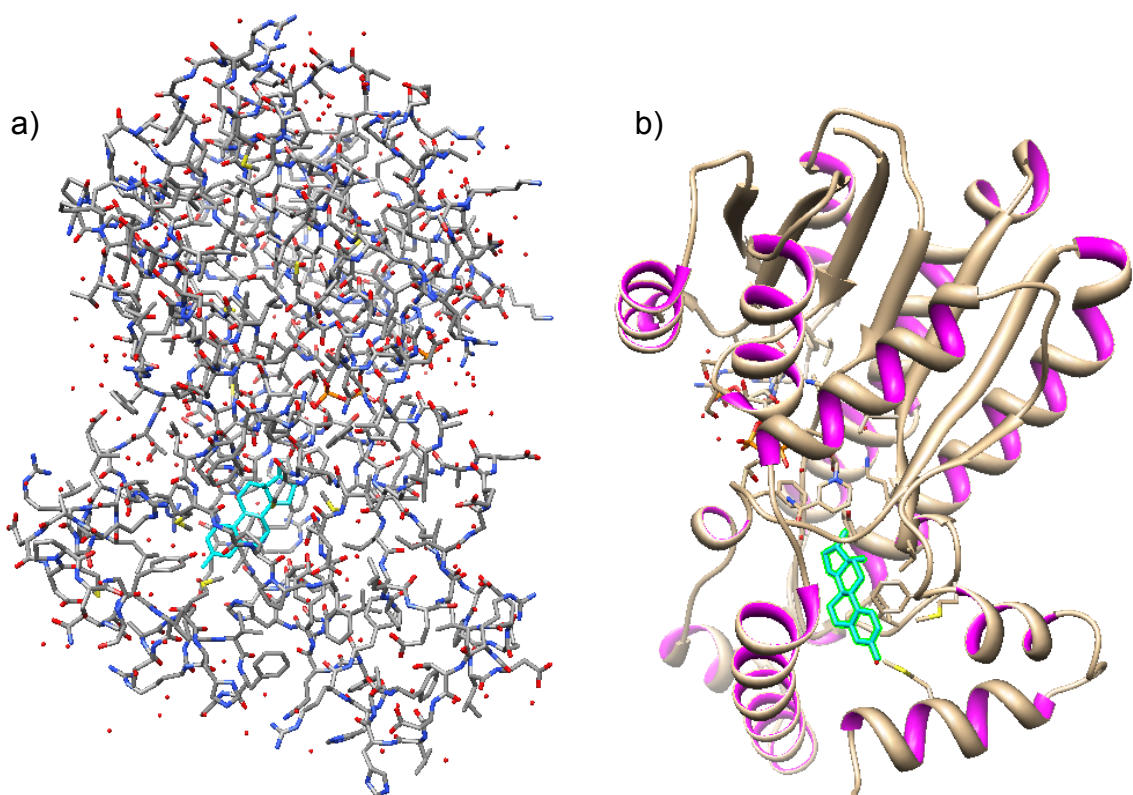


**Figure 3.1** a) Ball and stick representation of 17-beta-hydroxysteroid-dehydrogenase (PDB 1A27)<sup>1</sup> complexed with estradiol (cyan) b) ribbon representation of the same protein with estradiol (mint green).

The major advantage of molecular docking is the ability to screen a large library of compounds without physically obtaining the molecules required for biological assaying. Docking also gives structural insight into how the ligand binds to the protein with regards to its conformation and the residues it interacts with.<sup>2</sup>

One of the major restrictions to molecular docking however is that the protein target must be known and there must be an available X-ray crystal structure of the protein. Some of the other drawbacks are that docking studies do not give insight into the compounds toxicity, bioavailability, or other factors essential to its conversion into a drug; docking only gives information on how well the compound will bind to the protein.<sup>2</sup> Also, depending on the size of the compound library, the computational cost can be very high, so there might be a limit to how many compounds can actually be docked at a given time.<sup>2</sup>

### **3.3 The Search Algorithms**

Docking includes the generation of a series of different conformations or poses for each screened compound to aid in the search for the lowest binding energy conformer. A searching algorithm helps determine how a docking program will look for different ligand conformations within the binding site of a protein.<sup>2</sup> Some of the available algorithms are Monte Carlo, simulated annealing, tabu, and genetic algorithm.

Monte Carlo is based on randomly selecting a molecule's position in the binding site, which in this case refers to its conformation and orientation (fixed center of mass with rotations around the Cartesian axes) and it tests a large set of different ones.<sup>2</sup> Simulated annealing and tabu algorithms follow this similar process, however, they do not require as much time. This is due to the fact that Monte Carlo tends to repeat some of the positions it has already tested where as simulated annealing and the tabu algorithms keep

a record of which ones have already been tested and therefore avoid repetition. Simulated annealing then goes a step further and will spend more time testing positions that are close to positions that have already been shown to be low in energy.<sup>2</sup>

A genetic algorithm on the other hand is quite different and follows a “survival of the fittest” approach. It starts off by creating a large set of different positions at random. Then it will select the best positions (lowest energy) and generate more positions.<sup>2</sup> As it keeps generating newer positions, it will keep the best positions from each set every time.<sup>2</sup>

### **3.4 Scoring**

Every conformation that was generated for binding to the protein is assigned a score typically in the form of an energy value, which is a measure of binding affinity. That binding affinity or score decides which conformation is necessary for biological activity.

The different types of scoring functions are attempting to roughly calculate the binding free energy for the binding of the ligand to the receptor. An ideal scoring function would take into account all of the components in the following equation:<sup>3</sup>

$$\Delta G_{\text{binding}} = \Delta G_{\text{solvent}} + \Delta G_{\text{conf}} + \Delta G_{\text{interaction}} + \Delta G_{\text{rotation}} + \Delta G_{\text{t/r}} + \Delta G_{\text{vib}}$$

$\Delta G_{\text{solvent}}$  deals with the solvent effects,  $\Delta G_{\text{conf}}$  stands for any conformational changes,  $\Delta G_{\text{int}}$  accounts for any interactions between the protein and the ligand,  $\Delta G_{\text{rotation}}$  deals with the protein and ligand freezing internal rotations,  $\Delta G_{\text{tr}}$  takes into account the translational and rotational energy loss, and  $\Delta G_{\text{vib}}$  includes changes from vibrational modes.<sup>3</sup> Not all of these components are usually included in docking calculations, nor are they easy to figure out. They use simpler versions of these calculations. Despite the function that is used, it has been found that the combination of different scoring functions has delivered more favorable results than the application of just one type of function (consensus scoring).<sup>3</sup>

### **3.5 Docking Procedure**

#### **3.5.1 Preparing the Protein**

All docking procedures begin with an X-ray crystal structure of the protein. The most widely used source of proteins is the Protein Data Bank website.<sup>4</sup> Usually proteins that have a bound ligand in the active site are used. The ligand is eventually removed before docking, along with any water molecules. Hydrogen atoms are also added to the protein since they are usually not found on the protein. Then based on the selected force field, the protein is minimized.<sup>2</sup>

#### **3.5.2 The Ligand Set**

The ligands can be set up to dock automatically one after another or ligands from a particular database can be used. The automated process will usually involve the

generation of the different ligand conformations and poses. However, this can also be done separately before docking.<sup>2</sup>

### **3.5.3 The Binding Box**

Since protein structures are generally made up of multiple residues their large size can tend to increase computational time. One way around this is to set up a type of box around the binding site to focus computational efforts in that area, since residues faraway from the ligand do not seem to have an affect on the output score.<sup>2</sup> The box is usually set around the area of the bound ligand (if present).

### **3.5.4 The Results**

After the docking has been performed, more can be obtained from the output than just a binding score. The key benefit of using molecular docking is that one can observe the interactions between the ligand and the protein. Based on what residues are interacting with a specific part of the ligand, the important features of the ligand can be determined. The trivial parts of the structure can also be determined and the ligand can continue to be modified in this manner.<sup>2</sup> There are several available docking programs, some of which can be downloaded for free from the internet. DOCK was one of the first established docking programs, created by UCSF and incorporates a force field based scoring method. Developed by the Scripps Research Institute, AutoDock is another docking program that is available free of charge. It uses a linear regression analysis to establish its scoring

method. Some other programs include FlexX, FRED, Glide, GOLD, and Slide, but these are just a few examples from dozens of available docking programs.<sup>2</sup>

### **3.6 Error in CADD**

There is some error associated with CADD and the software devoted to it. Error in CADD can be found through the types of docking programs that are used and whether or not their accuracy is good enough to use the results.<sup>5</sup> Error can also result from the person running the program and their interpretation of the results. For example, when the QSAR (to be explained more thoroughly in the next chapter) technique was just developed, a lot of the computational methods were created out of pure curiosity, to test to see if something was possible and not so much because it was essential to CADD in terms of accuracy or efficiency.<sup>5</sup> The inability to comprehend basic principles in designing programs led to inaccurate interpretations of the results. If a better understanding of the methods that can be applied as well as the possible errors resulting from the calculations is obtained it will allow the opportunity for improvement and the realization of what is possible.<sup>5</sup>

Other errors can lie with the applied force fields. The force fields are considered approximations and these approximations affect the way torsion, dihedral, van der Waals, and electrostatic interactions are calculated.<sup>5</sup> Any changes made to the force field parameters can have an effect on the software and the time needed to run any calculations.<sup>5</sup>

However, the field of computational drug design is growing and there is great potential for its growth and improvement. Only through continued use of computational programs can specific weaknesses be identified and resolved. And if they cannot be resolved, how it can be avoided in order to reach the overall objective.<sup>5</sup> Error must be taken into account in order to establish CADD reliability to allow computational screening to continue in the drug discovery process.<sup>5</sup>

## REFERENCES:

1. PDB ID: 1A27  
Mazza, C. Human Type I 17Beta-Hydroxysteroid Dehydrogenase: Site Directed Mutagenesis and X-Ray Crystallography Structure-Function Analysis, Thesis, Universite Joseph Fourier, 1997.
2. Young, D.C., *Computational Drug Design: A Guide for Computational and Medicinal Chemists*, Wiley: New Jersey, 2009.
3. Leach, A.R., *Molecular Modelling: Principles and Applications*; 2<sup>nd</sup> Ed. Pearson Prentice Hall: England, 2001.
4. Protein Data Bank website <<http://www.rcsb.org/pdb/home/home.do>>
5. Stouch, T.R., *J Comput Aided Mol Des*, **2012**, 26 (1), 125-134.



## **Chapter 4**

### **CADD Approaches for Unknown Targets**

## **4.1 Introduction**

The previous section focused on molecular docking. As previously mentioned, an X-ray crystal structure of the target protein must have been deciphered in order to incorporate molecular docking in the drug design process. There are about 500,000 proteins in the human proteome and only 10,000 of these proteins possess an identified X-ray crystal structure.<sup>1</sup> Also, not only is there often not an available crystal structure, but usually the target protein(s) is not even known. The following sections will give a brief overview of current CADD programs and techniques that are used when the protein target is not available or known.

## **4.2 Predicting Intestinal Absorption: Lipinski's 'Rule of Five'**

One of the most widely used methods for filtering through a list of New Chemical Entities (NCEs) involves the application of Lipinski's 'Rule of Five'.<sup>2</sup> In fact, some of the methods to be discussed incorporate aspects of this method. By simply looking at the structure of a NCE, it can be determined whether it fits the likely criteria of a drug. In 1997, Lipinski and co-workers established a set of rules based on an analysis of 2245 drugs. If more than two of the following rules were violated, the NCE was likely going to have poor absorption. The necessary criteria for good absorption were i) a molecular weight less than 500 ii) less than 10 hydrogen bond acceptors (HBA) iii) less than five hydrogen bond donors (HBD) and iv) a calculated logP value less than five (for ClogP) or less than 4.15 (for MlogP).<sup>2,3</sup> Any oxygen and nitrogen atoms are considered HBAs. Any NH or OH groups are HBDs. The logP is the octanol/water partition coefficient and

assesses the lipophilicity of a compound. The ClogP is used synonymously with logP and is just one method of calculating the coefficient. The MlogP is a different way of calculating it that was established by Moriguchi and co-workers in 1992.<sup>3,4</sup>

### **4.3 Similarity and Substructure Searching**

Sometimes simple structural searches are performed on biologically active compounds. Substructure searches look for compounds that contain the same atoms and bonds that make up part of the active molecule.<sup>1</sup> For example, a search can be performed on molecules that integrate an indole within their structure. Similarity searching, on the other hand, helps find analogues of a particular compound. So instead of just searching for indoles, the search is expanded to quinolines (a bigger size ring system). These types of searches are rather easy to carry out and often just require drawing the part of the structure that is desired. For similarity searches, it can be decided how close or how far away from the structure the results should be.<sup>1</sup>

### **4.4 Pharmacophore models**

Molecules can also be searched based on pharmacophore. A pharmacophore includes the key parts of a drug and their placement that have been found necessary for protein binding or activity.<sup>5</sup> These type of searches allow for more chemical variability and can lead to what is called scaffold hopping; this involves altering lead structures to come up with an entirely new class of compounds that might turn out to be structurally different, but have similar affinity for the same receptor.<sup>1,6</sup> Not all molecules that were found to

have the same pharmacophore are necessarily that close in structure. Paclitaxel and Epothilone A (Fig. **4.1a**) are a great example of this. They do not look structurally similar, but their lowest energy conformers (as bound to the tubulin receptor) show similar pharmacophores when aligned against one another<sup>1,7,8,9</sup> (similarities are circled in yellow in Fig. **4.1b**<sup>10,11</sup>).

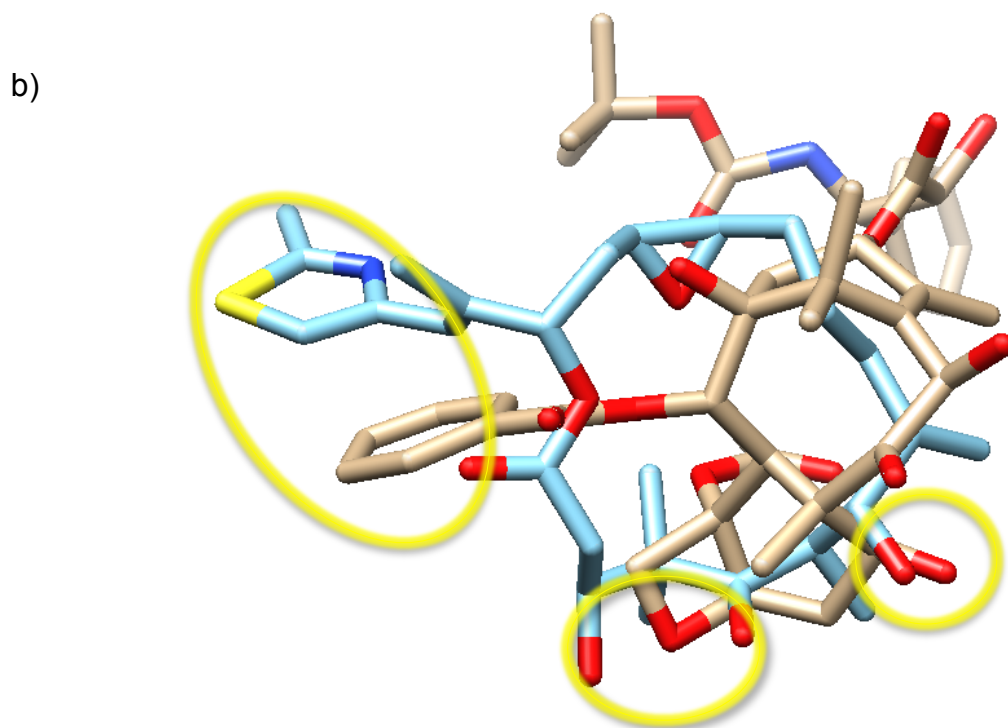
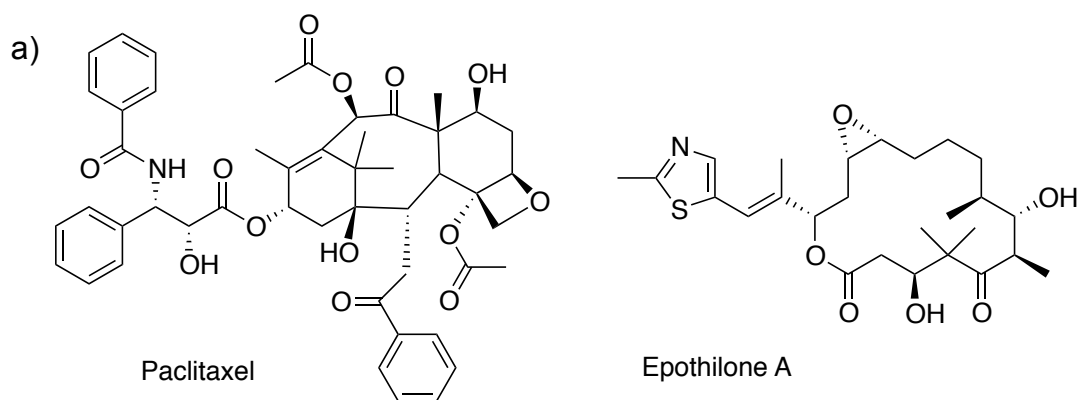


**Figure 4.1** a) Chemical structures of Paclitaxel and Epothilone A b) alignment of the lowest energy conformers of Paclitaxel (tan) and Epothilone A (cyan), as bound to tubulin receptors 1TUB<sup>8</sup> and 1TVK,<sup>9</sup> respectively (receptor omitted for clarity). The yellow circles show the similarities in pharmacophore (i.e., overlapping of aromatic or hydrophobic regions and hydrogen bond donors and acceptors).

Some of the key characteristics that can be included in a pharmacophore search are hydrogen bond donors and acceptors, aromaticity, hydrophobic regions, acidic or basic groups, and bulky groups that are involved in steric interactions.

Although this method is based on biologically active molecules, one of the disadvantages is that the lowest energy conformer for these molecules has to be known. Therefore, if the target protein is not known, this can be very difficult to determine.<sup>1</sup> It is also possible that there could be a key functional group present in all active compounds that might not be essential for binding. However, one-way around this is to use compounds that are not analogues of each other and do not have the same core structure.<sup>1</sup>

The first actual step to this process is to align the biologically active compounds, starting with the ones that are the most rigid in order to establish the pharmacophore model. Subsequent structures are then rotated and appropriately positioned to those structures to give the best alignment.<sup>1</sup> This can either be done manually or automatically through some software program, which overall can work rather well. MOE from the Chemical Computing Group, is one program that will allow manual manipulation.<sup>1</sup> Next, based on the established model, the compound searching can begin. The output is a ranking of the compounds that were found to best fit the model and is usually produced reasonably quickly.<sup>1</sup>

The pharmacophore model can also be established by using the active binding site of the protein and often works best this way since the actual interactions between the residues and molecule can be observed.<sup>1</sup>

#### **4.5 QSAR**

A common approach to computational drug design is the use of quantitative structure-activity relationships (QSAR). This method involves incorporating a mathematical formula to establish a relationship between a compound's biological activity and its physicochemical properties.<sup>5</sup> The molecular properties used in the equation are referred to as descriptors. A descriptor is a numerical value that details a specific part of a compound (e.g. molecular weight, log P value) and is not limited to the same set of descriptors every time this method is used.<sup>1,5</sup>

QSAR models generally work by establishing a training set of compounds with known biological activity. This “activity” is then going to be the desired value to predict for NCEs. The activity in the training set should cover a wide range of possible values. Every chosen parameter would then have at least 10 compounds in the set as part of the QSAR equation to avoid biasing the data.<sup>1,5</sup>

The compound descriptors for the test set are then calculated. This process should be relatively quick since computationally time-consuming descriptors are not usually chosen. Then the descriptors selection process begins. This includes choosing the one

with the highest correlation coefficient; Since QSAR models use equations that are mostly linear, taking into account the correlation coefficient tells how accurately the activity is being measured by the descriptors. In order to avoid descriptors that are too similar, the second descriptor that is chosen should not correlate too closely to the first selected descriptor, but should still have a high correlation with the activity. Figuring out the best fit from this data can then lead to the activity prediction of the test compounds.<sup>1,5</sup> QSAR models can also use nonlinear equations. However, some of these methods are considered to be trial-and-error since correlation coefficients cannot be used, and therefore descriptor selection becomes somewhat trickier.<sup>1</sup>

As previously mentioned, the types of descriptors that are chosen are usually computationally inexpensive, since computations of very large data sets can lead to an even bigger increase in computational cost. Among some of the different types of descriptors are constitutional, topological, electrostatic, geometrical, and quantum chemical.<sup>1</sup>

Constitutional descriptors can include properties like the molecular weight of a compound, the number of heteroatoms within a given structure, and the amount of rings encompassing it. These types of descriptors are usually used when molecule size changes with the resulting predicted activity value.<sup>1</sup> Topological descriptors are typically not directly related to the structure of the compound, but have been found to usually give the best predictions. These types of descriptors give details about the bonding arrangements



and can shed some light on a molecule's rigidity.<sup>1</sup> Electrostatic descriptors can give facts about the molecular charge distribution and includes properties like polarizability and topological polar surface area (TPSA). The TPSA is often used and gives information on the amount of polar groups compared to non-polar ones. The octanol-water partition coefficient (LogP) also falls into this category.<sup>1</sup> The geometrical descriptors can then give information about a compounds shape and size. A list of these types of descriptors can include molecule volume, moments of inertia, the molecular surface area, and other factors that can give information on a compounds height, length, and width.<sup>1</sup> Lastly, the quantum chemical descriptors give details about a compound's electronic structure. Some of these factors can include HOMO and LUMO energies, electron affinity, energy of protonation, and refractivity.<sup>1</sup>

The selected descriptors can manually be selected, but there are available software programs that can make the appropriate selections, which can often lead to more accurate predictions in a less amount of time. However, one of the disadvantages of using the available software is that the selected descriptors are chosen based solely on the inputted algorithms, with no scientific reasoning behind it. This leads to equations that are considered over-fitted, which work well for the training set, but give bad results for predicting test compounds.<sup>1</sup> Codessa by Semicem is one of the most widely used QSAR programs that allows for both manual and automatic descriptor selection. However, programs can also be obtained from Accelrys, the Chemical Computing Group, Schrödinger, and Tripos.<sup>1</sup>

The major disadvantage to using 2D-QSAR methods is that it does not take into account the 3D structure of the test drug or NCE. This makes it harder to see its potential interaction with the target receptor. One approach to dealing with this is to use 3D-QSAR methods.<sup>12</sup>

#### **4.6 Group Additivity**

Group additivity is also designed to run fast calculations of molecular properties for a set of compounds. This approach separates a molecule's parts into different groups, based on its backbone, its rings, and attached functional groups and each of these groups then contributes to a total added score. These methods have shown to be very good at anticipating toxicity.<sup>1</sup>

#### **4.7 Neural networks**

Neural networks use a training set of compounds to train a network that later goes on to predict the properties of a new molecule.<sup>1</sup> Neural networks are good for interpolation, which is making good predictions when the properties of the NCE lie within the range of the network or training set. However, accuracy decreases when it falls outside that specific area (extrapolation).<sup>1</sup>

#### **4.8 Hologram QSAR**

Hologram QSAR (HQSAR) deals with breaking down a molecule into its different fragments and arranging them into an array that is sort of like a fingerprint. The

fingerprint, represented in numerical values, is referred to as a hologram and is used to make the predictions.<sup>1</sup>

QSAR methods are usually utilized for predicting pharmacokinetic properties (e.g., permeability of the blood-brain barrier and passive intestinal absorption). Since more accurate methods exist, it is not really used for predicting whether or not a molecule will have biological activity.<sup>1</sup>

#### **4.9 3D-QSAR**

Three-dimensional QSAR is somewhat similar to 2D-QSAR, but incorporates properties in a grid type form around the molecule.<sup>1</sup> 3D-QSAR's main purpose is to try to figure out the properties of a target protein's binding site, without actually using or knowing the structure of the binding site, by incorporating the electrostatic and steric interactions around a biologically active molecule. This information is gathered for a training set of biologically active compounds and then a partial least squares (PLS) algorithm helps figure out what spatial arrangement of features might be present in the active site of the target protein that could interact with the training set.<sup>1</sup>

Much like the QSAR method, the 3D-QSAR process requires a training set (composed of at least 20 compounds) ranging in biological activity. Predictions tend to be more accurate when test compounds are somewhat structurally similar to those in the training

set. However, the training set should not be based on compounds that have the same framework.<sup>1</sup>

The next step is to establish a shape that is based on the biologically active conformer. However, since this information is not known at this stage of the process, the following three conditions help determine the likely conformer, a) every conformation that is used should have an energy close to that of the lowest energy conformer (within 10 kcal/mol) b) all conformations should have a similar shape and c) conformations should allow for easy alignment of pharmacophoric features. This can either be done automatically with a specific program or manually.<sup>1</sup>

Manual selection commences with all molecules in their ground state conformation. From this batch, the most rigid molecules are overlaid to establish a template based on shape and pharmacophore. The lowest energy conformers for similar molecules can then be aligned to this template, with non-similar compound conformations being modified to best fit the template. Then, based on the key features of the template, the best field parameters must be chosen. While the steric and electrostatic fields are normally included, other options can be based on hydrogen bonding, molecular lipophilic potential, and desolvation.<sup>1,5</sup>

The lowest energy conformer of each compound is then fit into a lattice, positioned to allow alignment of all compounds based on the pharmacophore. The steric and

electrostatic fields around the molecule are then measured by using a probe atom, located at each grid point. The probe atom can be a proton or  $sp^3$  hybridized carbocation. It then calculates the interactions amidst itself and the compound. The energy derived at each grid point can then be coupled using contour lines to figure out the shape (sterics) and positive and negative regions (electrostatics) of the compound.<sup>1,5</sup> Then, as briefly mentioned above, a PLS algorithm is used to help establish the best fit and select the most integral components. Then a simple equation based on the resulting data allows for predictions of biological activity by showing whether or not there is a relation between steric or electronic effects of the molecules and biological activity.<sup>1,5</sup> Figure 4.2 shows a brief schematic summarizing this entire process.

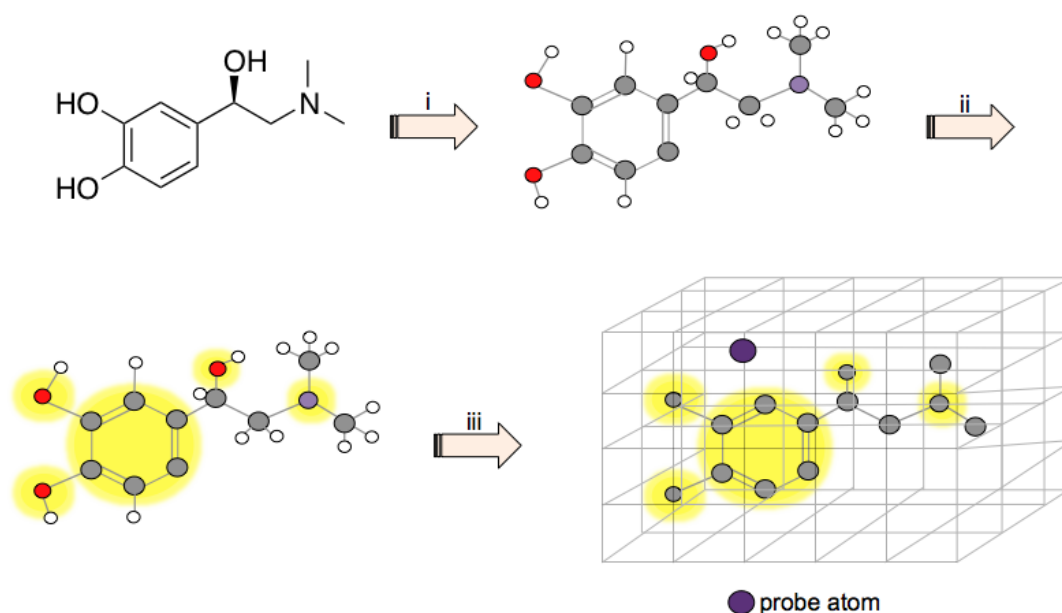


**Figure 4.2** 3D-QSAR process: i) starting with a training set ii) the lowest energy conformer is determined iii) which then establishes the pharmacophore iv) that is placed in a lattice to determine the interactions via a probe atom.

The most widely known software for performing 3D-QSAR methods is CoMFA (Comparative Molecular Field Analysis) from Tripos. Also from Tripos is Comparative Molecular Shape Indices Analysis (CoMSIA). It differs from CoMFA in that it is more selective in its activity predictions. Therefore the list of drugs predicted to be biologically active might be shorter, but its drawback is that it might not catch all biologically active compounds.<sup>1</sup>

3D-QSAR techniques have been found to be the most accurate of all ligand-based approaches.<sup>1</sup>

## REFERENCES:

1. Young, D.C., *Computational Drug Design: A Guide for Computational and Medicinal Chemists*, Wiley: New Jersey, 2009.
2. Lipinski, C.A.; Lombardo, F.; Dominy, B.W.; Feeney, P.J., *Advanced Drug Delivery Reviews*, **1997**, 23, 3-25.
3. Clark, D.E.; Pickett, S., *Drug Discovery Today*, **2000**, 5 (2), 49-58.
4. Moriguchi, I.; Hirono, S.; Liu, Q.; Matsushita, Y., *Chem Pharm Bull*, **1992**, 40, 127-130.
5. Patrick, G., *Medicinal Chemistry Instant Notes*, BIOS: Oxford, 2001.
6. Böhm, H.J.; Flohr, A.; Stahl, M., *Drug Discovery Today: Technologies. Lead Optimization*, **2004**, 1 (3), 217-224.
7. Giannakakou, P.; Gussio, R.; Nogales, E.; Downing, K.H.; Zaharevitz, D.; Bollbuck, B.; Poy, G.; Sackett, D.; Nicolaou, K.C; and Fojo, T., *Proc Natl Acad Sci* **2000**, 97 (6), 2904-2909.
8. PDB ID: 1TUB:  
Nogales, E.; Wolf, S.G.; Downing, K.H., *Nature*, **1998**, 391, 199-203.
9. PDB ID: 1TVK  
Nettles, J.H.; Li, H.; Cornett, B.; Krahn, J.M.; Snyder, J.P.; Downing, K.H., *Science*, **2004**, 305, 866-869.
10. Molecular graphics and alignment were performed with the UCSF Chimera package. Chimera is developed by the Resource for Biocomputing, Visualization, and Informatics at the University of California, San Francisco, with support from the National Institutes of Health (National Center for Research Resources grant 2P41RR001081, National Institute of General Medical Sciences grant 9P41GM103311).
11. Pettersen, E.F.; Goddard, T.D.; Huang, C.C.; Couch, G.S.; Greenblatt, D.M.; Meng, E.C.; Ferrin, T.E., *J Comput Chem*, **2004**, 25(13), 1605-1612.
12. Loew, G.H.; Villar, H.O.; Alkorta, I., *Pharmaceutical Research*, **1993**, 10, 475-486.

## **Chapter 5**

### **A New Approach to Computational Drug Design and Drug Rediscovery**



## 5.1 Introduction

It takes approximately \$800 million over about 15 years to introduce just one drug into market, with only 20-30 drugs receiving FDA approval each year.<sup>1</sup> Based on these results, it seems logical to look into existing drugs, where time and efforts have already been devoted as well as some biological testing performed. This alone can reduce cost by 40% since some of the biological assessments can be excluded as pharmacokinetic and toxicological profiles have already been established.<sup>1</sup> Drug rediscovery also decreases the amount of time necessary to attain next-generation lead compounds by eliminating the synthesis part of conventional drug discovery. Also, the rediscovery process has already been found to be effective as there are several drugs currently undergoing clinical and animal testing for an alternate use. Table **5.1** lists some of these drugs.<sup>1-11</sup> Therefore, it is worth designing a technique devoted to drug rediscovery. We have proposed an *in silico* approach to drug rediscovery that makes use of the binding affinity of non-target receptors (UBANTR) as a way of establishing new purposes for existing drugs. This approach can also be used to determine the potential indication of new chemical entities (NCEs). Discussion will focus on repurposing efforts, but hopefully it will be evident how this approach can be used in a similar fashion for NCEs.

**Table 5.1** Drugs Undergoing Testing for New Uses.<sup>1-11</sup>

<b>Drug</b>	<b>Current Use</b>	<b>New Use</b>
Amphotericin	Antifungal	Leishmaniasis
Ceftriaxone	Antibiotic	Amyotrophic Lateral Sclerosis
Dapsone	Leprosy	Malaria
Eflornithine	Cancer	African trypanosomes
Fosmidomycin	Urinary tract infections	Antimalarial
Miltefosine	Cancer	Visceral leishmania
Thalidomide	Sedative	Cancer

## **5.2 The UBANTR Approach**

The UBANTR approach's only requirement is the structures for a library of drug-like compounds to predict the indication class. The major advantage of this technique is that an X-ray crystal structure of the target protein is not required nor is prior knowledge of the protein(s). This is extremely valuable as one of the major disadvantages to the molecular docking approach to CADD is this requirement. And, as stated in the previous chapter, molecular docking is the preferred method to CADD.

This new approach only requires a three-dimensional coordinate file for each drug in the library. The actual docking to different receptors gives insight into a compound's actual behavior. Therefore, if the ligands are bound to other proteins, we should be able to derive certain information that allows us to see how the ligands interact, regardless of the fact that the target protein is not used. The gathering of this information should produce

enough data to analyze the potential biological activity of the screened compounds. By obtaining the binding affinity to a random set of proteins, specific “bits” of information can be derived and used to classify drugs by their major indication and give insights into potential new uses when they are groups with drugs of a different indication. Figure **5.1** explains how this process works. When a drug is docked to each receptor it produces a piece of a bar code or fingerprint. Once it has been docked to all 15 receptors, each drug is labeled with a very unique fingerprint. Each drug in the library is then grouped to other drugs that are found to have a similar fingerprint.



**Figure 5.1** Docking FDA-approved library to receptors produces unique fingerprint.

The concept of this approach is somewhat similar to the game “20 questions,” which is based on Shannon’s Theory.<sup>12</sup> Entropy is measured to be the amount of uncertainty about an object or event and information is then determined to be the degree of association between two systems, for example, between a ligand and receptor. Each of these interactions is a piece or “bit” of information that gives us insight into the properties of

the ligand.<sup>12</sup> Every question (or in this case, receptor) can help determine a bit of information, with most objects (drug activity) being identified (by indication) with a maximum of 20 questions. In our case, since we have 15 receptors, it would be 15 questions.

### **5.3 The Process**

A SMILES file containing information for each 487 FDA-approved drugs in the library was prepared. The stereochemistry for all compounds was specified and if a drug is found in its racemic form, both isomers were included. The SMILES file was then run through Omega (Open Eye Software)<sup>13</sup> to establish conformers of each drug, with the maximum amount of conformers generated set to 100. Then the file was run through Spartan '08 to add partial charges to the structures.<sup>14</sup>

X-ray crystal structures were obtained from the Protein Data Bank. The only requirement for the receptors was that the X-ray crystal structures must contain bound ligands ranging in volume similar to that of the drug library. The PDB files of 15 receptors were then run through FRED Receptor (Open Eye Software)<sup>15</sup> for optimization. The binding site was automatically selected based on the bound ligand.

All ligands were then docked to all 15 receptors by a batch process using FRED (Open Eye Software).<sup>16</sup> Every single conformer that was generated for each drug was docked. Then approximately 700,000 structures were examined to determine the lowest binding

energy conformer for the 487 drugs, which were then carried over to the data processing stage. Besides this, all default parameters were used, including the chemgauss3 scoring method, for all docking calculations. This produced 15 attributes for every FDA-approved drug. The volume of each 487 drugs was also included as a 16<sup>th</sup> attribute.

Once the binding affinities of the lowest energy conformers for each drug were selected, the data was normalized using values from 1 to 100. This data was then inputted into Orange<sup>17</sup>, a data mining and machine learning software, discretized, and applied a hierarchical clustering algorithm to group all FDA-approved drugs based on the binding affinity. Figure 5.2 shows a typical output from Orange.

From the 487 drugs, 80 were considered to be outliers based on a Euclidean distance metrics, resulting in only 407 drugs included in the hierarchical cluster.

## **5.4 Results and Discussion**

In an effort to stress the effectiveness of this method, focus is placed on certain sections of the data, instead of an analysis of all 407 drugs. Although it should be noted that the size and drug content of the library is significant and has an effect on the overall hierarchical clustering.

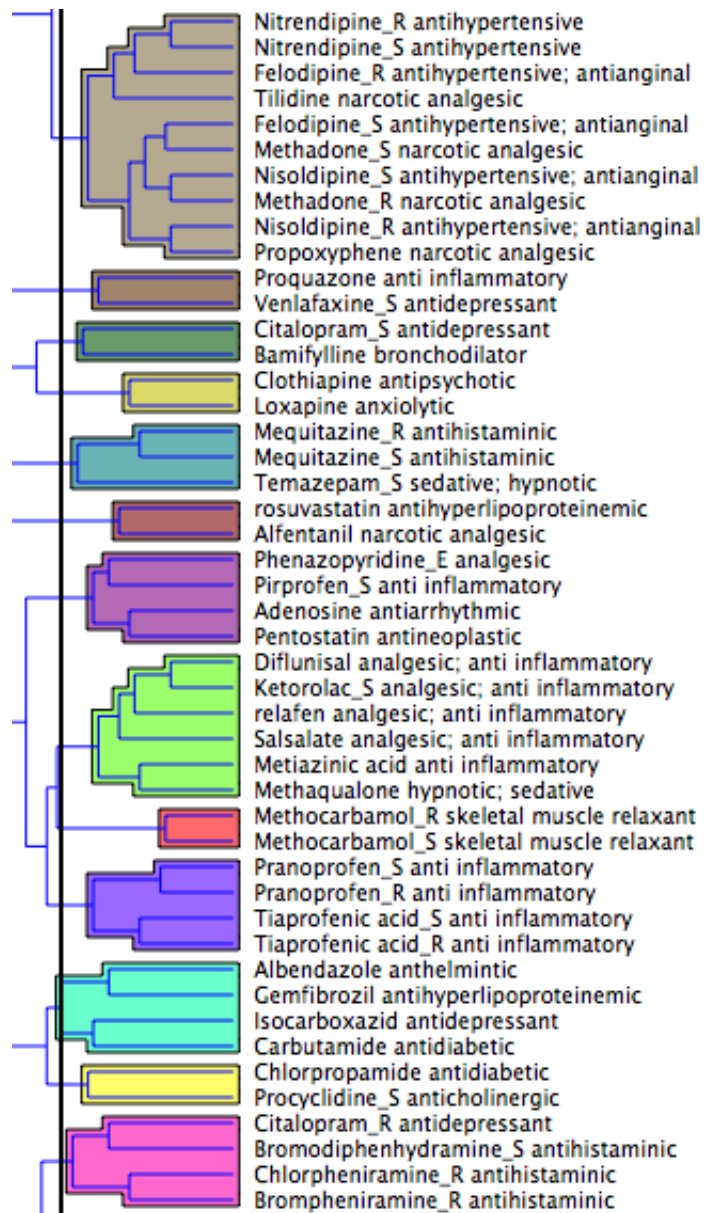
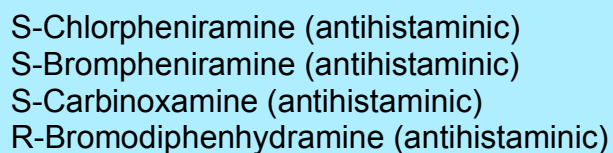


**Figure 5.2** Hierarchical clustering produced from Orange.<sup>17</sup>

Figure 5.2 is just a small representation of the 407 drugs. The drugs cluster into groups based on their binding similarity across all 15 non-target receptors. One of these clusters

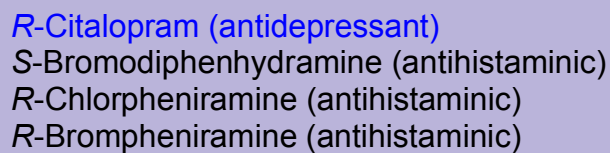
or groupings is found in Figure 5.3, which shows a clustered group of anti-histaminic drugs. Ideally what we are looking for are drugs to group or cluster together based on their indication class. Figure 5.3 is showing an example of this grouping.



S-Chlorpheniramine (antihistaminic)  
S-Brompheniramine (antihistaminic)  
S-Carbinoxamine (antihistaminic)  
R-Bromodiphenhydramine (antihistaminic)

**Figure 5.3** Clustered group of anti-histaminic drugs.

Figure 5.4 shows a drug cluster where not every drug that was shown to group together possesses the same indication. There are three anti-histaminic drugs and one anti-depressant. Based on the UBANTR approach, the first level of analysis includes looking for direct indication matches. The second level of analysis involves a deeper look into the connection between matching drugs.



R-Citalopram (antidepressant)  
S-Bromodiphenhydramine (antihistaminic)  
R-Chlorpheniramine (antihistaminic)  
R-Brompheniramine (antihistaminic)

**Figure 5.4** Clustered group of anti-histaminic drugs with one antidepressant.

This deeper connection can include secondary indications or alternate drug purposes, as well as any possible side effects. One method of investigating this deeper connection involves using STITCH.<sup>18</sup> STITCH will show a given interaction between chemicals and proteins by searching experiments, databases, and the literature.<sup>18</sup> It is important to note



that in our case, STITCH is used as a complimentary analysis, it is not complete, and it is not predictive. Inputting the drugs found in Figure 5.4 into the STITCH program will produce the diagram shown in Figure 5.5.<sup>18</sup>

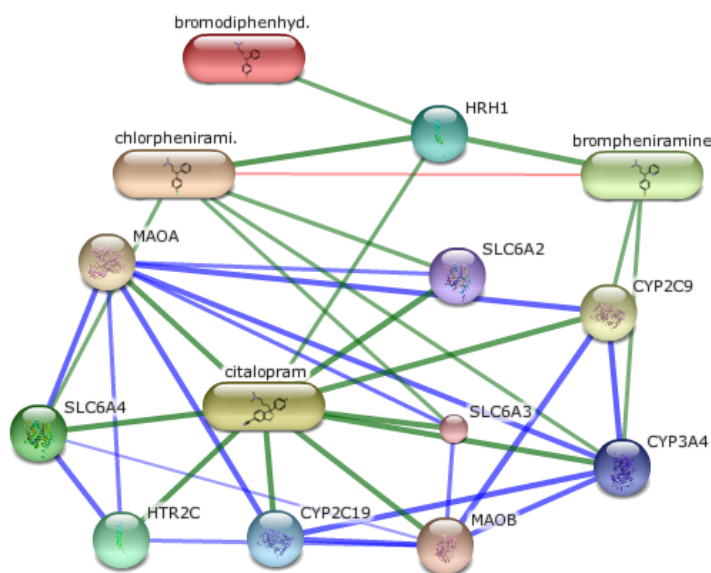


**Figure 5.5** STITCH output for clustered drugs from Figure 5.4<sup>18</sup>

Looking at the STITCH output, bromodiphenhydramine, brompheniramine and chlorpheniramine (all antihistamines) are linked to the HRH1 receptor, which is the histamine receptor. However, citalopram, the antidepressant, also shows a connection to the same histamine receptor. Therefore, the UBANTR approach is implying that there is a similarity between these four drugs and STITCH showed that the connection between all four of these drugs does exist.

Figure 5.6 lists another drug cluster example. The drugs are divided into two major indications, antihypertensive drugs and narcotic analgesics. A connection between both of these indications was not discovered through STITCH. However, this should not imply that a connection does not exist. In fact, this is one of the major objectives to the UBANTR approach. It is stating that there is a similarity amongst these drugs, which could lead to repurposing.

*R*-Nitrendipine (antihypertensive)  
*S*-Nitrendipine (antihypertensive)  
*R*-Felodipine (antihypertensive; antianginal)  
*S*-Felodipine (antihypertensive; antianginal)  
*S*-Nisoldipine (antihypertensive; antianginal)  
*R*-Nisoldipine (antihypertensive; antianginal)  
Tilidine (narcotic analgesic)  
*S*-Methadone (narcotic analgesic)  
*R*-Methadone (narcotic analgesic)  
Propoxyphene (narcotic analgesic)

**Figure 5.6** Drug cluster dividing into two major indications.

Drug repurposing involves taking existing drugs and discovering new uses for them (drug re-discovery). In this instance, we are implying that any of the antihypertensive drugs listed in Figure 5.6 should be screened as potential analgesics and/or the narcotic analgesics should be tested as antihypertensive drugs. The UBANTR approach is showing a similarity between all of these drugs, this is implying that they might have similar indications or some other potential connection, for example in the form of side-effects. This approach should be used as a starting point of where we can begin testing

particular drugs for other indications instead of randomly testing them for any available indication.

Two more clustered examples are shown in (Figure 5.7). The orange cluster is showing a group of diuretic; antihypertensive drugs clustered with one anticonvulsant drug. Again, the UBANTR approach is implying that Sulthiame, the anticonvulsant, might have biological properties as a diuretic; antihypertensive and/or any of the diuretic; antihypertensive drugs might also serve as an anticonvulsant drug. We are implying that testing for repurposing of these drugs should begin with the other matching indication. The UBANTR approach is showing a similarity, which should justify this screening. Despite the fact that a connection is not found through STITCH, does not imply that it does not exist; it just might not be known.

S-Trichlormethiazide (diuretic; antihypertensive)  
R-Trichlormethiazide (diuretic; antihypertensive)  
Sulthiame (anticonvulsant)  
S-Methyclothiazide (diuretic; antihypertensive)  
R-Methyclothiazide (diuretic; antihypertensive)

Diflunisal (analgesic; anti inflammatory)  
S-Ketorolac\_S (analgesic; anti inflammatory)  
relafen (analgesic; anti inflammatory)  
Salsalate (analgesic; anti inflammatory)  
Metiazinic acid (anti inflammatory)  
Methaqualone (sedative; hypnotic)

**Figure 5.7** Two different drug clusters.

The same reasoning can be applied to the second grouping in Figure 5.7. It shows predominantly analgesic; anti-inflammatory drugs with one sedative; hypnotic. There is an implied similarity base on the UBANTR approach and any repurposing efforts should begin with these matching indications.

In one more example (Figure 5.8), we see an anti-histaminic drug, triprolidine, amid anti-depressant drugs. In this example, a connection between amitriptyline, nortriptyline, doxepin, and triprolidine is known and can be seen in the STITCH output (Figure 5.8).

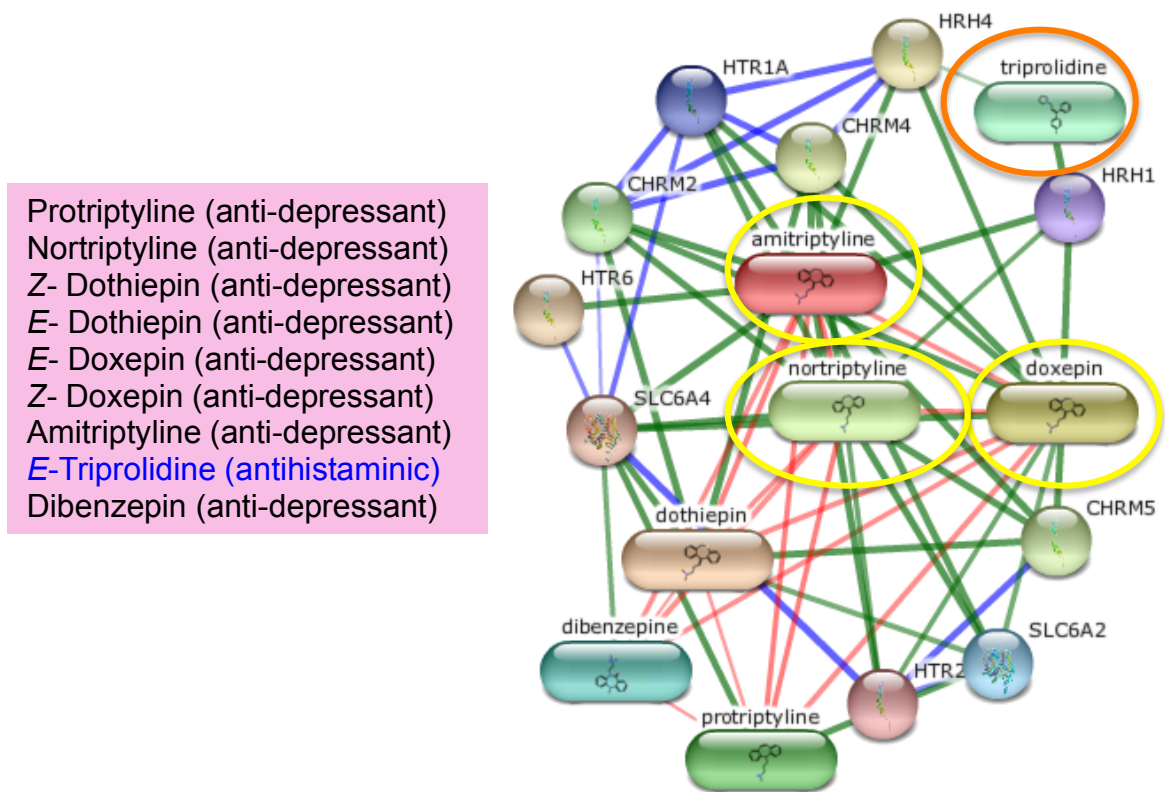


Figure 5.8 Drug cluster with its STITCH output.<sup>18</sup>

All four drugs are linked by the HRH1 (histamine) receptor and the three anti-depressant drugs are actually known to possess anti-histaminic effects.<sup>18</sup> This last cluster example is showing that a correlation does in fact exist for drugs that were determined to have similar properties by the UBANTR approach.

By looking at the previous clusters (Figures 5.3 to 5.7), it can be noticed that not all drugs of the same indication will always group together. For example, not all anti-histaminic drugs will appear within the same cluster or not all anti-hypertensive drugs will be grouped together. This has to do with the fact that not all drugs of the same indication will operate by the same biological pathway.

To analyze this further, focus was placed on antidepressants. The UBANTR drug library contains 25 anti-depressant drugs (not including isomers) that can be separated into 7 different types. For two of those types, only one drug is included in the library that follows that particular mechanism. Three other types each contain two drugs that follow that particular mechanism. The two major types of anti-depressants, selective serotonin reuptake inhibitors (SSRIs) and tricyclic antidepressants (TCAs), each consist of four and 13 drugs, respectively. Out of the four SSRIs, two of them were found to group together, fluoxetine and luvox (Fig. 5.9) and out of the 13 TCAs, 9 were found to group together in two different clusters. Six of them group together in the first cluster and three in the second (Fig. 5.9), which could imply that even among the TCAs, the drugs operate through two different methods.

No two antidepressants from different classes or types were found to group together; Groupings were only observed between their own types. Meaning, there were no SSRIs and TCAs (or any other types) found within the same cluster.

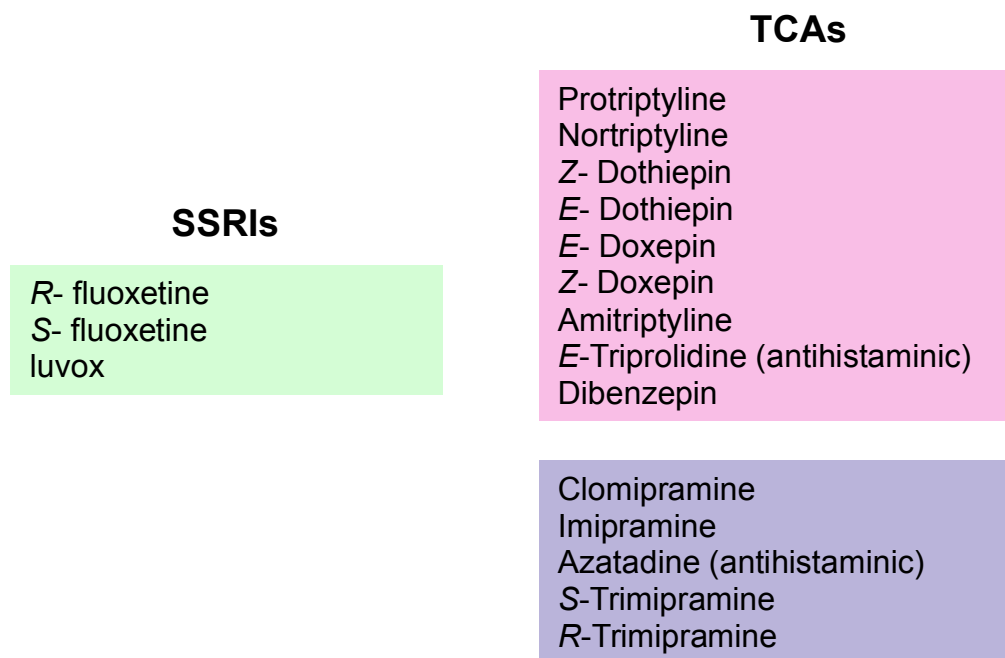


**Figure 5.9** Orange outputs for clustered SSRIs and TCA. Unless otherwise specified, all drugs are anti-depressants.

Taking a closer look at the ligand-protein interactions, focus will be place on the SSRI cluster, consisting of both isomers of fluoxetine (Fig. 5.10a) and luvox (Fig. 5.10b). Figure 5.11a shows *R*-fluoxetine bound into one of the 15 random receptors. Through this depiction, the interaction between the ligand and neighboring residues can be determined. Figure 5.11b then shows all clustered SSRIs aligned within the same random

protein. From this alignment it can be seen that the aromatic- $\text{CF}_3$  part of the molecule for each drug in this cluster have the same interactions with the same residues. Their similarity is apparent and helps explain why the three compounds were clustered together.

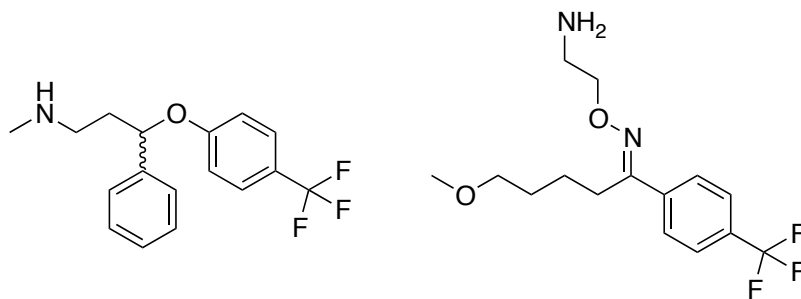


**Figure 5.10** a) fluoxetine b) luvox.

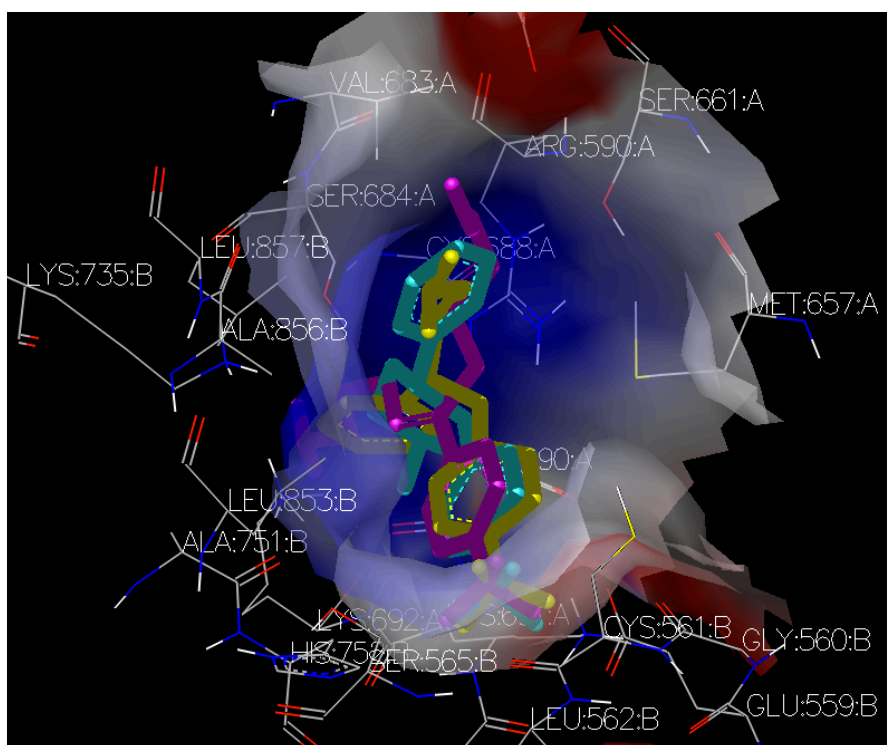
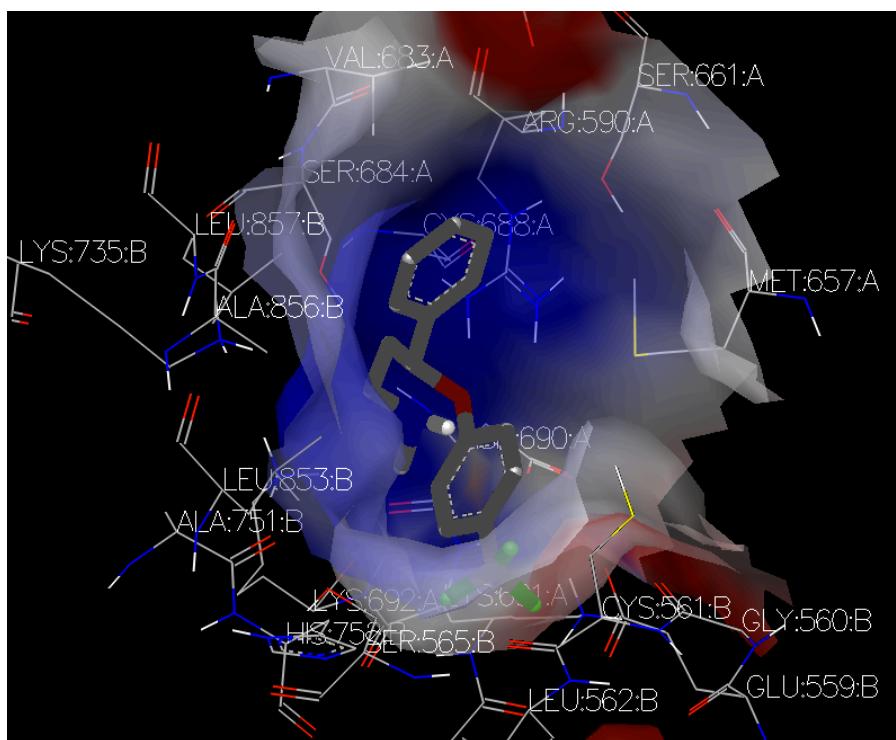


**Figure 5.11** a) *R*-fluoxetine bound into one of the 15 receptors. b) all SSRIs: cyan: (*R*)-fluoxetine (cyan), yellow: (*S*)- fluoxetine magenta (yellow), and luvox (magenta) bound into the same random receptor.<sup>19</sup>



This similarity is emphasized further through the depiction in Figure 5.12. This figure shows the alignment for the binding conformers of the same three compounds, for most of the 15 receptors. Looking through the sets of different overlaid structures, we can see how the structures align better for some of the proteins than for others. Therefore the UBANTR approach is helping to find drugs with a similar footprint across all 15 non-specific receptors.

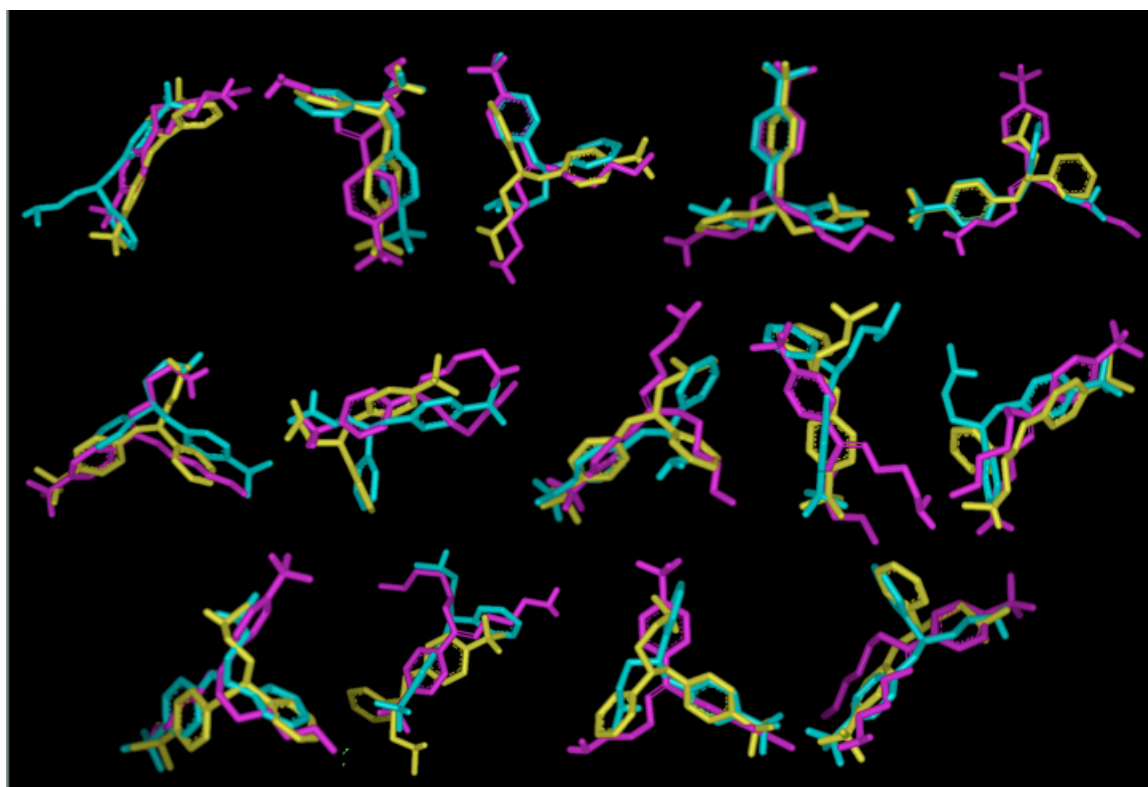


**Figure 5.12** Representation of lowest binding conformers for all clustered SSRIs to most of the 15 random receptors.<sup>19</sup>

A control was performed to help prove that there was no statistical bias with the UBANTR approach. Since the original data used for the UBANTR approach was normalized between values of one and 100, the control consisted of randomly generating numbers also between one and 100. Table 5.2 compares the data that was inputted into Orange for *S*-trimipramine in the UBANTR approach versus the control and shows the great difference in both data sets. Figure 5.13 then shows the results of this control test. The different clusters are represented by the alternating colors and as expected, it is evident that the outputted groupings are more random than the results produced through the UBANTR approach. The first four clusters of the control do not produce any drugs with the same indication. In the last cluster, there does appear to be three anti-depressant drugs that have been grouped together. However, paroxetine is an SSRI, trimipramine is a TCA, and nomifensine functions through a third differing pathway. Therefore, despite the fact that it does group drugs of the same indication, it does not distinguish between their biological pathways; a fact that differs greatly from the UBANTR approach.

**Table 5.2** Inputted data for trimipramine using the UBANTR (U) approach versus the control (C).

	<b>R<sub>1</sub></b>	<b>R<sub>2</sub></b>	<b>R<sub>3</sub></b>	<b>R<sub>4</sub></b>	<b>R<sub>5</sub></b>	<b>R<sub>6</sub></b>	<b>R<sub>7</sub></b>	<b>R<sub>8</sub></b>	<b>R<sub>9</sub></b>	<b>R<sub>10</sub></b>	<b>R<sub>11</sub></b>	<b>R<sub>12</sub></b>	<b>R<sub>13</sub></b>	<b>R<sub>14</sub></b>	<b>R<sub>15</sub></b>
<b>U</b>	46	17	93	54	72	94	68	97	64	21	98	77	48	49	62
<b>C</b>	18	72	86	66	54	45	4	24	2	93	38	1	47	50	44

<p>S-Mazindol (anorexic)  <i>E</i>-Vinbarbital (sedative; hypnotic)  S-Cifenline (antiarrhythmic)  <i>R</i>-Carbinoxamine (antihistaminic)</p>
<p>S-Oxybutynin (anticholinergic)  <i>S,R</i>-Mesoridazine (antipsychotic)  <i>R</i>-Lorazepam (anxiolytic)  Methylprednisolone (glucocorticoid)  <i>R</i>-Thalidomide (sedative; hypnotic)</p>
<p>Ethenzamide (analgesic)  Phenacemide (anticonvulsant)  Levamisole (anthelmintic)</p>
<p><i>R</i>-Butriptyline (antidepressant)  <i>R,S</i>-Secobarbital (sedative; hypnotic)  Promazine (antipsychotic)  Chlorambucil (antineoplastic)</p>
<p>bextra (analgesic; anti inflammatory)  Paroxetine (antidepressant)  <i>S</i>-Trimipramine (antidepressant)  <i>R</i>-Nomifensine (antidepressant)  <i>S</i>-Cetirizine (antihistaminic)  <i>Z</i>-Triprolidine (antihistaminic)  <i>R,R</i>-Secobarbital (sedative; hypnotic)</p>

**Figure 5.13** Control results showing random groupings of drugs.

The UBANTR approach can be used for NCEs as well. Any NCEs are docked to the same 15 random receptors and the data is normalized along with the entire FDA-approved drug library. The entire set is then inputted into Orange and depending on what the NCEs cluster with, it will predict its potential indication. For example, if we looked at Figure 5.3 and assumed we did not know the indication of *S*-Carbinoxamide, (so it is playing the role of a NCE for the purposes of this example) and it turned out to group

with three anti-histaminic drugs, we would imply that this NCE (*S*-Carbinoxamide) would be an anti-histamine or possess some anti-histaminic properties. Therefore NCEs would be treated in a similar fashion to the rest of the FDA-approved library and depending on which indications it grouped with, it is predicted to possess those similar properties, an approach that still only requires the structure of a biologically active compound.

## **5.5 Conclusion**

The UBANTR approach uses the data of a library of FDA-approved drugs docked to 15 non-specific receptors. This data allows insight into the properties of drugs included in the library without knowledge or availability of target receptors. There are two main objectives to the UBANTR approach; i) to repurpose drugs and ii) to predict the indication for New Chemical Entities (NCEs).

The first objective relates to any mismatches in indication from known drugs. These mismatches are revealing indications for potential repurposing, giving insight into a drug's alternate uses. For our purposes, STITCH was used to help find any known connections between drug matches and not as a method of validating the UBANTR approach. Therefore, a search resulting in no connection should not imply a link does not exist; it is possible this connection has simply not been established. The UBANTR approach can be a great starting point for testing existing drugs for alternate purposes.

The second objective is to predict the indication for NCEs. Although this was briefly discussed, this objective can be achieved through a similar process. Any known drug matching with unknown drugs (NCEs) is revealing their potential indication.

## REFERENCES:

1. Chong, C.R.; Sullivan Jr., D.J., *Nature*, **2007**, 448, 645- 646.
2. Rothstein, J. D. et al. *Nature*, **2005**, 433, 73-7.
3. Jomaa, H. et al., *Science*, **1999**, 285, 1573-6.
4. Lang, T. & Greenwood, B., *Lancet Infect Dis* **2003**, 3, 162-8.
5. Marton, L. J. & Pegg, A. E., *Annu Rev Pharmacol Toxicol*, **1995**, 35, 55-91.
6. Shigi, Y., *J Antimicrob Chemother*, **1989**, 24, 131-45.
7. Missinou, M. A. et al., *Lancet*, **2002**, 360, 1941-2.
8. Borrmann, S. et al., *J Infect Dis*, **2004**, 189, 901-8.
9. Fidock, D. A., Rosenthal, P. J., Croft, S. L., Brun, R. & Nwaka, S., *Nat Rev Drug Discov*, **2004**, 3, 509-20.
10. Sundar, S. et al., *N Engl J Med*, **2002**, 347, 1739-46.
11. D'Amato, R. J., Loughnan, M. S., Flynn, E. & Folkman, J., *Proc Natl Acad Sci U S A*, **1994**, 91, 4082-5.
12. Shannon, C.; Weaver, W., *The Bell System Technical Journal*, **1948**, 27, 379-423 and 623-656.
13. Omega, OpenEye Scientific Software, Inc., Santa Fe, NM, USA, [www.eyesopen.com](http://www.eyesopen.com), 2010.
14. Spartan' 06; Ver. 1.1.0; Wavefunction Inc., 18401 Von Karman Avenue, Suite 370 Irvine, CA 92612, USA.
15. Fred Receptor, OpenEye Scientific Software, Inc., Santa Fe, NM, USA, [www.eyesopen.com](http://www.eyesopen.com), 2010.
16. FRED, OpenEye Scientific Software, Inc., Santa Fe, NM, USA, [www.eyesopen.com](http://www.eyesopen.com), 2010.
17. Orange Data Mining Software:  
Curk, T.; Demšar, J.; Xu, Q.; Leban, G.; Petrovič, U.; Bratko, I.; Shaulsky, G.; Zupan, B., *Bioinformatics*, **2005**, 21(3), 396-398.

18. STITCH (version 3.1)  
Kuhn, M.; Szklarczyk, D., Franceschini, A., Campillos, M.; von Mering, C.; Jensen, L. J.; Beyer, A.; Bork, P., *Nucleic Acids Research*, **2009**, 1-5
19. Vida, version 4.0.2, OpenEye Scientific Software, Inc., Santa Fe, NM, USA,  
[www.eyesopen.com](http://www.eyesopen.com), 2010.

## Appendix A:

### Experimental Procedures and Spectroscopic Data

#### **CBC<sub>an</sub>**

To a flask containing 1,3- Cyclohexanedione (2.50g, 22.3 mmol) dissolved in THF (19 mL), was added citral (3.09g, 20.3 mmol), freshly prepared ZnBr<sub>2</sub> (20.3 mmol) in THF (20mL), and EDDA (0.63g, 3.50 mmol). Mixture was then heated using either oil bath or microwave (100 Watts) at 40 °C for 10 minutes. Mixture was then extracted 3x with diethyl ether and water. CBC<sub>an</sub> was then purified by column chromatography using a 1:4 Ethyl Acetate: Hexane solution. (4.41g, 88%). <sup>1</sup>H-NMR (300 MHz, CDCl<sub>3</sub>): δ 6.475- 6.441 p.p.m. (d, *J* = 10.1 Hz, 1H), 5.201- 5.167 (d, *J* = 10.08 Hz, 1H), 5.086 (m, 1H), 2.425- 2.165 (m, 6H), 2.079- 1.949 (m, 4H), 1.676 (bs, 3H), 1.589 (bs, 3H), 1.365 (s, 3H). <sup>13</sup>C-NMR (400 MHz, CDCl<sub>3</sub>): δ 194.76, 172.09, 132.15, 123.87, 121.85, 116.67, 110.52, 82.53, 41.91, 36.65, 28.80, 27.62, 25.86, 22.74, 20.87, 17.82. HRMS (*m/z*): [M]<sup>+</sup> calcd for C<sub>16</sub>H<sub>22</sub>O<sub>2</sub>, 246.1620; found, 246.1701.

#### **THC<sub>an</sub>**

CBC<sub>an</sub> (1.51g) was adsorbed onto silica (3.02g) and heated to 150 °C by microwave, under vacuum (300 Watts), for about 60 minutes. Compound was then filtered, concentrated, and columned with 1:4 Ethyl Acetate: Hexane solution, giving 1.16g (77%) of the product. Heating CBC<sub>an</sub> in the presence of EDDA decreases the rate of THC<sub>an</sub> formation (Table S1). <sup>1</sup>H-NMR (300 MHz, CDCl<sub>3</sub>): δ 6.09 p.p.m. (m, 1H), 6.02 (m, 1H), 3.18 (bs, 1H), 2.86-2.83 (br, 1H), 2.47- 2.20 (cm, 17H), 2.13-2.10 (m, 4H), 1.94- 1.78



(cm, 15H), 1.71 (s, 1H), 1.65 (s, 11H), 1.60 (m, 2H), 1.39-1.37 (d,  $J=5.00$  Hz, 12H), 1.28-1.26 (m, 4H), 1.22 (s, 6H), 1.07 (s, 6H).  $^{13}\text{C}$ -NMR (400 MHz,  $\text{CDCl}_3$ ):  $\delta$  198.04, 197.57, 170.94, 168.91, 133.67, 133.52, 123.84, 122.40, 114.18, 113.59, 80.84, 79.13, 45.59, 40.22, 37.65, 37.43, 32.22, 31.46, 30.17, 30.05, 29.60, 29.46, 27.21, 25.89, 25.24, 24.71, 23.68, 23.37, 20.41, 20.33, 20.00 (Ratio= 1.2:1 *trans:cis*). \*Data is for a mixture of isomers. Isolation of isomers proved to be difficult. Due to the peak overlap, multiplicity cannot be accurately determined for individual isomers. HRMS ( $m/z$ ):  $[\text{M}]^+$  calcd for  $\text{C}_{16}\text{H}_{22}\text{O}_2$ , 246.1620; found, 246.1693.

### $\Delta^1$ -THC

$\text{THC}_{\text{an}}$  (with  $\text{C}_5\text{H}_{11}$  alkyl side chain) (0.1777g, 0.5615 mmol) was dissolved in anhydrous THF (3.43 mL) and placed in a acetone/ dry ice bath ( $-78$  °C). *t*-BuLi in pentanes (1.202M, 0.4671 mL) was then added to the mixture. After 15 minutes,  $\text{I}_2$  was added and bath was replaced with a regular ice bath ( $0$  °C). Fifteen minutes after  $\text{I}_2$  was dissolved, 1,8-Diazabicycloundec-7-ene was added and mixture was allowed to stir at room temperature over night. Mixture was then extracted with 10% HCl and ether, dried over magnesium sulfate, and concentrated in vacuo. 0.0970g, 54.9% as a mixture of *cis/trans*-isomers.  $^1\text{H}$ -NMR (300 MHz,  $\text{CDCl}_3$ ):  $\delta$  6.39- 6.23 ppm (cm, 5H), 6.16- 6.13 (cm, 2H), 5.68 (d,  $J= 3.8$ , 1H), 5.21 (bs, 1H), 3.58\* (bs, 1H), 3.21 (d,  $J= 10.6$ , 2H), 2.62- 2.55\* (dd,  $J= 4.3$ , 9.3, 2H), 2.45- 2.38 (dd,  $J= 6.8$ , 13.3, 5H), 2.18- 2.11 (cm, 4H), 1.98- 1.89 (cm, 6H), 1.69 (d,  $J= 3.8$ , 9H), 1.64- 1.50 (cm, 12H), 1.42- 1.26 (cm, 33H), 1.11- 1.06 (m, 6H), 0.93- 0.85 (q,  $J= 6.9$ , 11H). Data is for a mixture of *cis*- [(*S,R*) and (*R,S*)] and *trans*-

[(*R,R*) and (*S,S*)] isomers in a 1:2 ratio. \*denotes peaks known to belong to *cis*- isomers. Underlined peaks denote those known to belong to the *trans*- isomers. Remaining peaks are for overlapping *cis/trans*- isomer peaks. Experimental integration is slightly higher for some peaks due to impurities. <sup>13</sup>C-NMR (300 MHz, CDCl<sub>3</sub>): δ 155.14, 154.93, 154.55, 154.01, 153.38, 153.01, 152.86, 144.01, 143.76, 142.95, 142.57, 134.99, 134.40, 124.06, 123.98, 122.31, 122.14, 111.21, 111.04, 110.12, 110.05, 108.21, 107.79, 77.84, 77.38, 76.36, 46.01, 45.10, 41.11, 40.28, 35.98, 35.63, 34.66, 33.81, 31.95, 31.73, 31.39, 30.79, 29.97, 29.77, 28.10, 27.78, 27.28, 26.08, 25.23, 24.74, 23.57, 22.75, 20.90, 19.47, 14.23. Data is for a mixture of *cis*- [(*S,R*) and (*R,S*)] and *trans*- [(*R,R*) and (*S,S*)] isomers in a 1:2 ratio. HRMS (*m/z*): [M]<sup>+</sup> calcd for C<sub>21</sub>H<sub>30</sub>O<sub>2</sub>, 314.2246; found, 314.2318.

### Compound A

THC<sub>an</sub> (1.37g, 5.58 mmol) was dissolved in anhydrous ether (24.3 mL) and added to a suspension of lithium aluminum hydride (1.22g, 32.03 mmol) in ether (97.1 mL). Mixture was stirred for half an hour at room temperature and then refluxed for an hour and a half. Then ammonium chloride (8.48g, 158.5mmol) was added to the mixture, followed by water (68.7 mL). It was then extracted with ether and dried with magnesium sulfate. Product was purified by column chromatography using 1:9 Ethyl Acetate: Hexane solution to yield separation of two major compounds (A and B) in a 1:4 ratio as *cis/trans* isomers (3:1 for compound A). Crude= 0.88g, 68.2%, Compound X= <sup>1</sup>H-NMR (500 MHz, CDCl<sub>3</sub>): δ 5.62 p.p.m. (bs, 1H), 5.53 (d, *J* = 5.1, 3H), 2.69 (bs, 3H), 2.47 (bs, 1H), 2.24- 2.16 (cm, 2H), 2.12- 2.03 (cm, 6H), 1.98- 1.86 (cm, 21H), 1.79- 1.69 (cm,

15H), 1.68 (bs, 9H), 1.67 (bs, 5H), 1.60 (s, 1H), 1.55- 1.31 (cm, 18H), 1.29 (s, 5H), 1.28 (s, 9H), 1.27- 1.22 (cm, 2H), 1.20 (s, 9H), 1.05 (s, 3H). Isolated fraction used for NMR experiments of this compound contained a *cis:trans* ratio of 3:1. Experimental integration is slightly higher for some cm due to impurities. <sup>13</sup>C-NMR (500 MHz, CDCl<sub>3</sub>): δ 144.64, 142.27, 134.54, 134.00, 122.10, 121.89, 105.24, 104.53, 76.16, 74.67, 45.84, 40.53, 36.47, 34.83, 31.68, 30.70, 28.33, 28.09, 27.83, 26.20, 25.06, 24.79, 23.79, 23.44, 23.23, 20.35, 19.92. \*Data is for a mixture of isomers. Isolation of isomers proved to be difficult. Due to the peak overlap, multiplicity cannot be accurately determined for individual isomers. HRMS (*m/z*): [M]<sup>+</sup> calcd for C<sub>16</sub>H<sub>24</sub>O, 232.1827; found, 232.1902.

### Compound B

<sup>1</sup>H-NMR (500 MHz, CDCl<sub>3</sub>): δ 5.54 p.p.m. (bs, 1H), 5.51 (bs, 1H), 5.47 (d, *J* = 4.1, 1H), 5.39 (bs, 1H), 4.14 (bs, 1H), 4.08 (t, *J* = 6.5, 1H), 3.08 (bs, 1H), 2.70 (d, *J* = 9.0, 1H), 2.09- 1.90 (cm, 12H)<sup>a</sup>, 1.71 (bs, 3H), 1.69 (bs, 3H), 1.71- 1.64 (cm, 5H)<sup>b</sup>, 1.57- 1.43 (cm, 6H), 1.41-1.40 (cm, 1H), 1.39 (s, 3H), 1.36- 1.24 (cm, 3H)<sup>c</sup>, 1.23 (s, 3H), 1.20 (s, 3H), 1.18 (s, 3H). Experimental integration is slightly higher for some cm due to impurities: a) 12H should integrate to 10H b) 5H should integrate to 4H and c) 3H should integrate to 1H. Isolated fraction used for NMR experiments of this compound contained a *cis:trans* ratio of 1:1. <sup>13</sup>C-NMR (500 MHz, CDCl<sub>3</sub>): δ 139.79, 138.37, 135.23, 135.02, 124.33, 122.10, 120.53, 117.81, 74.66, 72.91, 67.83, 67.70, 49.81, 43.30, 38.60, 36.77, 31.39, 30.91, 30.60, 30.53, 28.88, 28.04, 25.83, 25.42, 25.17, 24.43, 23.72, 23.24, 20.68, 20.30,

19.00, 18.16. (Ratio= 1:1 *trans:cis*). \*Data is for a mixture of isomers. Isolation of isomers proved to be difficult. Due to the peak overlap, multiplicity cannot be accurately determined for individual isomers. HRMS (*m/z*): [M]<sup>+</sup> calcd for C<sub>16</sub>H<sub>24</sub>O, 232.18; found, 232.19.

### $\Delta^0$ -THC<sub>gem</sub>

5,5-dimethyl -1,3-cyclohexanedione (1.49, 10.62 mmol) was dissolved in THF (18.6 mL), then (+) citronellal (1.74 mL, 9.65 mmol) was added, followed by zinc bromide (2.17g, 9.65 mmol), and EDDA (0.30g, 1.66 mmol). The mixture was then heated to 40 °C, for 30 minutes. It was then cooled, extracted with water and ether, dried over magnesium sulfate, and concentrated. Compound was recrystallized from hexane to afford white crystals. (0.337g, 12.7%) <sup>1</sup>H-NMR (400 MHz, CDCl<sub>3</sub>): δ 2.84 ppm (m, 1H), 2.23- 2.03 (cm, 5H), 1.81-1.20 (cm, 4H), 1.31 (s, 3H), 1.09- 0.96 (cm, 2H), 1.04 (s, 3H), 1.03 (s, 3H), 1.01 (s, 3H), 0.88 (d *J* = 6.6, 3H), 0.46 (dd, *J*= 11.5, 24.0, 1H). <sup>13</sup>C-NMR (400 MHz, CDCl<sub>3</sub>): δ 197.78, 168.55, 113.32, 80.42, 51.69, 48.91, 43.33, 38.73, 35.69, 33.66, 32.47, 31.67, 29.42, 27.66, 27.36, 22.56, 19.62. Data is for a mixture of isomers. Isolation of isomers proved to be difficult. Due to the peak overlap, multiplicity cannot be accurately determined for individual isomers. HRMS (*m/z*): [M]<sup>+</sup> calcd for C<sub>18</sub>H<sub>28</sub>O<sub>2</sub>, 276.2089; found, 276.2174.

### **CBC<sub>gem</sub>**

5,5-dimethyl -1,3-cyclohexanedione (1.84, 13.12 mmol) was dissolved in THF (21.0 mL), then (+) citral (1.87 mL, 10.93 mmol) was added, followed by zinc bromide (2.46g, 10.93 mmol), and EDDA (0.339g, 1.880 mmol). The mixture was then heated to 40 °C, for 40 minutes. It was then cooled, extracted with water and ether, dried over magnesium sulfate, and concentrated. Compound was purified by column chromatography with 1:3 Ethyl Acetate: Hexanes (2.28g, 75.9%). <sup>1</sup>H-NMR (300 MHz, CDCl<sub>3</sub>): δ 6.45 ppm (d, *J*= 10.1, 1H), 5.17 (d, *J*= 10.0, 1H), 5.13-5.04 (m, 1H), 2.27 (d, *J*=2.2, 2H), 2.25 (s, 2H), 2.10- 1.99 (cm, 2H), 1.77-1.52 (cm, 2H), 1.68 (d, *J*= 1.0, 3H), 1.59 (s, 3H), 1.37 (s, 3H), 1.07 (d, *J*= 3.2, 6H).

### **Δ<sup>1</sup>-THC<sub>gem</sub>**

CBC<sub>gem</sub> (0.506g) was adsorbed onto silica (1.00g) and heated to 150 °C for 50 minutes, then mixture was filtered through sand. No purification needed (0.641g, quantitative yield). <sup>1</sup>H-NMR (400 MHz, CDCl<sub>3</sub>): δ 6.09 ppm (bs, 1H), 6.06 (s, 1H), 3.17 (bs, 1H), 2.81 (bs, 1H), 2.35- 2.10 (cm, 15H), 1.98- 1.76 (cm, 7H), 1.64 (bs, 6H), 1.62- 1.43 (cm, 5H), 1.38 (s, 3H), 1.36 (s, 4H), 1.30 (d, *J*= 2.2, 1H), 1.22 (s, 3H), 1.06 (s, 6H), 1.02 (d, *J*= 2.2, 9H). Experimental integration is slightly higher for some cm due to impurities. <sup>13</sup>C-NMR (400 MHz, CDCl<sub>3</sub>): δ 198.26, 197.74, 169.13, 167.25, 133.62, 133.42, 122.15, 112.12, 80.89, 79.30, 51.66, 51.59, 45.67, 43.35, 43.22, 40.15, 32.17, 32.04, 31.47, 30.04, 28.97, 27.21, 25.45, 24.76, 23.44, 20.60, 20.11. Isolated fraction used for NMR experiments of this compound contained a *cis:trans* ratio of 1:1. Isolation of isomers

proved to be difficult. Due to the peak overlap, multiplicity cannot be accurately determined for individual isomers. HRMS ( $m/z$ ):  $[M]^+$  calcd for  $C_{18}H_{26}O_2$ , 274.1933; found, 274.2241.

### $\Delta^0$ -THC<sub>est</sub>

Methyl acetoacetate (3.30 mL, 30.56 mmol) and ( $\pm$ )citronellal (4.99 mL, 27.78 mmol) were mixed with THF (53.42 mL). Then zinc bromide (6.25g, 27.78 mmol) and EDDA (1.00g, 5.55 mmol) were added, respectively. The mixture was then heated to 40 °C for 2.5 hours. It was then extracted with water and ether, dried with magnesium sulfate, and concentrated. Crude = 6.50g, 92.7%. Crude compound (6.2g, 24.57 mmol) was dissolved in methylene chloride (61.4 mL). Then acetic acid (6.4 mL, 112.04 mmol) and HCl (2.0 mL, 24.57 mmol, 12.1 N) were added. Mixture was allowed to stir at room temperature for 2 hours. Methylene chloride was evaporated and residue was dissolved in ether and extracted with water. Organic phase was washed with saturated sodium bicarbonate solution, water, then brine. Then it was dried over magnesium sulfate and concentrated (5.91g, 90.9% crude). Compound was then run through a silica plug and eluted with 5:95 Ethyl acetate: Hexanes (1.6g, 47.1%).  $^1H$ -NMR (300 MHz,  $CDCl_3$ ):  $\delta$  3.69 ppm (s, 3H), 2.13- 2.07 (cm, 2H), 2.07 (d,  $J$ = 1.3, 3H), 1.79- 1.46 (cm, 5H), 1.29 (s, 3H), 1.26- 0.91 (cm, 4H), 1.07 (s, 3H), 0.90 (d,  $J$ = 6.5, 3H), 0.61 (dd,  $J$ = 11.7, 24.3, 1H). Integration slightly higher due to some impurity, but seems consistent with the literature.

### **CBC<sub>est</sub>**

(±)Citral (19.4 mL, 0.1132 mol) is mixed with THF (218 mL), then methyl acetoacetate (13.44 mL, 0.1245 mol) is added, followed by EDDA (2.04g, 11.3 mmol). Mixture is stirred for 2 hours and 35 minutes at 40 °C. It is then extracted with ether and water, dried with sodium sulfate, and concentrated. Product was next purified for next reaction (quantitative yield). <sup>1</sup>H-NMR (400 MHz, CDCl<sub>3</sub>): δ 6.32 ppm (d, *J* = 10.0, 1H), 5.11-5.06 (cm, 2H), 3.72 (s, 3H), 2.39- 2.34 (cm, 2H), 2.27 (s, 3H), 2.23- 2.11 (cm, 3H), 2.06-1.92 (cm, 4H), 1.67 (bs, 6H), 1.59 (bs, 6H), 1.32 (s, 3H). Experimental integration is higher for some peaks due to the presence of some uncyclized product (the result of the Knoevenagel reaction, prior to the 6π-oxo-electrocyclization). <sup>13</sup>C-NMR (400 MHz, CDCl<sub>3</sub>): δ 167.15, 166.51, 156.67, 156.51, 140.45, 140.32, 131.98, 124.09, 124.01, 123.22, 120.40, 119.99, 119.91, 102.53, 80.86, 52.25, 51.22, 41.20, 41.06, 33.30, 33.11, 31.49, 27.18, 26.65, 26.46, 25.88, 25.80, 22.74, 20.36, 17.81, 17.74. HRMS (*m/z*): [M]<sup>+</sup> calcd for C<sub>15</sub>H<sub>22</sub>O<sub>3</sub>, 250.1569; found, 250.1683.

### **Δ<sup>1</sup>-THC<sub>est</sub>**

CBC<sub>est</sub> (5.26g) was adsorbed onto silica (10.5g) and heated at 150 °C for 4.5 hours. Compound was purified by column chromatography using 1:4 Ethyl acetate: Hexanes (1.43g, 28.3%). <sup>1</sup>H-NMR (400 MHz, CDCl<sub>3</sub>): δ 5.59 ppm (bs, 1H) 5.49 (s, 2H), 3.75 (d, *J* = 1.0, 4H), 3.74 (d, *J* = 0.9, 3H), 3.21 (bs, 1H), 2.84 (bs, 2H), 2.12 (dd, 6H), 2.08 (s, 4H), 1.94 (d, *J* = 7.7, 2H), 1.82- 1.79 (cm, 3H), 1.64 (bs, 8H), 1.33 (d, *J* = 5.0, 9H), 1.25 (s, 3H), 1.09 (s, 5H). Experimental integration is higher than expected due to a mixture of

*cis:trans* isomers (1:2) and slight impurities.  $^{13}\text{C}$ -NMR (400 MHz,  $\text{CDCl}_3$ ):  $\delta$  168.99, 160.96, 158.73, 135.22, 134.13, 124.35, 121.94, 120.40, 119.38, 104.22, 78.91, 77.48, 50.90, 45.29, 39.89, 34.03, 31.37, 30.11, 29.87, 27.32, 25.32, 23.74, 23.47, 23.39, 20.17, 20.04, 18.74. HRMS ( $m/z$ ):  $[\text{M}]^+$  calcd for  $\text{C}_{15}\text{H}_{22}\text{O}_3$ , 250.1569; found, 250.1729.

### Compound E

per-THC<sub>est</sub> (0.4845g, 1.920 mmol) and tetramethylethylenediamine (TMEDA) (0.288 mL, 1.920 mmol) were diluted in anhydrous diethyl ether (11.9 mL) and the temperature was lowered to  $-20\text{ }^\circ\text{C}$ . Then *t*-BuLi in pentanes (2.3 mL, 2.304 mmol) was added dropwise. After 45 minutes, the dimethyl acetylenedicarboxylate (0.235 mL, 1.920 mmol) was added. It was left to stir at  $-20\text{ }^\circ\text{C}$  for 2 hours and then left to stir at room temperature over night. Mixture was then extracted with 10% HCl, dried over sodium sulfate, and concentrated. (< 1% yield recovered).  $^1\text{H}$ -NMR (400 MHz,  $\text{CDCl}_3$ ):  $\delta$  11.62 p.p.m. (s, 1H), 6.39 (s, 1H), 3.85 (d,  $J= 2.7$ , 6H), 3.16 (d,  $J= 12.8$ , 1H), 2.48 (td,  $J= 2.7$ , 11.0, 1H), 1.88-1.83 (m, 3H), 1.71- 1.57 (cm, 2H), 1.38 (s, 4H), 1.35- 1.29 (cm, 1H), 1.16- 1.08 (cm, 4H), 1.05 (s, 4H), 0.95 (d,  $J= 6.5$ , 4H), 0.93-0.84 (cm, 2H), 0.66 (dd,  $J= 11.5$ , 24.0, 1H) Data is for a mixture of *cis* and *trans*- isomers.  $^{13}\text{C}$ -NMR (400 MHz,  $\text{CDCl}_3$ ):  $\delta$  170.27, 169.80, 162.77, 159.48, 134.65, 131.19, 129.07, 129.00, 115.03, 110.05, 101.44, 79.14, 68.36, 66.04, 52.67, 48.90, 38.94, 38.31, 35.61, 35.53, 32.96, 29.90, 29.11, 28.11, 27.61, 23.91, 23.16, 22.69, 19.33, 15.46, 14.30, 14.24, 11.15. \*Data is for a mixture of isomers. Isolation of isomers proved to be difficult. Due to the peak



overlap, multiplicity cannot be accurately determined for individual isomers. HRMS

( $m/z$ ):  $[M]^+$  calcd for  $C_{20}H_{26}O_6$ , 362.1729; found, 362.1808.

## Appendix B:

### NMR spectra for THC<sub>an</sub> with C<sub>5</sub> alkyl chain and NMR Analysis

THC<sub>an</sub> with the C<sub>5</sub> alkyl chain was obtained as a mixture of all stereoisomers by the same pathway as CBC<sub>an</sub> to THC<sub>an</sub> (with no alkyl chain). The following table gives the carbon and proton assignments for the 4 isomers produced from the reaction. The NMR spectra show groupings of four for all atoms in the structure, representing four stereoisomers. One of the key factors used in the identification of all four isomers involves the *gem*-dimethyl groups (labeled 8 and 9) and the NOESY spectrum. For the *cis* isomers, it was found that one of the methyl groups correlated to both protons 1 and 6, while the methyl group from the *trans* isomers showed correlation to only one proton, either 1 or 6. Formal stereochemical designation of *cis* and *trans* isomers could not be determined.

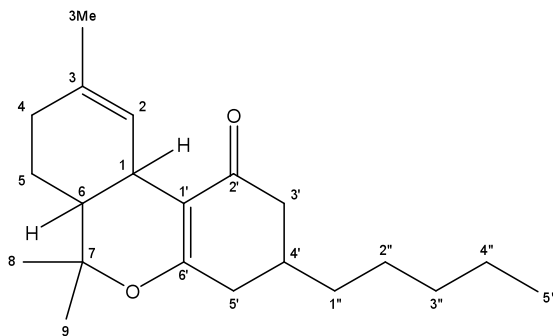
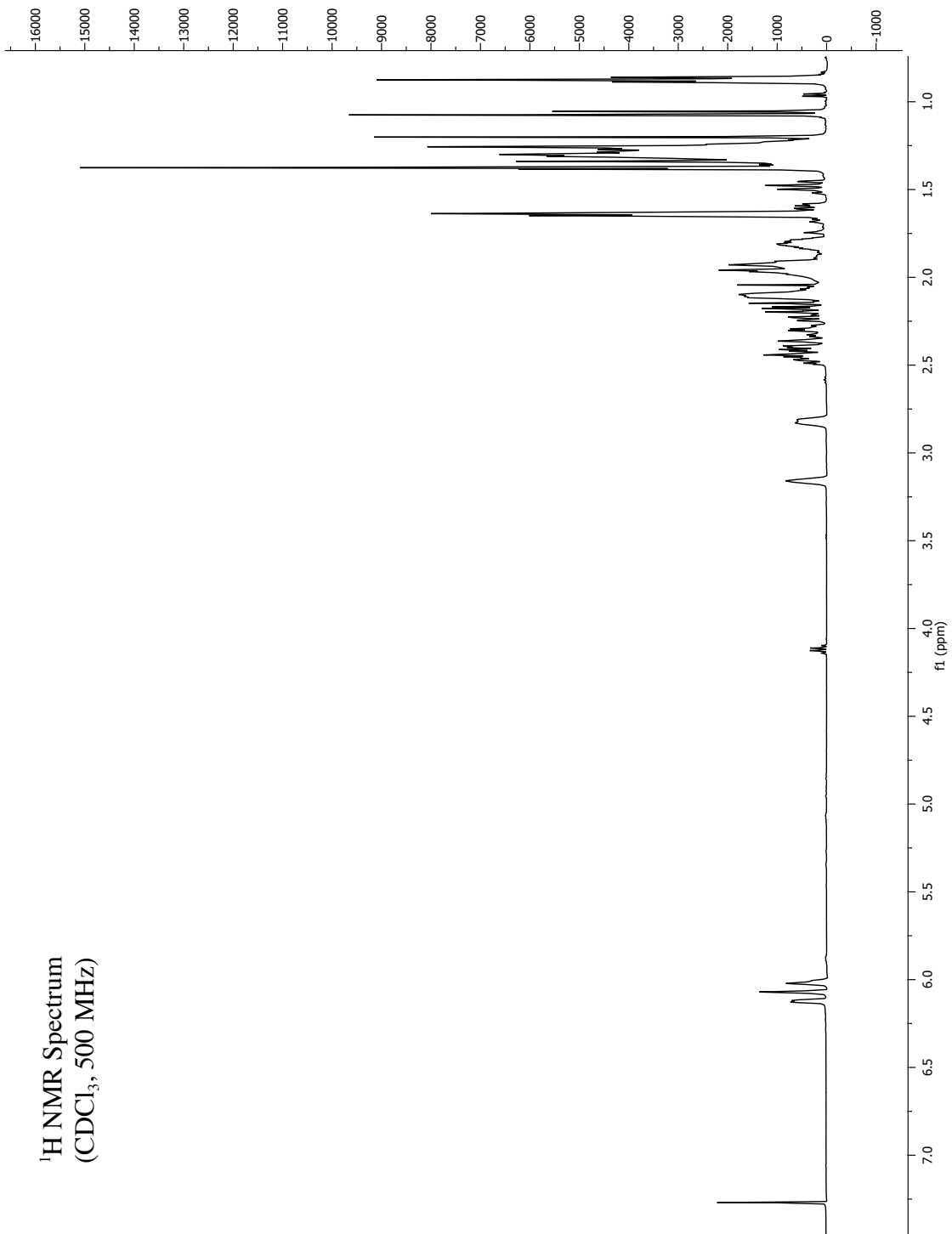
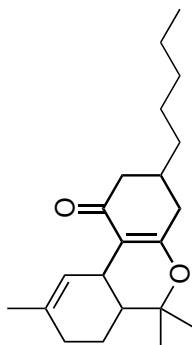


Table analysis on next page.

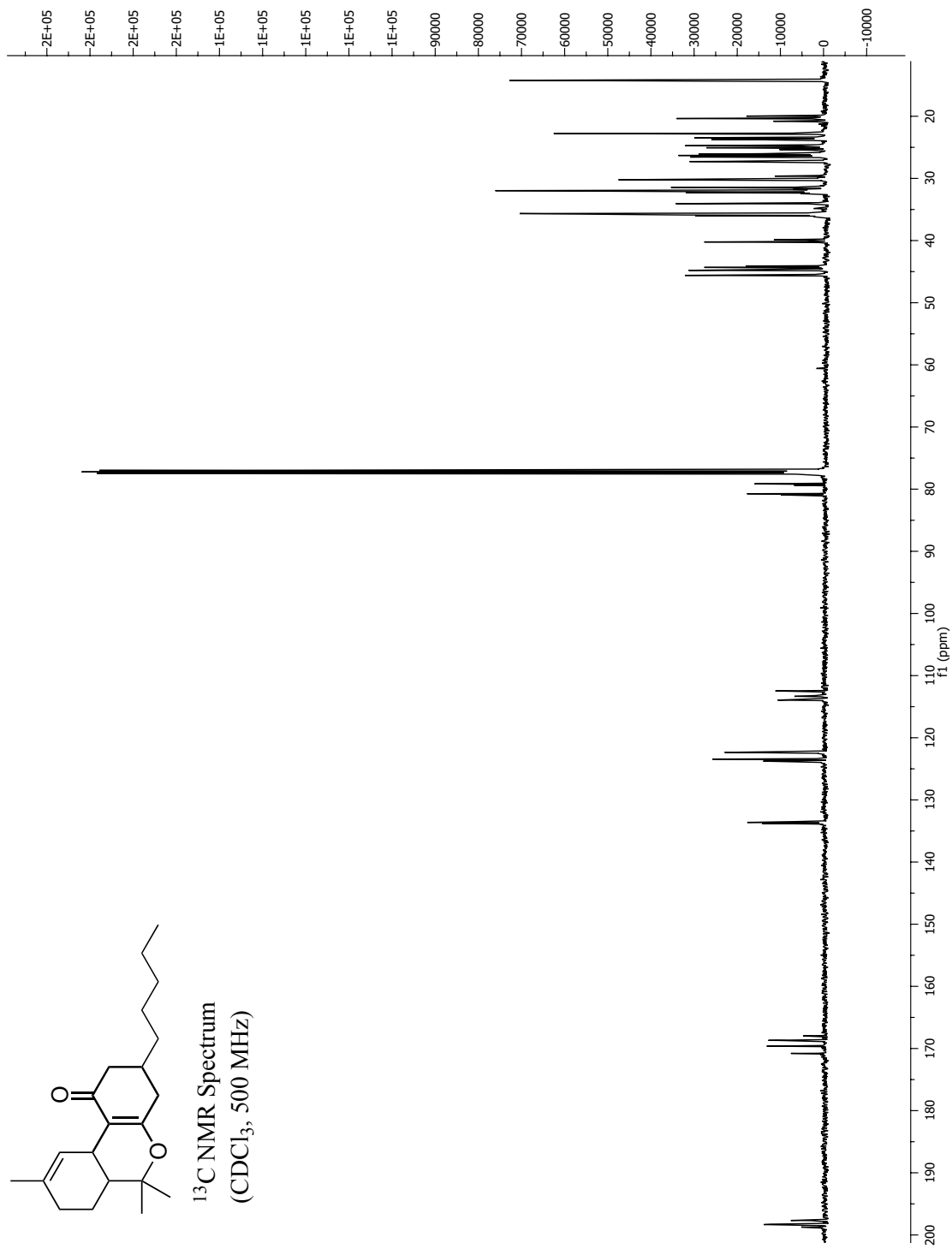
Position	<i>cis</i> I					<i>cis</i> II					<i>trans</i> I					<i>trans</i> II				
	<sup>1</sup> H	<sup>13</sup> C	NOESY	HMBC	<sup>1</sup> H	<sup>13</sup> C	NOESY	HMBC	<sup>1</sup> H	<sup>13</sup> C	NOESY	HMBC	<sup>1</sup> H	<sup>13</sup> C	NOESY	HMBC	<sup>1</sup> H	<sup>13</sup> C	NOESY	HMBC
1	3.14	29.97	4,5,6,9,5"	2,3,5,6,1',6'	3.15	29.79	4,5,6,8		2.81	31.90	4,5,9,5"		2.81	32.05	4,5,8		2.81	32.05	4,5,8	
2	6.11	122.12	1,4,3 <sub>Me</sub>	4,3 <sub>Me</sub> ,6,1'	5.99	122.03	1,4,3 <sub>Me</sub>	4,3 <sub>Me</sub> ,6	6.06	123.20	1,4,3 <sub>Me</sub> ,6	1,3 <sub>Me</sub> ,4,6,1'	6.01	123.55	1,4,3 <sub>Me</sub> ,6	1,3 <sub>Me</sub> ,4,6,1'		133.34		
3		133.55				133.25				133.39				133.34						
3 <sub>Me</sub>	1.64	23.52	2,4	2,3,4	1.61	23.45	2,4	2,3,4	1.62	23.23	2,4	2,3,4	1.62	23.18	2,4	2,3,4				
4	1.92	29.97	3 <sub>Me</sub> ,5,6	2,3,3 <sub>Me</sub> ,5,6,1'	1.91	29.39	3 <sub>Me</sub> ,5,6	2,3,3 <sub>Me</sub> ,5,6	2.09	31.22	3 <sub>Me</sub> ,5,6	2,3,3 <sub>Me</sub> ,5,6	2.10	31.24	3 <sub>Me</sub> ,5,6	2,3,3 <sub>Me</sub> ,5,6				
5	1.23,1.80	20.08	4,6	1,3,4,6	1.31,1.84	20.57	4,6	1,4,6,7	1.33,1.79	24.53	4,6	1,3,6,7,1'	1.33,1.80	24.49	4,6	1,3,6,1'				
6	1.59	39.99	1,5,8,9	1,2,5,1'	1.64	39.65	1,5,8,9	1,2,7,5,1'	1.48	45.37	5,8,9	1,2,5,7,9	1.48	45.37	5,8,9	1,2,5,7,9				
7		78.92				79.13				80.50				80.70						
8	1.37	25.88	6,9	1,7,6,9	1.25	25.81	1,6,9	6,7,9	1.37	27.05	6,9	1,7,6,9	1.05	19.75	1,9	6,7,9				
9	1.19	24.83	1,6,8	6,7,8	1.33	25.13	6,8	6,7,8	1.07	20.14	1,8	6,7,8	1.37	27.03	6,8	6,7,8				
1'		113.71				112.99				112.25				113.10						
2'		198.03				197.44				198.11				198.51						
3'	1.92,2.44	44.09	4'	1',2',4',5'	1.92,2.44	43.87	4'	2',4',5'	2.17,2.42	44.56	4'	1',2',4',5'	2.11,2.40	44.51	4'	1',2',4',5'				
4'	1.95	32.06	3',5'	2',5',1"	1.98	32.20	3',5'	5',1"	2.05	33.84	3',5'	2',3',5',6',1"	2.05	33.73	3',5'	3',5',6',1"				
5'	1.90,2.36	35.79	4'	1',3',4',6'	1.92,2.36	35.90	4'	3',4',6'	2.20,2.31	35.65	4'	1',3',4',6'	2.16,2.29	35.65	4'	3',4',6'				
6'		168.47				170.57				169.39				167.75						
1"	1.31	31.73	2"	3',4',5',2"	1.31	31.73	2"	3',4',5',2"	1.31	31.73	4"	3',4',5',2"	1.31	31.73	4"	3',4',5',2"				
2"	1.27	26.33		1",3"	1.27	26.25		1",3"	1.27	26.08		1",3"	1.27	26.06		1",3"				
3"	1.23	31.73		2",4"	1.23	31.73		2",4"	1.23	31.73		2",4"	1.23	31.73		2",4"				
4"	1.27	22.53		3",5"	1.27	22.53		3",5"	1.27	22.53		3",5"	1.27	22.53		3",5"				
5"	0.86	13.99	1,4"	3",4"	0.86	13.99	4"	3",4"	0.86	13.99	1,4"	3",4"	0.86	13.99	4"	3",4"				

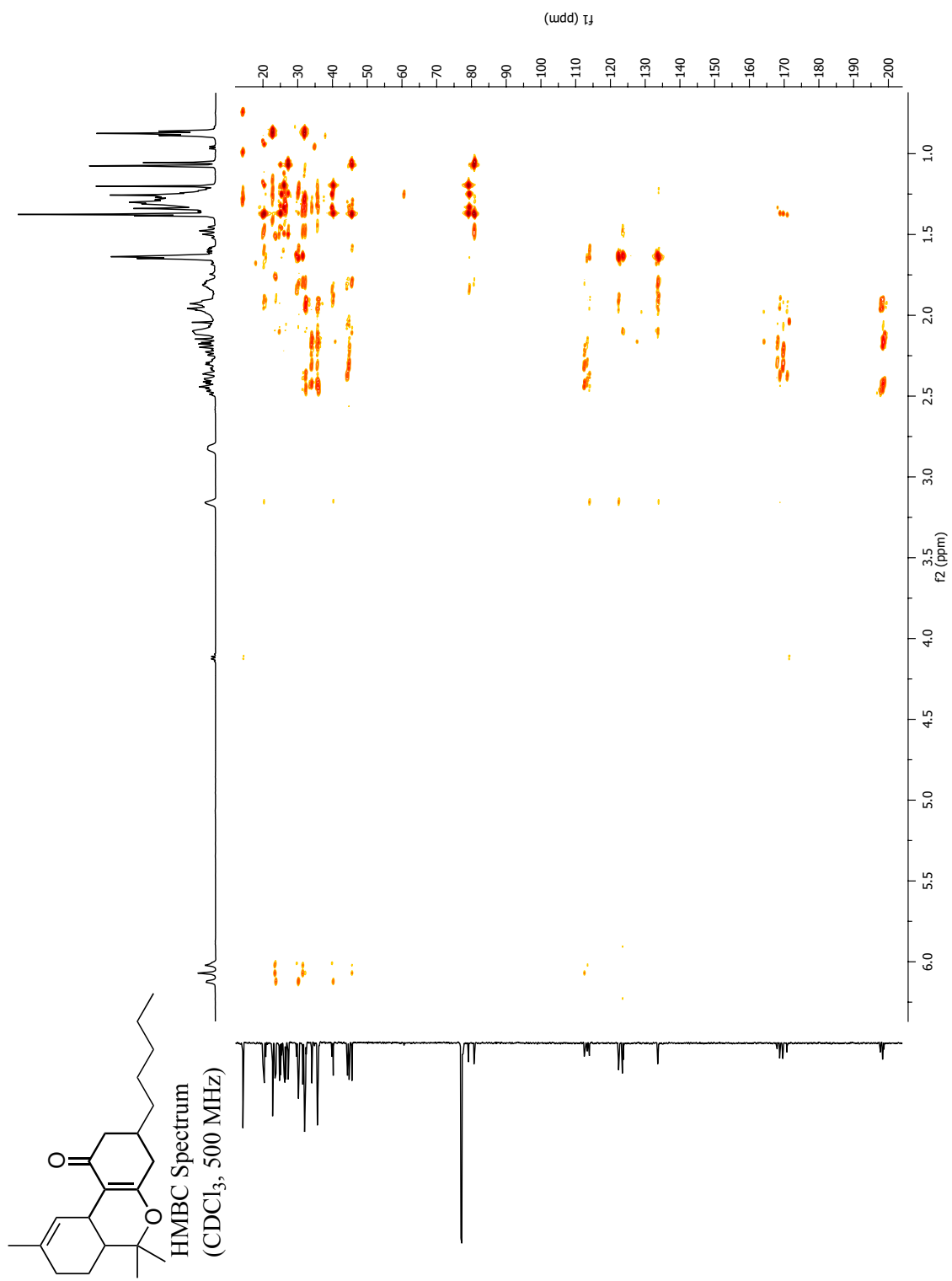
<sup>1</sup>H NMR Spectrum  
(CDCl<sub>3</sub>, 500 MHz)

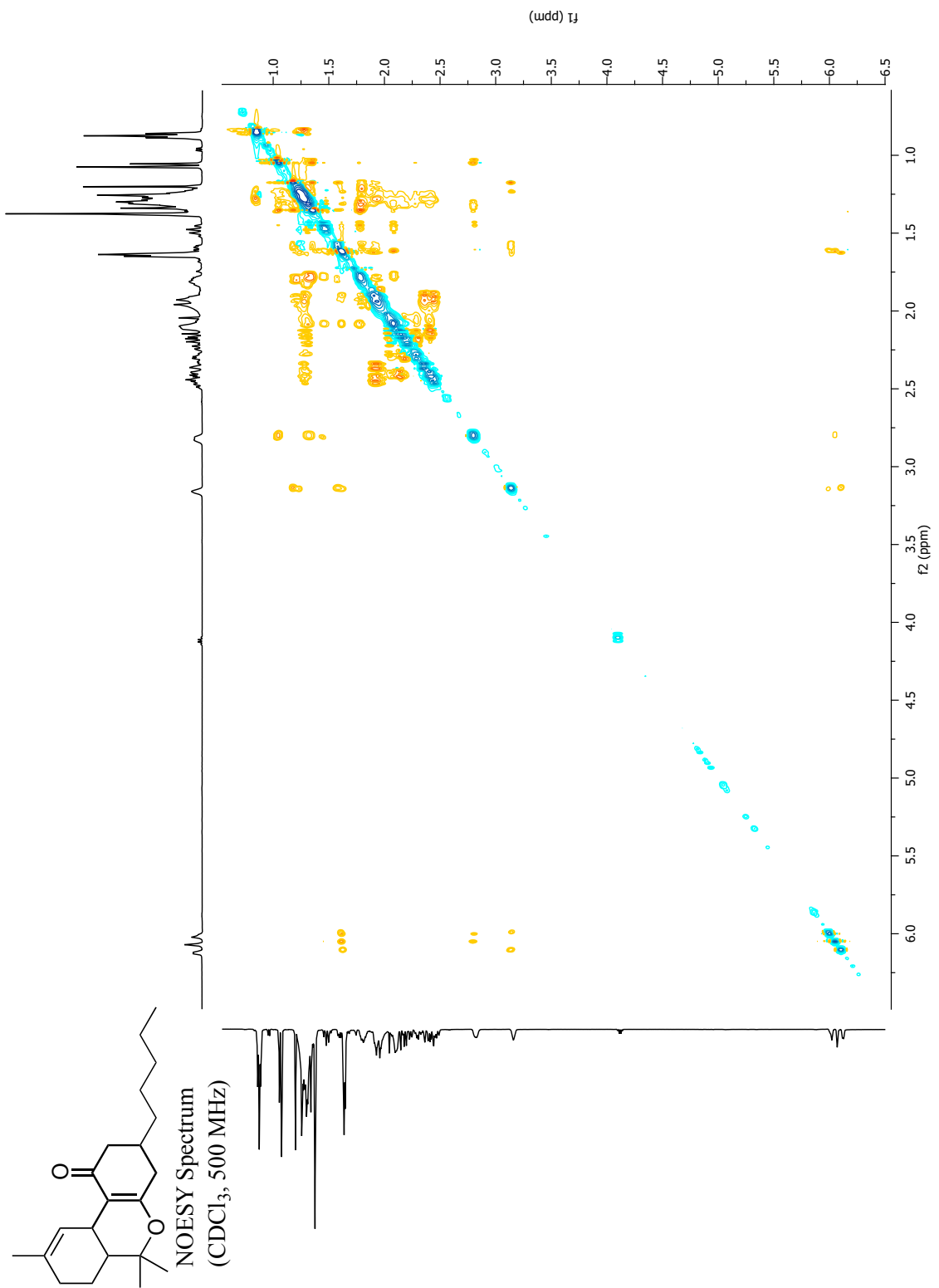




<sup>13</sup>C NMR Spectrum  
(CDCl<sub>3</sub>, 500 MHz)







## Appendix C:

### Ground State and TS Coordinates (DFT B3LYP/6-31G\*)

**Figure 2.3 (p.32)**

**1** (set to 0 kcal/mol)

Energy= -509199.718 kcal/mol

HEADER

REMARK Spartan `06 exported M001

HETATM	1	C	UNK	0001	4.180	-1.103	-0.082
HETATM	2	C	UNK	0001	5.438	-0.594	-0.202
HETATM	3	H	UNK	0001	6.286	-1.261	-0.349
HETATM	4	C	UNK	0001	3.016	-0.249	0.117
HETATM	5	C	UNK	0001	3.251	1.234	0.188
HETATM	6	C	UNK	0001	5.670	0.828	-0.136
HETATM	7	C	UNK	0001	4.629	1.687	0.050
HETATM	8	H	UNK	0001	4.781	2.761	0.102
HETATM	9	O	UNK	0001	2.329	2.046	0.354
HETATM	10	C	UNK	0001	1.778	-0.837	0.228
HETATM	11	H	UNK	0001	1.773	-1.920	0.150
HETATM	12	C	UNK	0001	0.514	-0.190	0.433
HETATM	13	H	UNK	0001	0.542	0.890	0.518
HETATM	14	C	UNK	0001	-0.685	-0.829	0.527
HETATM	15	C	UNK	0001	-1.941	-0.015	0.729
HETATM	16	H	UNK	0001	-1.673	1.005	1.027
HETATM	17	H	UNK	0001	-2.533	-0.445	1.549
HETATM	18	C	UNK	0001	-2.848	0.058	-0.533
HETATM	19	H	UNK	0001	-3.177	-0.948	-0.812
HETATM	20	H	UNK	0001	-2.238	0.431	-1.368
HETATM	21	C	UNK	0001	-4.019	0.980	-0.322
HETATM	22	H	UNK	0001	-3.740	2.027	-0.185
HETATM	23	C	UNK	0001	-5.325	0.678	-0.265
HETATM	24	C	UNK	0001	-6.356	1.758	-0.031
HETATM	25	H	UNK	0001	-6.944	1.555	0.875
HETATM	26	H	UNK	0001	-7.075	1.808	-0.861
HETATM	27	H	UNK	0001	-5.896	2.745	0.078
HETATM	28	C	UNK	0001	-5.899	-0.708	-0.425
HETATM	29	H	UNK	0001	-6.483	-0.991	0.463
HETATM	30	H	UNK	0001	-5.139	-1.476	-0.581
HETATM	31	H	UNK	0001	-6.594	-0.746	-1.276
HETATM	32	C	UNK	0001	-0.888	-2.318	0.436
HETATM	33	H	UNK	0001	0.041	-2.887	0.358
HETATM	34	H	UNK	0001	-1.507	-2.574	-0.434
HETATM	35	H	UNK	0001	-1.432	-2.679	1.320
HETATM	36	C	UNK	0001	7.088	1.320	-0.277
HETATM	37	H	UNK	0001	7.514	1.016	-1.242
HETATM	38	H	UNK	0001	7.731	0.891	0.503
HETATM	39	H	UNK	0001	7.144	2.409	-0.206
HETATM	40	O	UNK	0001	3.924	-2.445	-0.140



```

HETATM 41 H UNK 0001 4.763 -2.912 -0.277
CONNECT 1 2 4 40
CONNECT 2 3 1 6
CONNECT 3 2
CONNECT 4 1 5 10
CONNECT 5 4 7 9
CONNECT 6 2 7 36
CONNECT 7 8 5 6
CONNECT 8 7
CONNECT 9 5
CONNECT 10 11 4 12
CONNECT 11 10
CONNECT 12 13 10 14
CONNECT 13 12
CONNECT 14 12 15 32
CONNECT 15 16 17 14 18
CONNECT 16 15
CONNECT 17 15
CONNECT 18 19 20 15 21
CONNECT 19 18
CONNECT 20 18
CONNECT 21 22 18 23
CONNECT 22 21
CONNECT 23 21 24 28
CONNECT 24 25 26 27 23
CONNECT 25 24
CONNECT 26 24
CONNECT 27 24
CONNECT 28 29 30 31 23
CONNECT 29 28
CONNECT 30 28
CONNECT 31 28
CONNECT 32 33 34 35 14
CONNECT 33 32
CONNECT 34 32
CONNECT 35 32
CONNECT 36 37 38 39 6
CONNECT 37 36
CONNECT 38 36
CONNECT 39 36
CONNECT 40 41 1
CONNECT 41 40
END

```

**TS CBC** (14.6 kcal/mol)  
Energy= -509185.065 kcal/mol

```

HEADER
REMARK Spartan `06 exported M001
HETATM 1 O UNK 0001 0.028 -1.445 0.611
HETATM 2 C UNK 0001 1.226 -1.551 1.000

```

HETATM	3	C	UNK	0001	-0.903	0.512	1.286
HETATM	4	C	UNK	0001	0.277	1.253	1.290
HETATM	5	H	UNK	0001	0.286	2.200	0.750
HETATM	6	C	UNK	0001	1.500	0.797	1.793
HETATM	7	H	UNK	0001	2.277	1.549	1.954
HETATM	8	C	UNK	0001	1.902	-0.547	1.854
HETATM	9	C	UNK	0001	3.199	-0.877	2.386
HETATM	10	C	UNK	0001	3.858	-2.028	2.042
HETATM	11	H	UNK	0001	4.826	-2.240	2.483
HETATM	12	C	UNK	0001	3.269	-2.927	1.103
HETATM	13	C	UNK	0001	2.029	-2.666	0.571
HETATM	14	H	UNK	0001	1.557	-3.360	-0.118
HETATM	15	C	UNK	0001	-1.351	-0.289	2.476
HETATM	16	H	UNK	0001	-2.108	0.305	3.014
HETATM	17	H	UNK	0001	-0.534	-0.506	3.165
HETATM	18	H	UNK	0001	-1.820	-1.225	2.164
HETATM	19	C	UNK	0001	-1.984	0.859	0.286
HETATM	20	H	UNK	0001	-2.334	1.882	0.490
HETATM	21	H	UNK	0001	-2.849	0.203	0.442
HETATM	22	C	UNK	0001	-1.524	0.767	-1.190
HETATM	23	H	UNK	0001	-0.697	1.463	-1.356
HETATM	24	H	UNK	0001	-1.112	-0.239	-1.339
HETATM	25	C	UNK	0001	-2.656	1.007	-2.151
HETATM	26	H	UNK	0001	-3.439	0.245	-2.120
HETATM	27	C	UNK	0001	-2.821	2.018	-3.019
HETATM	28	C	UNK	0001	-4.033	2.074	-3.918
HETATM	29	H	UNK	0001	-3.739	2.071	-4.978
HETATM	30	H	UNK	0001	-4.606	2.999	-3.759
HETATM	31	H	UNK	0001	-4.705	1.226	-3.752
HETATM	32	C	UNK	0001	-1.856	3.164	-3.201
HETATM	33	H	UNK	0001	-1.487	3.202	-4.236
HETATM	34	H	UNK	0001	-0.988	3.110	-2.540
HETATM	35	H	UNK	0001	-2.358	4.125	-3.017
HETATM	36	C	UNK	0001	4.021	-4.183	0.737
HETATM	37	H	UNK	0001	3.535	-4.717	-0.085
HETATM	38	H	UNK	0001	4.085	-4.866	1.594
HETATM	39	H	UNK	0001	5.051	-3.951	0.437
HETATM	40	O	UNK	0001	3.821	-0.009	3.244
HETATM	41	H	UNK	0001	3.158	0.598	3.607
CONNECT	1	2	3				
CONNECT	2	1	8	13			
CONNECT	3	1	4	15	19		
CONNECT	4	5	3	6			
CONNECT	5	4					
CONNECT	6	7	4	8			
CONNECT	7	6					
CONNECT	8	6	2	9			
CONNECT	9	8	10	40			
CONNECT	10	11	9	12			
CONNECT	11	10					
CONNECT	12	10	13	36			

CONECT 13 14 2 12  
 CONECT 14 13  
 CONECT 15 16 17 18 3  
 CONECT 16 15  
 CONECT 17 15  
 CONECT 18 15  
 CONECT 19 20 21 3 22  
 CONECT 20 19  
 CONECT 21 19  
 CONECT 22 23 24 19 25  
 CONECT 23 22  
 CONECT 24 22  
 CONECT 25 26 22 27  
 CONECT 26 25  
 CONECT 27 25 28 32  
 CONECT 28 29 30 31 27  
 CONECT 29 28  
 CONECT 30 28  
 CONECT 31 28  
 CONECT 32 33 34 35 27  
 CONECT 33 32  
 CONECT 34 32  
 CONECT 35 32  
 CONECT 36 37 38 39 12  
 CONECT 37 36  
 CONECT 38 36  
 CONECT 39 36  
 CONECT 40 41 9  
 CONECT 41 40  
 END

**TS *cis*-THC** (25.5 kcal/mol)  
 Energy= -509174.181 kcal/mol

HEADER

REMARK Spartan `06 exported M001

HETATM	1	C	UNK	0001	0.172	-1.858	2.407
HETATM	2	C	UNK	0001	1.039	-1.670	1.405
HETATM	3	H	UNK	0001	2.064	-2.025	1.539
HETATM	4	C	UNK	0001	-1.282	-1.443	2.363
HETATM	5	H	UNK	0001	-1.500	-0.821	3.243
HETATM	6	H	UNK	0001	-1.897	-2.349	2.495
HETATM	7	C	UNK	0001	-1.733	-0.707	1.094
HETATM	8	H	UNK	0001	-2.830	-0.628	1.108
HETATM	9	H	UNK	0001	-1.352	0.321	1.103
HETATM	10	C	UNK	0001	-1.271	-1.430	-0.159
HETATM	11	H	UNK	0001	-1.125	-2.503	-0.033
HETATM	12	C	UNK	0001	0.803	-1.062	0.071
HETATM	13	H	UNK	0001	0.986	-1.725	-0.772
HETATM	14	C	UNK	0001	1.076	0.284	-0.265
HETATM	15	C	UNK	0001	-1.619	-1.035	-1.449

HETATM	16	O	UNK	0001	0.462	-0.290	-2.463
HETATM	17	C	UNK	0001	0.902	0.604	-1.686
HETATM	18	C	UNK	0001	1.446	1.344	0.624
HETATM	19	C	UNK	0001	1.729	2.604	0.141
HETATM	20	H	UNK	0001	2.064	3.379	0.830
HETATM	21	C	UNK	0001	1.601	2.912	-1.246
HETATM	22	C	UNK	0001	1.170	1.948	-2.124
HETATM	23	H	UNK	0001	1.041	2.160	-3.182
HETATM	24	C	UNK	0001	0.604	-2.526	3.689
HETATM	25	H	UNK	0001	-0.007	-3.414	3.904
HETATM	26	H	UNK	0001	0.479	-1.848	4.546
HETATM	27	H	UNK	0001	1.653	-2.835	3.654
HETATM	28	C	UNK	0001	-1.678	-2.044	-2.560
HETATM	29	H	UNK	0001	-2.711	-2.408	-2.675
HETATM	30	H	UNK	0001	-1.044	-2.912	-2.350
HETATM	31	H	UNK	0001	-1.365	-1.606	-3.510
HETATM	32	C	UNK	0001	-2.219	0.318	-1.691
HETATM	33	H	UNK	0001	-3.233	0.371	-1.264
HETATM	34	H	UNK	0001	-2.280	0.549	-2.757
HETATM	35	H	UNK	0001	-1.633	1.106	-1.202
HETATM	36	C	UNK	0001	1.945	4.306	-1.712
HETATM	37	H	UNK	0001	3.016	4.512	-1.580
HETATM	38	H	UNK	0001	1.401	5.066	-1.137
HETATM	39	H	UNK	0001	1.706	4.443	-2.771
HETATM	40	O	UNK	0001	1.557	1.055	1.958
HETATM	41	H	UNK	0001	1.861	1.857	2.412
CONNECT	1	2	4	24			
CONNECT	2	3	1	12			
CONNECT	3	2					
CONNECT	4	5	6	1	7		
CONNECT	5	4					
CONNECT	6	4					
CONNECT	7	8	9	4	10		
CONNECT	8	7					
CONNECT	9	7					
CONNECT	10	11	7	12	15		
CONNECT	11	10					
CONNECT	12	13	10	2	14		
CONNECT	13	12					
CONNECT	14	12	17	18			
CONNECT	15	10	16	28	32		
CONNECT	16	15	17				
CONNECT	17	14	16	22			
CONNECT	18	14	19	40			
CONNECT	19	20	18	21			
CONNECT	20	19					
CONNECT	21	19	22	36			
CONNECT	22	23	17	21			
CONNECT	23	22					
CONNECT	24	25	26	27	1		
CONNECT	25	24					

CONECT 26 24  
 CONECT 27 24  
 CONECT 28 29 30 31 15  
 CONECT 29 28  
 CONECT 30 28  
 CONECT 31 28  
 CONECT 32 33 34 35 15  
 CONECT 33 32  
 CONECT 34 32  
 CONECT 35 32  
 CONECT 36 37 38 39 21  
 CONECT 37 36  
 CONECT 38 36  
 CONECT 39 36  
 CONECT 40 41 18  
 CONECT 41 40  
 END

**TS *trans*-THC (24.1 kcal/mol)**

Energy= -509175.659 kcal/mol

HEADER

REMARK Spartan `06 exported M001

HETATM	1	C	UNK	0001	0.874	0.658	-0.458
HETATM	2	C	UNK	0001	1.558	1.701	0.241
HETATM	3	C	UNK	0001	1.653	-0.501	-0.885
HETATM	4	C	UNK	0001	3.073	-0.500	-0.665
HETATM	5	H	UNK	0001	3.630	-1.367	-1.006
HETATM	6	C	UNK	0001	3.699	0.562	-0.057
HETATM	7	C	UNK	0001	2.926	1.665	0.407
HETATM	8	H	UNK	0001	3.427	2.496	0.904
HETATM	9	C	UNK	0001	-0.518	0.553	-0.722
HETATM	10	C	UNK	0001	-1.347	-1.026	0.412
HETATM	11	H	UNK	0001	-1.225	-0.482	1.348
HETATM	12	C	UNK	0001	-0.517	-2.139	0.245
HETATM	13	O	UNK	0001	1.041	-1.500	-1.375
HETATM	14	C	UNK	0001	-2.746	-0.994	-0.182
HETATM	15	H	UNK	0001	-3.338	-1.834	0.210
HETATM	16	H	UNK	0001	-2.695	-1.152	-1.268
HETATM	17	C	UNK	0001	-3.506	0.305	0.105
HETATM	18	H	UNK	0001	-4.458	0.289	-0.445
HETATM	19	H	UNK	0001	-3.797	0.336	1.168
HETATM	20	C	UNK	0001	-2.777	1.589	-0.211
HETATM	21	C	UNK	0001	-1.473	1.667	-0.526
HETATM	22	H	UNK	0001	-1.042	2.658	-0.637
HETATM	23	H	UNK	0001	-0.699	-0.105	-1.569
HETATM	24	C	UNK	0001	0.568	-2.385	1.254
HETATM	25	H	UNK	0001	1.361	-3.018	0.849
HETATM	26	H	UNK	0001	0.151	-2.886	2.142
HETATM	27	C	UNK	0001	-0.896	-3.269	-0.670
HETATM	28	H	UNK	0001	-1.687	-3.880	-0.207

HETATM	29	H	UNK	0001	-0.039	-3.914	-0.876
HETATM	30	H	UNK	0001	-1.280	-2.902	-1.625
HETATM	31	C	UNK	0001	-3.609	2.840	-0.072
HETATM	32	H	UNK	0001	-4.034	2.924	0.938
HETATM	33	H	UNK	0001	-4.460	2.826	-0.767
HETATM	34	H	UNK	0001	-3.022	3.742	-0.270
HETATM	35	C	UNK	0001	5.193	0.578	0.159
HETATM	36	H	UNK	0001	5.672	-0.296	-0.293
HETATM	37	H	UNK	0001	5.440	0.583	1.230
HETATM	38	H	UNK	0001	5.648	1.478	-0.276
HETATM	39	H	UNK	0001	1.013	-1.443	1.595
HETATM	40	O	UNK	0001	0.816	2.753	0.717
HETATM	41	H	UNK	0001	1.423	3.385	1.132
CONNECT	1	2	3	9			
CONNECT	2	1	7	40			
CONNECT	3	1	4	13			
CONNECT	4	5	3	6			
CONNECT	5	4					
CONNECT	6	4	7	35			
CONNECT	7	8	6	2			
CONNECT	8	7					
CONNECT	9	1	10	23	21		
CONNECT	10	11	9	12	14		
CONNECT	11	10					
CONNECT	12	10	13	24	27		
CONNECT	13	12	3				
CONNECT	14	15	16	10	17		
CONNECT	15	14					
CONNECT	16	14					
CONNECT	17	18	19	14	20		
CONNECT	18	17					
CONNECT	19	17					
CONNECT	20	17	21	31			
CONNECT	21	22	20	9			
CONNECT	22	21					
CONNECT	23	9					
CONNECT	24	25	26	12	39		
CONNECT	25	24					
CONNECT	26	24					
CONNECT	27	28	29	30	12		
CONNECT	28	27					
CONNECT	29	27					
CONNECT	30	27					
CONNECT	31	32	33	34	20		
CONNECT	32	31					
CONNECT	33	31					
CONNECT	34	31					
CONNECT	35	36	37	38	6		
CONNECT	36	35					
CONNECT	37	35					
CONNECT	38	35					

CONNECT 39 24  
CONNECT 40 41 2  
CONNECT 41 40  
END

**CBC** (-16.8 kcal/mol)  
Energy= -509216.547 kcal/mol

HEADER

REMARK Spartan `06 exported M001

HETATM	1	O	UNK	0001	0.844	-0.324	0.872
HETATM	2	C	UNK	0001	2.062	-0.170	0.281
HETATM	3	C	UNK	0001	0.004	0.845	1.115
HETATM	4	C	UNK	0001	0.163	1.867	0.011
HETATM	5	H	UNK	0001	-0.642	2.585	-0.119
HETATM	6	C	UNK	0001	1.278	1.926	-0.731
HETATM	7	H	UNK	0001	1.414	2.686	-1.493
HETATM	8	C	UNK	0001	2.333	0.942	-0.535
HETATM	9	C	UNK	0001	3.594	1.004	-1.154
HETATM	10	C	UNK	0001	4.539	-0.004	-0.967
HETATM	11	H	UNK	0001	5.512	0.073	-1.452
HETATM	12	C	UNK	0001	4.246	-1.112	-0.159
HETATM	13	C	UNK	0001	2.999	-1.190	0.464
HETATM	14	H	UNK	0001	2.738	-2.032	1.097
HETATM	15	C	UNK	0001	0.421	1.449	2.468
HETATM	16	H	UNK	0001	-0.202	2.317	2.711
HETATM	17	H	UNK	0001	1.464	1.779	2.430
HETATM	18	H	UNK	0001	0.315	0.706	3.267
HETATM	19	C	UNK	0001	-1.430	0.291	1.190
HETATM	20	H	UNK	0001	-2.101	1.115	1.468
HETATM	21	H	UNK	0001	-1.468	-0.435	2.012
HETATM	22	C	UNK	0001	-1.929	-0.372	-0.108
HETATM	23	H	UNK	0001	-1.931	0.365	-0.918
HETATM	24	H	UNK	0001	-1.200	-1.141	-0.394
HETATM	25	C	UNK	0001	-3.281	-1.008	0.069
HETATM	26	H	UNK	0001	-3.301	-1.818	0.802
HETATM	27	C	UNK	0001	-4.441	-0.705	-0.535
HETATM	28	C	UNK	0001	-5.702	-1.471	-0.212
HETATM	29	H	UNK	0001	-6.116	-1.950	-1.111
HETATM	30	H	UNK	0001	-6.487	-0.803	0.172
HETATM	31	H	UNK	0001	-5.526	-2.249	0.537
HETATM	32	C	UNK	0001	-4.616	0.381	-1.569
HETATM	33	H	UNK	0001	-4.977	-0.040	-2.518
HETATM	34	H	UNK	0001	-3.696	0.931	-1.778
HETATM	35	H	UNK	0001	-5.376	1.106	-1.245
HETATM	36	C	UNK	0001	5.278	-2.197	0.041
HETATM	37	H	UNK	0001	4.901	-2.991	0.694
HETATM	38	H	UNK	0001	6.195	-1.799	0.494
HETATM	39	H	UNK	0001	5.565	-2.657	-0.913
HETATM	40	O	UNK	0001	3.839	2.097	-1.943
HETATM	41	H	UNK	0001	4.717	1.999	-2.342

```

CONNECT 1 2 3
CONNECT 2 1 8 13
CONNECT 3 1 4 15 19
CONNECT 4 5 3 6
CONNECT 5 4
CONNECT 6 7 4 8
CONNECT 7 6
CONNECT 8 6 2 9
CONNECT 9 8 10 40
CONNECT 10 11 9 12
CONNECT 11 10
CONNECT 12 10 13 36
CONNECT 13 14 2 12
CONNECT 14 13
CONNECT 15 16 17 18 3
CONNECT 16 15
CONNECT 17 15
CONNECT 18 15
CONNECT 19 20 21 3 22
CONNECT 20 19
CONNECT 21 19
CONNECT 22 23 24 19 25
CONNECT 23 22
CONNECT 24 22
CONNECT 25 26 22 27
CONNECT 26 25
CONNECT 27 25 28 32
CONNECT 28 29 30 31 27
CONNECT 29 28
CONNECT 30 28
CONNECT 31 28
CONNECT 32 33 34 35 27
CONNECT 33 32
CONNECT 34 32
CONNECT 35 32
CONNECT 36 37 38 39 12
CONNECT 37 36
CONNECT 38 36
CONNECT 39 36
CONNECT 40 41 9
CONNECT 41 40
END

```

*cis*-THC (-25.4 kcal/mol)  
Energy= -509225.085 kcal/mol

```

HEADER
REMARK Spartan `06 exported M001
HETATM 1 C UNK 0001 2.571 1.482 0.147
HETATM 2 C UNK 0001 1.238 1.432 0.281
HETATM 3 H UNK 0001 0.728 1.974 1.077

```



HETATM	4	C	UNK	0001	3.174	0.602	-0.926
HETATM	5	H	UNK	0001	4.265	0.561	-0.838
HETATM	6	H	UNK	0001	2.958	1.014	-1.924
HETATM	7	C	UNK	0001	2.581	-0.823	-0.821
HETATM	8	H	UNK	0001	2.983	-1.450	-1.626
HETATM	9	H	UNK	0001	2.944	-1.259	0.116
HETATM	10	C	UNK	0001	1.030	-0.844	-0.858
HETATM	11	H	UNK	0001	0.713	-1.190	-1.851
HETATM	12	C	UNK	0001	0.426	0.584	-0.686
HETATM	13	C	UNK	0001	-1.058	0.528	-0.390
HETATM	14	C	UNK	0001	0.392	-1.850	0.133
HETATM	15	O	UNK	0001	-1.040	-1.879	-0.101
HETATM	16	C	UNK	0001	-1.709	-0.686	-0.144
HETATM	17	C	UNK	0001	-1.852	1.690	-0.442
HETATM	18	C	UNK	0001	-3.232	1.640	-0.260
HETATM	19	H	UNK	0001	-3.798	2.566	-0.310
HETATM	20	C	UNK	0001	-3.866	0.413	-0.026
HETATM	21	C	UNK	0001	-3.096	-0.748	0.037
HETATM	22	H	UNK	0001	-3.550	-1.716	0.224
HETATM	23	C	UNK	0001	3.479	2.297	1.025
HETATM	24	H	UNK	0001	4.192	1.654	1.560
HETATM	25	H	UNK	0001	2.918	2.874	1.767
HETATM	26	H	UNK	0001	4.080	2.999	0.431
HETATM	27	C	UNK	0001	0.838	-3.282	-0.176
HETATM	28	H	UNK	0001	1.904	-3.415	0.029
HETATM	29	H	UNK	0001	0.649	-3.529	-1.226
HETATM	30	H	UNK	0001	0.276	-3.987	0.446
HETATM	31	C	UNK	0001	0.618	-1.524	1.617
HETATM	32	H	UNK	0001	1.680	-1.523	1.879
HETATM	33	H	UNK	0001	0.118	-2.283	2.228
HETATM	34	H	UNK	0001	0.201	-0.549	1.880
HETATM	35	C	UNK	0001	-5.364	0.358	0.165
HETATM	36	H	UNK	0001	-5.891	0.755	-0.712
HETATM	37	H	UNK	0001	-5.680	0.958	1.028
HETATM	38	H	UNK	0001	-5.709	-0.668	0.326
HETATM	39	O	UNK	0001	-1.305	2.921	-0.698
HETATM	40	H	UNK	0001	-0.337	2.852	-0.702
HETATM	41	H	UNK	0001	0.534	1.051	-1.682
CONNECT	1	2	4	23			
CONNECT	2	3	1	12			
CONNECT	3	2					
CONNECT	4	5	6	1	7		
CONNECT	5	4					
CONNECT	6	4					
CONNECT	7	8	9	4	10		
CONNECT	8	7					
CONNECT	9	7					
CONNECT	10	11	7	12	14		
CONNECT	11	10					
CONNECT	12	10	13	41	2		
CONNECT	13	12	16	17			

CONECT 14 10 15 27 31  
 CONECT 15 14 16  
 CONECT 16 13 15 21  
 CONECT 17 13 18 39  
 CONECT 18 19 17 20  
 CONECT 19 18  
 CONECT 20 18 21 35  
 CONECT 21 22 16 20  
 CONECT 22 21  
 CONECT 23 24 25 26 1  
 CONECT 24 23  
 CONECT 25 23  
 CONECT 26 23  
 CONECT 27 28 29 30 14  
 CONECT 28 27  
 CONECT 29 27  
 CONECT 30 27  
 CONECT 31 32 33 34 14  
 CONECT 32 31  
 CONECT 33 31  
 CONECT 34 31  
 CONECT 35 36 37 38 20  
 CONECT 36 35  
 CONECT 37 35  
 CONECT 38 35  
 CONECT 39 40 17  
 CONECT 40 39  
 CONECT 41 12  
 END

**trans-THC** (-27.5 kcal/mol)  
 Energy= -509227.168 kcal/mol

HEADER

REMARK Spartan `06 exported M001

HETATM	1	C	UNK	0001	2.611	1.679	-0.241
HETATM	2	C	UNK	0001	1.326	1.695	0.140
HETATM	3	H	UNK	0001	0.800	2.642	0.195
HETATM	4	C	UNK	0001	3.417	0.400	-0.321
HETATM	5	H	UNK	0001	4.373	0.532	0.209
HETATM	6	H	UNK	0001	3.695	0.224	-1.374
HETATM	7	C	UNK	0001	2.676	-0.830	0.232
HETATM	8	H	UNK	0001	3.155	-1.742	-0.141
HETATM	9	H	UNK	0001	2.759	-0.851	1.327
HETATM	10	C	UNK	0001	1.194	-0.766	-0.165
HETATM	11	H	UNK	0001	1.150	-0.565	-1.246
HETATM	12	C	UNK	0001	0.553	0.447	0.542
HETATM	13	H	UNK	0001	0.686	0.318	1.630
HETATM	14	C	UNK	0001	-0.945	0.485	0.269
HETATM	15	C	UNK	0001	0.364	-2.048	0.030
HETATM	16	O	UNK	0001	-0.942	-1.805	-0.564

HETATM	17	C	UNK	0001	-1.590	-0.634	-0.283
HETATM	18	C	UNK	0001	-1.772	1.574	0.606
HETATM	19	C	UNK	0001	-3.134	1.590	0.309
HETATM	20	H	UNK	0001	-3.729	2.462	0.575
HETATM	21	C	UNK	0001	-3.739	0.490	-0.312
HETATM	22	C	UNK	0001	-2.959	-0.627	-0.589
HETATM	23	H	UNK	0001	-3.389	-1.520	-1.031
HETATM	24	C	UNK	0001	3.338	2.940	-0.634
HETATM	25	H	UNK	0001	3.732	2.868	-1.658
HETATM	26	H	UNK	0001	4.204	3.124	0.019
HETATM	27	H	UNK	0001	2.684	3.816	-0.584
HETATM	28	C	UNK	0001	0.908	-3.220	-0.789
HETATM	29	H	UNK	0001	1.842	-3.604	-0.368
HETATM	30	H	UNK	0001	1.087	-2.919	-1.827
HETATM	31	H	UNK	0001	0.175	-4.033	-0.792
HETATM	32	C	UNK	0001	0.169	-2.460	1.496
HETATM	33	H	UNK	0001	1.133	-2.675	1.971
HETATM	34	H	UNK	0001	-0.447	-3.364	1.546
HETATM	35	H	UNK	0001	-0.331	-1.679	2.075
HETATM	36	C	UNK	0001	-5.208	0.523	-0.665
HETATM	37	H	UNK	0001	-5.390	1.147	-1.550
HETATM	38	H	UNK	0001	-5.808	0.940	0.152
HETATM	39	H	UNK	0001	-5.587	-0.480	-0.886
HETATM	40	O	UNK	0001	-1.189	2.630	1.266
HETATM	41	H	UNK	0001	-1.872	3.296	1.436
CONNECT	1	2	4	24			
CONNECT	2	3	1	12			
CONNECT	3	2					
CONNECT	4	5	6	1	7		
CONNECT	5	4					
CONNECT	6	4					
CONNECT	7	8	9	4	10		
CONNECT	8	7					
CONNECT	9	7					
CONNECT	10	11	7	12	15		
CONNECT	11	10					
CONNECT	12	13	10	2	14		
CONNECT	13	12					
CONNECT	14	12	17	18			
CONNECT	15	10	16	28	32		
CONNECT	16	15	17				
CONNECT	17	14	16	22			
CONNECT	18	14	19	40			
CONNECT	19	20	18	21			
CONNECT	20	19					
CONNECT	21	19	22	36			
CONNECT	22	23	17	21			
CONNECT	23	22					
CONNECT	24	25	26	27	1		
CONNECT	25	24					
CONNECT	26	24					

```

CONNECT 27 24
CONNECT 28 29 30 31 15
CONNECT 29 28
CONNECT 30 28
CONNECT 31 28
CONNECT 32 33 34 35 15
CONNECT 33 32
CONNECT 34 32
CONNECT 35 32
CONNECT 36 37 38 39 21
CONNECT 37 36
CONNECT 38 36
CONNECT 39 36
CONNECT 40 41 18
CONNECT 41 40
END

```

**Figure 2.2 (p.28)**

$I_{an}$  (set to 0 kcal/mol)  
Energy= -509971.466 kcal/mol

```

HEADER
REMARK Spartan `06 exported M001
HETATM  1 C UNK 0001  3.006 -0.005  1.455
HETATM  2 C UNK 0001  4.272 -0.846  1.349
HETATM  3 H UNK 0001  4.492 -1.233  2.358
HETATM  4 H UNK 0001  5.093 -0.169  1.091
HETATM  5 C UNK 0001  1.687 -0.667  1.195
HETATM  6 C UNK 0001  1.631 -2.105  0.821
HETATM  7 C UNK 0001  4.155 -2.026  0.377
HETATM  8 H UNK 0001  3.969 -1.624 -0.631
HETATM  9 C UNK 0001  2.946 -2.877  0.783
HETATM 10 H UNK 0001  3.119 -3.286  1.793
HETATM 11 H UNK 0001  2.799 -3.735  0.119
HETATM 12 O UNK 0001  3.085  1.181  1.755
HETATM 13 O UNK 0001  0.584 -2.690  0.559
HETATM 14 C UNK 0001  0.581  0.137  1.325
HETATM 15 H UNK 0001  0.825  1.159  1.607
HETATM 16 C UNK 0001 -0.799 -0.201  1.138
HETATM 17 H UNK 0001 -1.014 -1.227  0.867
HETATM 18 C UNK 0001 -1.834  0.676  1.264
HETATM 19 C UNK 0001 -3.245  0.190  1.032
HETATM 20 H UNK 0001 -3.836  0.368  1.944
HETATM 21 H UNK 0001 -3.235 -0.893  0.867
HETATM 22 C UNK 0001 -3.982  0.876 -0.151
HETATM 23 H UNK 0001 -4.099  1.945  0.053
HETATM 24 H UNK 0001 -5.001  0.460 -0.173

```

HETATM	25	C	UNK	0001	-3.312	0.634	-1.478
HETATM	26	H	UNK	0001	-3.076	-0.413	-1.674
HETATM	27	C	UNK	0001	-2.984	1.524	-2.427
HETATM	28	C	UNK	0001	-2.316	1.074	-3.705
HETATM	29	H	UNK	0001	-1.344	1.569	-3.839
HETATM	30	H	UNK	0001	-2.922	1.338	-4.584
HETATM	31	H	UNK	0001	-2.149	-0.008	-3.720
HETATM	32	C	UNK	0001	-3.236	3.010	-2.348
HETATM	33	H	UNK	0001	-2.297	3.571	-2.454
HETATM	34	H	UNK	0001	-3.711	3.322	-1.414
HETATM	35	H	UNK	0001	-3.884	3.336	-3.174
HETATM	36	C	UNK	0001	-1.695	2.132	1.618
HETATM	37	H	UNK	0001	-0.703	2.400	1.984
HETATM	38	H	UNK	0001	-2.428	2.410	2.386
HETATM	39	H	UNK	0001	-1.906	2.760	0.742
HETATM	40	C	UNK	0001	5.442	-2.856	0.329
HETATM	41	H	UNK	0001	5.675	-3.276	1.316
HETATM	42	H	UNK	0001	6.297	-2.245	0.017
HETATM	43	H	UNK	0001	5.349	-3.690	-0.375
CONNECT	1	2	5	12			
CONNECT	2	3	4	1	7		
CONNECT	3	2					
CONNECT	4	2					
CONNECT	5	1	6	14			
CONNECT	6	5	9	13			
CONNECT	7	8	2	9	40		
CONNECT	8	7					
CONNECT	9	10	11	6	7		
CONNECT	10	9					
CONNECT	11	9					
CONNECT	12	1					
CONNECT	13	6					
CONNECT	14	15	5	16			
CONNECT	15	14					
CONNECT	16	17	14	18			
CONNECT	17	16					
CONNECT	18	16	19	36			
CONNECT	19	20	21	18	22		
CONNECT	20	19					
CONNECT	21	19					
CONNECT	22	23	24	19	25		
CONNECT	23	22					
CONNECT	24	22					
CONNECT	25	26	22	27			
CONNECT	26	25					
CONNECT	27	25	28	32			
CONNECT	28	29	30	31	27		
CONNECT	29	28					
CONNECT	30	28					
CONNECT	31	28					
CONNECT	32	33	34	35	27		

CONECT 33 32  
 CONECT 34 32  
 CONECT 35 32  
 CONECT 36 37 38 39 18  
 CONECT 37 36  
 CONECT 38 36  
 CONECT 39 36  
 CONECT 40 41 42 43 7  
 CONECT 41 40  
 CONECT 42 40  
 CONECT 43 40  
 END

**TS CBC<sub>an</sub>** (17.8 kcal/mol)  
 Energy= -509953.660 kcal/mol

HEADER

REMARK Spartan `06 exported M001

HETATM	1	O	UNK	0001	-0.145	-1.172	0.724
HETATM	2	C	UNK	0001	1.043	-1.297	1.120
HETATM	3	C	UNK	0001	-0.984	0.722	1.286
HETATM	4	C	UNK	0001	0.183	1.508	1.253
HETATM	5	H	UNK	0001	0.154	2.449	0.704
HETATM	6	C	UNK	0001	1.408	1.064	1.730
HETATM	7	H	UNK	0001	2.218	1.779	1.865
HETATM	8	C	UNK	0001	1.780	-0.294	1.845
HETATM	9	C	UNK	0001	3.131	-0.578	2.368
HETATM	10	C	UNK	0001	3.684	-1.985	2.169
HETATM	11	H	UNK	0001	3.306	-2.627	2.982
HETATM	12	H	UNK	0001	4.771	-1.932	2.282
HETATM	13	C	UNK	0001	3.265	-2.580	0.817
HETATM	14	H	UNK	0001	3.635	-1.910	0.026
HETATM	15	C	UNK	0001	1.735	-2.603	0.741
HETATM	16	H	UNK	0001	1.375	-2.881	-0.256
HETATM	17	H	UNK	0001	1.349	-3.374	1.428
HETATM	18	O	UNK	0001	3.790	0.277	2.955
HETATM	19	C	UNK	0001	-1.435	0.072	2.566
HETATM	20	H	UNK	0001	-2.144	0.758	3.055
HETATM	21	H	UNK	0001	-0.606	-0.100	3.255
HETATM	22	H	UNK	0001	-1.959	-0.869	2.374
HETATM	23	C	UNK	0001	-2.075	0.975	0.271
HETATM	24	H	UNK	0001	-2.519	1.957	0.499
HETATM	25	H	UNK	0001	-2.877	0.241	0.413
HETATM	26	C	UNK	0001	-1.609	0.956	-1.201
HETATM	27	H	UNK	0001	-0.829	1.709	-1.350
HETATM	28	H	UNK	0001	-1.135	-0.018	-1.381
HETATM	29	C	UNK	0001	-2.755	1.151	-2.157
HETATM	30	H	UNK	0001	-3.506	0.359	-2.123
HETATM	31	C	UNK	0001	-2.964	2.156	-3.021
HETATM	32	C	UNK	0001	-4.186	2.169	-3.910
HETATM	33	H	UNK	0001	-3.901	2.180	-4.972

HETATM	34	H	UNK	0001	-4.789	3.073	-3.743
HETATM	35	H	UNK	0001	-4.827	1.298	-3.741
HETATM	36	C	UNK	0001	-2.046	3.340	-3.209
HETATM	37	H	UNK	0001	-1.688	3.391	-4.247
HETATM	38	H	UNK	0001	-1.171	3.319	-2.555
HETATM	39	H	UNK	0001	-2.584	4.279	-3.021
HETATM	40	C	UNK	0001	3.861	-3.972	0.584
HETATM	41	H	UNK	0001	3.560	-4.374	-0.391
HETATM	42	H	UNK	0001	3.528	-4.678	1.356
HETATM	43	H	UNK	0001	4.957	-3.941	0.611
CONNECT	1	2	3				
CONNECT	2	1	8	15			
CONNECT	3	1	4	19	23		
CONNECT	4	5	3	6			
CONNECT	5	4					
CONNECT	6	7	4	8			
CONNECT	7	6					
CONNECT	8	6	2	9			
CONNECT	9	8	10	18			
CONNECT	10	11	12	9	13		
CONNECT	11	10					
CONNECT	12	10					
CONNECT	13	14	10	15	40		
CONNECT	14	13					
CONNECT	15	16	17	2	13		
CONNECT	16	15					
CONNECT	17	15					
CONNECT	18	9					
CONNECT	19	20	21	22	3		
CONNECT	20	19					
CONNECT	21	19					
CONNECT	22	19					
CONNECT	23	24	25	3	26		
CONNECT	24	23					
CONNECT	25	23					
CONNECT	26	27	28	23	29		
CONNECT	27	26					
CONNECT	28	26					
CONNECT	29	30	26	31			
CONNECT	30	29					
CONNECT	31	29	32	36			
CONNECT	32	33	34	35	31		
CONNECT	33	32					
CONNECT	34	32					
CONNECT	35	32					
CONNECT	36	37	38	39	31		
CONNECT	37	36					
CONNECT	38	36					
CONNECT	39	36					
CONNECT	40	41	42	43	13		
CONNECT	41	40					

CONNECT 42 40  
CONNECT 43 40  
END

**TS *cis*-THC<sub>an</sub>** (29.3 kcal/mol)  
Energy= -509942.187 kcal/mol

HEADER

REMARK Spartan `06 exported M001

HETATM	1	C	UNK	0001	-1.290	-2.123	0.129
HETATM	2	C	UNK	0001	-0.622	-3.476	0.383
HETATM	3	H	UNK	0001	-1.399	-4.172	0.718
HETATM	4	H	UNK	0001	-0.262	-3.860	-0.586
HETATM	5	C	UNK	0001	-0.488	-0.931	0.380
HETATM	6	C	UNK	0001	0.925	-0.999	0.605
HETATM	7	C	UNK	0001	1.562	-2.355	0.895
HETATM	8	H	UNK	0001	2.364	-2.201	1.627
HETATM	9	H	UNK	0001	2.053	-2.706	-0.026
HETATM	10	C	UNK	0001	0.550	-3.405	1.374
HETATM	11	H	UNK	0001	0.149	-3.067	2.341
HETATM	12	O	UNK	0001	-2.453	-2.071	-0.284
HETATM	13	C	UNK	0001	-1.095	0.357	0.194
HETATM	14	H	UNK	0001	-2.168	0.240	0.028
HETATM	15	C	UNK	0001	-0.818	1.073	-1.536
HETATM	16	H	UNK	0001	-1.317	0.263	-2.070
HETATM	17	C	UNK	0001	0.574	1.092	-1.766
HETATM	18	O	UNK	0001	1.640	0.019	0.484
HETATM	19	C	UNK	0001	1.432	2.279	-1.478
HETATM	20	H	UNK	0001	1.076	3.166	-2.021
HETATM	21	H	UNK	0001	2.475	2.097	-1.747
HETATM	22	H	UNK	0001	1.389	2.509	-0.406
HETATM	23	C	UNK	0001	1.168	-0.118	-2.409
HETATM	24	H	UNK	0001	0.716	-1.025	-1.981
HETATM	25	H	UNK	0001	2.253	-0.165	-2.297
HETATM	26	H	UNK	0001	0.922	-0.133	-3.482
HETATM	27	C	UNK	0001	1.206	-4.774	1.584
HETATM	28	H	UNK	0001	1.618	-5.162	0.643
HETATM	29	H	UNK	0001	0.481	-5.508	1.957
HETATM	30	H	UNK	0001	2.028	-4.713	2.307
HETATM	31	C	UNK	0001	-0.742	1.460	1.133
HETATM	32	H	UNK	0001	-0.310	1.135	2.076
HETATM	33	C	UNK	0001	-0.933	2.775	0.939
HETATM	34	C	UNK	0001	-1.395	3.353	-0.375
HETATM	35	H	UNK	0001	-2.298	3.960	-0.212
HETATM	36	H	UNK	0001	-0.634	4.075	-0.707
HETATM	37	C	UNK	0001	-1.692	2.333	-1.489
HETATM	38	H	UNK	0001	-1.642	2.839	-2.462
HETATM	39	H	UNK	0001	-2.727	1.986	-1.385
HETATM	40	C	UNK	0001	-0.630	3.782	2.020
HETATM	41	H	UNK	0001	-0.252	3.300	2.927
HETATM	42	H	UNK	0001	-1.530	4.353	2.288



```

HETATM 43 H UNK 0001 0.117 4.517 1.688
CONNECT 1 2 5 12
CONNECT 2 3 4 1 10
CONNECT 3 2
CONNECT 4 2
CONNECT 5 1 6 13
CONNECT 6 5 7 18
CONNECT 7 8 9 6 10
CONNECT 8 7
CONNECT 9 7
CONNECT 10 11 7 2 27
CONNECT 11 10
CONNECT 12 1
CONNECT 13 14 5 15 31
CONNECT 14 13
CONNECT 15 16 13 17 37
CONNECT 16 15
CONNECT 17 15 18 19 23
CONNECT 18 17 6
CONNECT 19 20 21 22 17
CONNECT 20 19
CONNECT 21 19
CONNECT 22 19
CONNECT 23 24 25 26 17
CONNECT 24 23
CONNECT 25 23
CONNECT 26 23
CONNECT 27 28 29 30 10
CONNECT 28 27
CONNECT 29 27
CONNECT 30 27
CONNECT 31 32 13 33
CONNECT 32 31
CONNECT 33 31 34 40
CONNECT 34 35 36 33 37
CONNECT 35 34
CONNECT 36 34
CONNECT 37 38 39 34 15
CONNECT 38 37
CONNECT 39 37
CONNECT 40 41 42 43 33
CONNECT 41 40
CONNECT 42 40
CONNECT 43 40
END

```

**TS *trans*-THC<sub>an</sub>** (26.9 kcal/mol)  
Energy= -509944.552 kcal/mol

HEADER  
REMARK Spartan `06 exported M001

HETATM	1	C	UNK	0001	0.683	0.542	-0.321
HETATM	2	C	UNK	0001	1.262	1.661	0.425
HETATM	3	C	UNK	0001	1.489	-0.582	-0.694
HETATM	4	C	UNK	0001	3.002	-0.532	-0.542
HETATM	5	H	UNK	0001	3.278	-1.064	0.382
HETATM	6	H	UNK	0001	3.439	-1.109	-1.366
HETATM	7	C	UNK	0001	3.546	0.901	-0.495
HETATM	8	C	UNK	0001	2.786	1.681	0.585
HETATM	9	H	UNK	0001	3.091	2.732	0.626
HETATM	10	H	UNK	0001	3.018	1.254	1.574
HETATM	11	C	UNK	0001	-0.715	0.406	-0.616
HETATM	12	C	UNK	0001	-1.597	-0.968	0.494
HETATM	13	H	UNK	0001	-1.543	-0.389	1.417
HETATM	14	C	UNK	0001	-0.798	-2.124	0.486
HETATM	15	O	UNK	0001	0.945	-1.642	-1.091
HETATM	16	O	UNK	0001	0.596	2.567	0.930
HETATM	17	C	UNK	0001	-2.975	-0.993	-0.162
HETATM	18	H	UNK	0001	-3.576	-1.812	0.258
HETATM	19	H	UNK	0001	-2.869	-1.215	-1.231
HETATM	20	C	UNK	0001	-3.741	0.322	0.013
HETATM	21	H	UNK	0001	-4.639	0.301	-0.621
HETATM	22	H	UNK	0001	-4.123	0.395	1.045
HETATM	23	C	UNK	0001	-2.948	1.571	-0.283
HETATM	24	C	UNK	0001	-1.624	1.578	-0.509
HETATM	25	H	UNK	0001	-1.127	2.540	-0.600
HETATM	26	H	UNK	0001	-0.862	-0.218	-1.498
HETATM	27	C	UNK	0001	0.223	-2.284	1.571
HETATM	28	H	UNK	0001	0.970	-3.044	1.330
HETATM	29	H	UNK	0001	-0.269	-2.567	2.513
HETATM	30	C	UNK	0001	-1.129	-3.304	-0.376
HETATM	31	H	UNK	0001	-1.972	-3.859	0.066
HETATM	32	H	UNK	0001	-0.280	-3.983	-0.467
HETATM	33	H	UNK	0001	-1.432	-2.997	-1.380
HETATM	34	C	UNK	0001	-3.733	2.857	-0.230
HETATM	35	H	UNK	0001	-4.214	2.987	0.750
HETATM	36	H	UNK	0001	-4.540	2.858	-0.976
HETATM	37	H	UNK	0001	-3.097	3.728	-0.413
HETATM	38	H	UNK	0001	3.332	1.374	-1.465
HETATM	39	C	UNK	0001	5.061	0.934	-0.269
HETATM	40	H	UNK	0001	5.593	0.393	-1.060
HETATM	41	H	UNK	0001	5.323	0.468	0.690
HETATM	42	H	UNK	0001	5.437	1.964	-0.253
HETATM	43	H	UNK	0001	0.728	-1.327	1.761
CONNECT	1	2	3	11			
CONNECT	2	1	8	16			
CONNECT	3	1	4	15			
CONNECT	4	5	6	3	7		
CONNECT	5	4					
CONNECT	6	4					
CONNECT	7	4	8	38	39		
CONNECT	8	9	10	7	2		

CONNECT 9 8  
CONNECT 10 8  
CONNECT 11 1 12 26 24  
CONNECT 12 13 11 14 17  
CONNECT 13 12  
CONNECT 14 12 15 27 30  
CONNECT 15 14 3  
CONNECT 16 2  
CONNECT 17 18 19 12 20  
CONNECT 18 17  
CONNECT 19 17  
CONNECT 20 21 22 17 23  
CONNECT 21 20  
CONNECT 22 20  
CONNECT 23 20 24 34  
CONNECT 24 25 23 11  
CONNECT 25 24  
CONNECT 26 11  
CONNECT 27 28 29 14 43  
CONNECT 28 27  
CONNECT 29 27  
CONNECT 30 31 32 33 14  
CONNECT 31 30  
CONNECT 32 30  
CONNECT 33 30  
CONNECT 34 35 36 37 23  
CONNECT 35 34  
CONNECT 36 34  
CONNECT 37 34  
CONNECT 38 7  
CONNECT 39 40 41 42 7  
CONNECT 40 39  
CONNECT 41 39  
CONNECT 42 39  
CONNECT 43 27  
END

**CBC<sub>an</sub>** (-3.4 kcal/mol)  
Energy= -509974.861 kcal/mol

HEADER

REMARK Spartan `06 exported M001

HETATM	1	O	UNK	0001	-0.690	-1.054	-0.508
HETATM	2	C	UNK	0001	-1.734	-0.258	-0.791
HETATM	3	C	UNK	0001	0.578	-0.970	-1.266
HETATM	4	C	UNK	0001	0.720	0.370	-1.953
HETATM	5	H	UNK	0001	1.711	0.618	-2.324
HETATM	6	C	UNK	0001	-0.326	1.184	-2.138
HETATM	7	H	UNK	0001	-0.241	2.129	-2.666
HETATM	8	C	UNK	0001	-1.637	0.834	-1.603
HETATM	9	C	UNK	0001	-2.810	1.672	-1.878

HETATM	10	C	UNK	0001	-4.141	1.213	-1.284
HETATM	11	H	UNK	0001	-4.619	0.536	-2.010
HETATM	12	H	UNK	0001	-4.788	2.092	-1.200
HETATM	13	C	UNK	0001	-3.983	0.488	0.061
HETATM	14	H	UNK	0001	-3.540	1.199	0.773
HETATM	15	C	UNK	0001	-2.995	-0.679	-0.093
HETATM	16	H	UNK	0001	-2.728	-1.111	0.879
HETATM	17	H	UNK	0001	-3.462	-1.494	-0.671
HETATM	18	O	UNK	0001	-2.738	2.683	-2.570
HETATM	19	C	UNK	0001	0.539	-2.110	-2.294
HETATM	20	H	UNK	0001	1.470	-2.131	-2.871
HETATM	21	H	UNK	0001	-0.291	-1.960	-2.992
HETATM	22	H	UNK	0001	0.414	-3.077	-1.795
HETATM	23	C	UNK	0001	1.684	-1.209	-0.221
HETATM	24	H	UNK	0001	2.644	-1.250	-0.752
HETATM	25	H	UNK	0001	1.529	-2.200	0.224
HETATM	26	C	UNK	0001	1.754	-0.144	0.889
HETATM	27	H	UNK	0001	1.910	0.841	0.438
HETATM	28	H	UNK	0001	0.773	-0.103	1.382
HETATM	29	C	UNK	0001	2.811	-0.460	1.914
HETATM	30	H	UNK	0001	2.636	-1.383	2.471
HETATM	31	C	UNK	0001	3.921	0.234	2.212
HETATM	32	C	UNK	0001	4.868	-0.249	3.286
HETATM	33	H	UNK	0001	4.973	0.498	4.085
HETATM	34	H	UNK	0001	5.877	-0.413	2.881
HETATM	35	H	UNK	0001	4.529	-1.185	3.741
HETATM	36	C	UNK	0001	4.337	1.525	1.551
HETATM	37	H	UNK	0001	4.393	2.339	2.288
HETATM	38	H	UNK	0001	3.660	1.843	0.755
HETATM	39	H	UNK	0001	5.343	1.432	1.118
HETATM	40	C	UNK	0001	-5.327	0.017	0.625
HETATM	41	H	UNK	0001	-5.200	-0.488	1.590
HETATM	42	H	UNK	0001	-5.818	-0.686	-0.060
HETATM	43	H	UNK	0001	-6.007	0.863	0.778
CONNECT	1	2	3				
CONNECT	2	1	8	15			
CONNECT	3	1	4	19	23		
CONNECT	4	5	3	6			
CONNECT	5	4					
CONNECT	6	7	4	8			
CONNECT	7	6					
CONNECT	8	6	2	9			
CONNECT	9	8	10	18			
CONNECT	10	11	12	9	13		
CONNECT	11	10					
CONNECT	12	10					
CONNECT	13	14	10	15	40		
CONNECT	14	13					
CONNECT	15	16	17	2	13		
CONNECT	16	15					
CONNECT	17	15					

```

CONNECT 18 9
CONNECT 19 20 21 22 3
CONNECT 20 19
CONNECT 21 19
CONNECT 22 19
CONNECT 23 24 25 3 26
CONNECT 24 23
CONNECT 25 23
CONNECT 26 27 28 23 29
CONNECT 27 26
CONNECT 28 26
CONNECT 29 30 26 31
CONNECT 30 29
CONNECT 31 29 32 36
CONNECT 32 33 34 35 31
CONNECT 33 32
CONNECT 34 32
CONNECT 35 32
CONNECT 36 37 38 39 31
CONNECT 37 36
CONNECT 38 36
CONNECT 39 36
CONNECT 40 41 42 43 13
CONNECT 41 40
CONNECT 42 40
CONNECT 43 40
END

```

*cis*-**THC**<sub>an</sub> (-16.8 kcal/mol)  
Energy= -509988.300 kcal/mol

```

HEADER
REMARK Spartan `06 exported M001
HETATM 1 C UNK 0001 -2.537 -1.884 0.033
HETATM 2 C UNK 0001 -1.559 -1.615 -0.840
HETATM 3 H UNK 0001 -1.209 -2.389 -1.516
HETATM 4 C UNK 0001 -3.031 -0.846 1.011
HETATM 5 H UNK 0001 -3.193 -1.309 1.995
HETATM 6 H UNK 0001 -4.024 -0.483 0.695
HETATM 7 C UNK 0001 -2.063 0.334 1.151
HETATM 8 H UNK 0001 -2.546 1.132 1.723
HETATM 9 H UNK 0001 -1.184 0.017 1.726
HETATM 10 C UNK 0001 -1.616 0.851 -0.230
HETATM 11 H UNK 0001 -2.521 1.117 -0.794
HETATM 12 C UNK 0001 -0.879 -0.267 -1.014
HETATM 13 C UNK 0001 0.602 -0.301 -0.643
HETATM 14 C UNK 0001 -0.743 2.125 -0.159
HETATM 15 O UNK 0001 0.521 1.800 0.507
HETATM 16 C UNK 0001 1.166 0.681 0.113
HETATM 17 C UNK 0001 1.472 -1.338 -1.215
HETATM 18 C UNK 0001 3.194 -0.738 0.584

```

HETATM	19	C	UNK	0001	-3.209	-3.233	0.086
HETATM	20	H	UNK	0001	-3.076	-3.706	1.070
HETATM	21	H	UNK	0001	-2.812	-3.913	-0.674
HETATM	22	H	UNK	0001	-4.294	-3.144	-0.070
HETATM	23	C	UNK	0001	-0.415	2.676	-1.555
HETATM	24	H	UNK	0001	-1.335	2.981	-2.066
HETATM	25	H	UNK	0001	0.092	1.936	-2.179
HETATM	26	H	UNK	0001	0.235	3.553	-1.469
HETATM	27	C	UNK	0001	-1.342	3.239	0.702
HETATM	28	H	UNK	0001	-2.344	3.501	0.344
HETATM	29	H	UNK	0001	-0.713	4.133	0.648
HETATM	30	H	UNK	0001	-1.412	2.943	1.751
HETATM	31	O	UNK	0001	1.070	-2.139	-2.056
HETATM	32	H	UNK	0001	-0.942	-0.042	-2.090
HETATM	33	C	UNK	0001	2.943	-1.356	-0.795
HETATM	34	H	UNK	0001	3.287	-2.394	-0.853
HETATM	35	H	UNK	0001	3.511	-0.797	-1.557
HETATM	36	C	UNK	0001	2.587	0.668	0.606
HETATM	37	H	UNK	0001	2.600	1.098	1.616
HETATM	38	H	UNK	0001	3.187	1.348	-0.020
HETATM	39	H	UNK	0001	2.657	-1.344	1.329
HETATM	40	C	UNK	0001	4.680	-0.726	0.956
HETATM	41	H	UNK	0001	5.091	-1.742	0.968
HETATM	42	H	UNK	0001	4.838	-0.289	1.949
HETATM	43	H	UNK	0001	5.263	-0.138	0.235
CONNECT	1	2	4	19			
CONNECT	2	3	1	12			
CONNECT	3	2					
CONNECT	4	5	6	1	7		
CONNECT	5	4					
CONNECT	6	4					
CONNECT	7	8	9	4	10		
CONNECT	8	7					
CONNECT	9	7					
CONNECT	10	11	7	12	14		
CONNECT	11	10					
CONNECT	12	10	13	32	2		
CONNECT	13	12	16	17			
CONNECT	14	10	15	23	27		
CONNECT	15	14	16				
CONNECT	16	13	15	36			
CONNECT	17	13	31	33			
CONNECT	18	33	39	36	40		
CONNECT	19	20	21	22	1		
CONNECT	20	19					
CONNECT	21	19					
CONNECT	22	19					
CONNECT	23	24	25	26	14		
CONNECT	24	23					
CONNECT	25	23					
CONNECT	26	23					

CONECT 27 28 29 30 14  
 CONECT 28 27  
 CONECT 29 27  
 CONECT 30 27  
 CONECT 31 17  
 CONECT 32 12  
 CONECT 33 34 35 18 17  
 CONECT 34 33  
 CONECT 35 33  
 CONECT 36 37 38 16 18  
 CONECT 37 36  
 CONECT 38 36  
 CONECT 39 18  
 CONECT 40 41 42 43 18  
 CONECT 41 40  
 CONECT 42 40  
 CONECT 43 40  
 END

*trans*-THC<sub>an</sub> (-15.8 kcal/mol)  
 Energy= -509987.258 kcal/mol

HEADER

REMARK Spartan `06 exported M001

HETATM	1	C	UNK	0001	2.824	1.728	-0.108
HETATM	2	C	UNK	0001	1.542	1.730	0.282
HETATM	3	H	UNK	0001	1.024	2.670	0.433
HETATM	4	C	UNK	0001	3.616	0.451	-0.294
HETATM	5	H	UNK	0001	4.585	0.540	0.219
HETATM	6	H	UNK	0001	3.865	0.337	-1.362
HETATM	7	C	UNK	0001	2.877	-0.803	0.204
HETATM	8	H	UNK	0001	3.348	-1.698	-0.218
HETATM	9	H	UNK	0001	2.972	-0.877	1.295
HETATM	10	C	UNK	0001	1.390	-0.714	-0.171
HETATM	11	H	UNK	0001	1.334	-0.465	-1.241
HETATM	12	C	UNK	0001	0.755	0.466	0.594
HETATM	13	H	UNK	0001	0.860	0.283	1.677
HETATM	14	C	UNK	0001	-0.733	0.538	0.277
HETATM	15	C	UNK	0001	0.572	-2.007	-0.012
HETATM	16	O	UNK	0001	-0.788	-1.738	-0.500
HETATM	17	C	UNK	0001	-1.369	-0.545	-0.254
HETATM	18	C	UNK	0001	-1.529	1.720	0.642
HETATM	19	C	UNK	0001	-3.669	0.418	0.156
HETATM	20	C	UNK	0001	3.569	3.008	-0.393
HETATM	21	H	UNK	0001	3.974	3.013	-1.416
HETATM	22	H	UNK	0001	4.429	3.128	0.282
HETATM	23	H	UNK	0001	2.924	3.885	-0.279
HETATM	24	C	UNK	0001	1.061	-3.125	-0.934
HETATM	25	H	UNK	0001	2.021	-3.524	-0.592
HETATM	26	H	UNK	0001	1.178	-2.761	-1.960
HETATM	27	H	UNK	0001	0.334	-3.943	-0.941

HETATM	28	C	UNK	0001	0.448	-2.508	1.432
HETATM	29	H	UNK	0001	1.434	-2.765	1.836
HETATM	30	H	UNK	0001	-0.177	-3.406	1.461
HETATM	31	H	UNK	0001	-0.004	-1.756	2.085
HETATM	32	C	UNK	0001	-5.110	0.492	-0.358
HETATM	33	H	UNK	0001	-5.143	0.849	-1.396
HETATM	34	H	UNK	0001	-5.708	1.179	0.251
HETATM	35	H	UNK	0001	-5.594	-0.492	-0.328
HETATM	36	O	UNK	0001	-1.068	2.641	1.313
HETATM	37	C	UNK	0001	-2.975	1.784	0.154
HETATM	38	H	UNK	0001	-3.501	2.512	0.779
HETATM	39	H	UNK	0001	-2.966	2.186	-0.872
HETATM	40	H	UNK	0001	-3.694	0.056	1.195
HETATM	41	C	UNK	0001	-2.822	-0.569	-0.657
HETATM	42	H	UNK	0001	-2.895	-0.324	-1.729
HETATM	43	H	UNK	0001	-3.193	-1.594	-0.549
CONNECT	1	2	4	20			
CONNECT	2	3	1	12			
CONNECT	3	2					
CONNECT	4	5	6	1	7		
CONNECT	5	4					
CONNECT	6	4					
CONNECT	7	8	9	4	10		
CONNECT	8	7					
CONNECT	9	7					
CONNECT	10	11	7	12	15		
CONNECT	11	10					
CONNECT	12	13	10	2	14		
CONNECT	13	12					
CONNECT	14	12	17	18			
CONNECT	15	10	16	24	28		
CONNECT	16	15	17				
CONNECT	17	14	16	41			
CONNECT	18	14	36	37			
CONNECT	19	32	37	40	41		
CONNECT	20	21	22	23	1		
CONNECT	21	20					
CONNECT	22	20					
CONNECT	23	20					
CONNECT	24	25	26	27	15		
CONNECT	25	24					
CONNECT	26	24					
CONNECT	27	24					
CONNECT	28	29	30	31	15		
CONNECT	29	28					
CONNECT	30	28					
CONNECT	31	28					
CONNECT	32	33	34	35	19		
CONNECT	33	32					
CONNECT	34	32					
CONNECT	35	32					



```

CONNECT 36 18
CONNECT 37 38 39 19 18
CONNECT 38 37
CONNECT 39 37
CONNECT 40 19
CONNECT 41 42 43 17 19
CONNECT 42 41
CONNECT 43 41
END

```

**Scheme 2.9 (p.43)**

*trans*- $\Delta^1$ -THC<sub>est</sub> (-13.88 kcal/mol)  
Energy= -508606.086 kcal/mol

```

HEADER
REMARK Spartan `06 exported M001
HETATM 1 C UNK 0001 2.034 -0.765 -1.594
HETATM 2 C UNK 0001 1.325 1.660 -1.222
HETATM 3 C UNK 0001 -0.108 -0.208 -0.381
HETATM 4 C UNK 0001 0.637 1.080 0.021
HETATM 5 C UNK 0001 0.902 -1.164 -0.999
HETATM 6 C UNK 0001 2.426 0.695 -1.697
HETATM 7 H UNK 0001 1.762 2.644 -1.019
HETATM 8 H UNK 0001 0.666 -2.223 -0.971
HETATM 9 H UNK 0001 2.709 0.929 -2.734
HETATM 10 H UNK 0001 0.585 1.798 -2.021
HETATM 11 H UNK 0001 -0.841 0.042 -1.166
HETATM 12 H UNK 0001 1.429 0.784 0.725
HETATM 13 H UNK 0001 3.342 0.856 -1.106
HETATM 14 C UNK 0001 -0.869 -0.773 0.817
HETATM 15 C UNK 0001 -0.273 2.024 0.819
HETATM 16 O UNK 0001 -0.700 1.296 2.014
HETATM 17 C UNK 0001 -1.071 -0.006 1.927
HETATM 18 C UNK 0001 3.009 -1.748 -2.192
HETATM 19 H UNK 0001 4.000 -1.659 -1.722
HETATM 20 H UNK 0001 3.156 -1.562 -3.265
HETATM 21 H UNK 0001 2.669 -2.781 -2.070
HETATM 22 C UNK 0001 0.485 3.226 1.385
HETATM 23 H UNK 0001 1.400 2.905 1.895
HETATM 24 H UNK 0001 -0.144 3.753 2.109
HETATM 25 H UNK 0001 0.754 3.929 0.591
HETATM 26 C UNK 0001 -1.531 2.481 0.069
HETATM 27 H UNK 0001 -1.259 3.032 -0.837
HETATM 28 H UNK 0001 -2.127 3.142 0.707
HETATM 29 H UNK 0001 -2.157 1.632 -0.219
HETATM 30 C UNK 0001 -1.503 -2.104 0.713
HETATM 31 O UNK 0001 -1.861 -2.849 1.610
HETATM 32 O UNK 0001 -1.698 -2.440 -0.597
HETATM 33 C UNK 0001 -2.331 -3.706 -0.816
HETATM 34 H UNK 0001 -3.332 -3.720 -0.376
HETATM 35 H UNK 0001 -1.744 -4.517 -0.375

```

```

HETATM 36 H UNK 0001 -2.388 -3.821 -1.899
HETATM 37 C UNK 0001 -1.725 -0.408 3.218
HETATM 38 H UNK 0001 -2.052 -1.444 3.201
HETATM 39 H UNK 0001 -2.571 0.260 3.423
HETATM 40 H UNK 0001 -1.005 -0.268 4.034
CONNECT 1 5 6 18
CONNECT 2 7 10 4 6
CONNECT 3 11 5 4 14
CONNECT 4 2 3 12 15
CONNECT 5 1 3 8
CONNECT 6 1 2 9 13
CONNECT 7 2
CONNECT 8 5
CONNECT 9 6
CONNECT 10 2
CONNECT 11 3
CONNECT 12 4
CONNECT 13 6
CONNECT 14 3 17 30
CONNECT 15 4 16 22 26
CONNECT 16 15 17
CONNECT 17 16 14 37
CONNECT 18 19 20 21 1
CONNECT 19 18
CONNECT 20 18
CONNECT 21 18
CONNECT 22 23 24 25 15
CONNECT 23 22
CONNECT 24 22
CONNECT 25 22
CONNECT 26 27 28 29 15
CONNECT 27 26
CONNECT 28 26
CONNECT 29 26
CONNECT 30 14 31 32
CONNECT 31 30
CONNECT 32 30 33
CONNECT 33 34 35 36 32
CONNECT 34 33
CONNECT 35 33
CONNECT 36 33
CONNECT 37 38 39 40 17
CONNECT 38 37
CONNECT 39 37
CONNECT 40 37
END

```

*cis*- $\Delta^1$ -THC<sub>est</sub> (-12.93 kcal/mol)  
 Energy= -508605.137 kcal/mol

HEADER

REMARK Spartan `06 exported M001

HETATM	1	C	UNK	0001	2.330	-0.677	-0.956
HETATM	2	C	UNK	0001	2.346	1.020	0.947
HETATM	3	C	UNK	0001	0.412	-0.584	0.704
HETATM	4	C	UNK	0001	0.813	0.869	1.028
HETATM	5	C	UNK	0001	1.181	-1.163	-0.471
HETATM	6	C	UNK	0001	2.982	0.557	-0.375
HETATM	7	H	UNK	0001	2.758	0.401	1.755
HETATM	8	H	UNK	0001	0.681	-1.198	1.578
HETATM	9	H	UNK	0001	0.765	-2.071	-0.901
HETATM	10	H	UNK	0001	2.970	1.362	-1.126
HETATM	11	H	UNK	0001	2.649	2.049	1.173
HETATM	12	H	UNK	0001	0.535	1.050	2.076
HETATM	13	H	UNK	0001	4.050	0.356	-0.203
HETATM	14	C	UNK	0001	-1.101	-0.723	0.566
HETATM	15	C	UNK	0001	-0.035	1.899	0.241
HETATM	16	O	UNK	0001	-1.440	1.639	0.560
HETATM	17	C	UNK	0001	-1.914	0.370	0.568
HETATM	18	C	UNK	0001	-1.581	-2.113	0.575
HETATM	19	O	UNK	0001	-0.866	-3.072	0.821
HETATM	20	O	UNK	0001	-2.896	-2.272	0.252
HETATM	21	C	UNK	0001	-3.360	-3.628	0.258
HETATM	22	H	UNK	0001	-2.815	-4.226	-0.478
HETATM	23	H	UNK	0001	-4.419	-3.575	-0.001
HETATM	24	H	UNK	0001	-3.228	-4.082	1.244
HETATM	25	C	UNK	0001	-3.420	0.414	0.610
HETATM	26	H	UNK	0001	-3.840	0.233	-0.386
HETATM	27	H	UNK	0001	-3.726	1.411	0.938
HETATM	28	H	UNK	0001	-3.834	-0.342	1.277
HETATM	29	C	UNK	0001	0.189	3.320	0.763
HETATM	30	H	UNK	0001	1.180	3.687	0.480
HETATM	31	H	UNK	0001	0.100	3.356	1.854
HETATM	32	H	UNK	0001	-0.559	3.996	0.336
HETATM	33	C	UNK	0001	0.069	1.875	-1.290
HETATM	34	H	UNK	0001	1.070	2.159	-1.623
HETATM	35	H	UNK	0001	-0.643	2.597	-1.703
HETATM	36	H	UNK	0001	-0.159	0.889	-1.698
HETATM	37	C	UNK	0001	3.042	-1.322	-2.117
HETATM	38	H	UNK	0001	4.060	-1.631	-1.839
HETATM	39	H	UNK	0001	3.148	-0.623	-2.959
HETATM	40	H	UNK	0001	2.506	-2.206	-2.477
CONNECT	1	5	6	37			
CONNECT	2	7	11	4	6		
CONNECT	3	8	5	4	14		
CONNECT	4	2	3	12	15		
CONNECT	5	1	3	9			
CONNECT	6	1	2	10	13		
CONNECT	7	2					
CONNECT	8	3					
CONNECT	9	5					
CONNECT	10	6					

```

CONNECT 11 2
CONNECT 12 4
CONNECT 13 6
CONNECT 14 3 17 18
CONNECT 15 4 16 29 33
CONNECT 16 15 17
CONNECT 17 16 14 25
CONNECT 18 14 19 20
CONNECT 19 18
CONNECT 20 18 21
CONNECT 21 22 23 24 20
CONNECT 22 21
CONNECT 23 21
CONNECT 24 21
CONNECT 25 26 27 28 17
CONNECT 26 25
CONNECT 27 25
CONNECT 28 25
CONNECT 29 30 31 32 15
CONNECT 30 29
CONNECT 31 29
CONNECT 32 29
CONNECT 33 34 35 36 15
CONNECT 34 33
CONNECT 35 33
CONNECT 36 33
CONNECT 37 38 39 40 1
CONNECT 38 37
CONNECT 39 37
CONNECT 40 37
END

```

$CBC_{est}$  (-2.84 kcal/mol)  
 Energy= -508595.047 kcal/mol

```

HEADER
REMARK Spartan`06 exported M001
HETATM 1 C UNK 0001 0.542 -1.775 -1.179
HETATM 2 C UNK 0001 1.252 -0.215 0.605
HETATM 3 C UNK 0001 -0.226 -2.126 1.093
HETATM 4 O UNK 0001 0.225 -0.897 1.412
HETATM 5 C UNK 0001 -0.052 -2.648 -0.163
HETATM 6 C UNK 0001 1.113 -0.612 -0.843
HETATM 7 H UNK 0001 1.524 0.061 -1.591
HETATM 8 H UNK 0001 0.475 -2.087 -2.215
HETATM 9 C UNK 0001 -0.524 -3.998 -0.517
HETATM 10 O UNK 0001 -0.998 -4.839 0.230
HETATM 11 O UNK 0001 -0.358 -4.244 -1.848
HETATM 12 C UNK 0001 2.616 -0.640 1.169
HETATM 13 H UNK 0001 3.423 -0.137 0.624
HETATM 14 H UNK 0001 2.754 -1.720 1.057

```

HETATM	15	H	UNK	0001	2.694	-0.380	2.231
HETATM	16	C	UNK	0001	1.007	1.285	0.837
HETATM	17	H	UNK	0001	1.805	1.838	0.325
HETATM	18	H	UNK	0001	1.122	1.489	1.909
HETATM	19	C	UNK	0001	-0.366	1.792	0.357
HETATM	20	H	UNK	0001	-1.142	1.202	0.863
HETATM	21	H	UNK	0001	-0.477	1.587	-0.713
HETATM	22	C	UNK	0001	-0.567	3.252	0.666
HETATM	23	H	UNK	0001	-0.569	3.488	1.732
HETATM	24	C	UNK	0001	-0.725	4.277	-0.186
HETATM	25	C	UNK	0001	-0.745	4.156	-1.691
HETATM	26	H	UNK	0001	-1.697	4.521	-2.098
HETATM	27	H	UNK	0001	-0.604	3.132	-2.045
HETATM	28	H	UNK	0001	0.042	4.779	-2.139
HETATM	29	C	UNK	0001	-0.906	5.686	0.327
HETATM	30	H	UNK	0001	-0.120	6.352	-0.057
HETATM	31	H	UNK	0001	-0.882	5.730	1.421
HETATM	32	H	UNK	0001	-1.863	6.111	-0.008
HETATM	33	C	UNK	0001	-0.956	-2.726	2.254
HETATM	34	H	UNK	0001	-0.238	-3.022	3.030
HETATM	35	H	UNK	0001	-1.529	-3.601	1.959
HETATM	36	H	UNK	0001	-1.605	-1.960	2.695
HETATM	37	C	UNK	0001	-0.785	-5.539	-2.285
HETATM	38	H	UNK	0001	-0.245	-6.326	-1.751
HETATM	39	H	UNK	0001	-0.560	-5.576	-3.352
HETATM	40	H	UNK	0001	-1.857	-5.673	-2.114
CONNECT	1	8	5	6			
CONNECT	2	4	6	12	16		
CONNECT	3	5	4	33			
CONNECT	4	2	3				
CONNECT	5	1	3	9			
CONNECT	6	1	2	7			
CONNECT	7	6					
CONNECT	8	1					
CONNECT	9	5	10	11			
CONNECT	10	9					
CONNECT	11	9	37				
CONNECT	12	13	14	15	2		
CONNECT	13	12					
CONNECT	14	12					
CONNECT	15	12					
CONNECT	16	17	18	2	19		
CONNECT	17	16					
CONNECT	18	16					
CONNECT	19	20	21	16	22		
CONNECT	20	19					
CONNECT	21	19					
CONNECT	22	23	19	24			
CONNECT	23	22					
CONNECT	24	22	25	29			
CONNECT	25	26	27	28	24		
CONNECT	26	25					

```

CONNECT 27 25
CONNECT 28 25
CONNECT 29 30 31 32 24
CONNECT 30 29
CONNECT 31 29
CONNECT 32 29
CONNECT 33 34 35 36 3
CONNECT 34 33
CONNECT 35 33
CONNECT 36 33
CONNECT 37 38 39 40 11
CONNECT 38 37
CONNECT 39 37
CONNECT 40 37
END

```

**Knoev<sub>est</sub>** ( 0 kcal/mol)  
 Energy= -508592.209 kcal/mol

HEADER

REMARK Spartan `06 exported M001

HETATM	1	C	UNK	0001	0.306	-2.064	0.932
HETATM	2	C	UNK	0001	1.780	-2.145	0.634
HETATM	3	C	UNK	0001	2.599	-3.343	1.084
HETATM	4	H	UNK	0001	3.512	-3.369	0.485
HETATM	5	H	UNK	0001	2.050	-4.284	0.980
HETATM	6	H	UNK	0001	2.866	-3.242	2.141
HETATM	7	O	UNK	0001	2.322	-1.265	-0.024
HETATM	8	C	UNK	0001	-0.360	-2.862	1.992
HETATM	9	O	UNK	0001	-1.547	-3.130	2.047
HETATM	10	O	UNK	0001	0.506	-3.249	2.965
HETATM	11	C	UNK	0001	-0.075	-4.003	4.039
HETATM	12	H	UNK	0001	-0.539	-4.919	3.663
HETATM	13	H	UNK	0001	-0.834	-3.411	4.557
HETATM	14	H	UNK	0001	0.752	-4.238	4.710
HETATM	15	C	UNK	0001	-0.402	-1.175	0.170
HETATM	16	H	UNK	0001	0.216	-0.631	-0.539
HETATM	17	C	UNK	0001	-1.801	-0.849	0.202
HETATM	18	H	UNK	0001	-2.438	-1.427	0.862
HETATM	19	C	UNK	0001	-2.348	0.157	-0.533
HETATM	20	C	UNK	0001	-3.813	0.471	-0.407
HETATM	21	H	UNK	0001	-4.322	0.334	-1.372
HETATM	22	H	UNK	0001	-3.964	1.524	-0.128
HETATM	23	H	UNK	0001	-4.309	-0.158	0.337
HETATM	24	C	UNK	0001	-1.560	1.060	-1.457
HETATM	25	H	UNK	0001	-2.234	1.485	-2.211
HETATM	26	H	UNK	0001	-0.795	0.502	-2.007
HETATM	27	C	UNK	0001	-0.860	2.225	-0.697
HETATM	28	H	UNK	0001	-1.617	2.769	-0.115
HETATM	29	H	UNK	0001	-0.164	1.797	0.030

HETATM	30	C	UNK	0001	-0.167	3.181	-1.631
HETATM	31	H	UNK	0001	-0.835	3.849	-2.179
HETATM	32	C	UNK	0001	1.149	3.283	-1.876
HETATM	33	C	UNK	0001	2.219	2.434	-1.234
HETATM	34	H	UNK	0001	2.908	3.059	-0.648
HETATM	35	H	UNK	0001	2.830	1.944	-2.004
HETATM	36	H	UNK	0001	1.836	1.648	-0.580
HETATM	37	C	UNK	0001	1.670	4.309	-2.855
HETATM	38	H	UNK	0001	2.373	4.998	-2.365
HETATM	39	H	UNK	0001	0.864	4.904	-3.296
HETATM	40	H	UNK	0001	2.227	3.830	-3.673
CONNECT	1	2	8	15			
CONNECT	2	1	3	7			
CONNECT	3	4	5	6	2		
CONNECT	4	3					
CONNECT	5	3					
CONNECT	6	3					
CONNECT	7	2					
CONNECT	8	1	9	10			
CONNECT	9	8					
CONNECT	10	8	11				
CONNECT	11	12	13	14	10		
CONNECT	12	11					
CONNECT	13	11					
CONNECT	14	11					
CONNECT	15	16	1	17			
CONNECT	16	15					
CONNECT	17	18	15	19			
CONNECT	18	17					
CONNECT	19	17	20	24			
CONNECT	20	21	22	23	19		
CONNECT	21	20					
CONNECT	22	20					
CONNECT	23	20					
CONNECT	24	25	26	19	27		
CONNECT	25	24					
CONNECT	26	24					
CONNECT	27	28	29	24	30		
CONNECT	28	27					
CONNECT	29	27					
CONNECT	30	31	27	32			
CONNECT	31	30					
CONNECT	32	30	33	37			
CONNECT	33	34	35	36	32		
CONNECT	34	33					
CONNECT	35	33					
CONNECT	36	33					
CONNECT	37	38	39	40	32		
CONNECT	38	37					
CONNECT	39	37					
CONNECT	40	37					
END							

TS *trans*- $\Delta^1$ -THC<sub>est</sub> (+28.83 kcal/mol)

Energy= -508563.376 kcal/mol

HEADER

REMARK Spartan `06 exported M001

HETATM	1	C	UNK	0001	1.179	0.463	-0.424
HETATM	2	C	UNK	0001	1.634	1.560	0.437
HETATM	3	C	UNK	0001	1.979	-0.658	-0.843
HETATM	4	C	UNK	0001	3.491	-0.732	-0.722
HETATM	5	H	UNK	0001	3.816	-0.698	0.323
HETATM	6	H	UNK	0001	3.817	-1.673	-1.174
HETATM	7	C	UNK	0001	-0.214	0.341	-0.745
HETATM	8	C	UNK	0001	-1.126	-1.024	0.323
HETATM	9	H	UNK	0001	-1.060	-0.470	1.260
HETATM	10	C	UNK	0001	-0.346	-2.194	0.283
HETATM	11	O	UNK	0001	1.378	-1.668	-1.292
HETATM	12	O	UNK	0001	0.905	2.286	1.099
HETATM	13	C	UNK	0001	-2.508	-1.014	-0.324
HETATM	14	H	UNK	0001	-3.119	-1.831	0.084
HETATM	15	H	UNK	0001	-2.414	-1.216	-1.399
HETATM	16	C	UNK	0001	-3.247	0.310	-0.118
HETATM	17	H	UNK	0001	-4.163	0.310	-0.727
HETATM	18	H	UNK	0001	-3.597	0.383	0.925
HETATM	19	C	UNK	0001	-2.437	1.544	-0.432
HETATM	20	C	UNK	0001	-1.115	1.526	-0.656
HETATM	21	H	UNK	0001	-0.613	2.482	-0.783
HETATM	22	H	UNK	0001	-0.340	-0.261	-1.645
HETATM	23	C	UNK	0001	0.679	-2.394	1.356
HETATM	24	H	UNK	0001	1.399	-3.177	1.106
HETATM	25	H	UNK	0001	0.188	-2.661	2.303
HETATM	26	C	UNK	0001	-0.700	-3.344	-0.609
HETATM	27	H	UNK	0001	-1.552	-3.898	-0.182
HETATM	28	H	UNK	0001	0.137	-4.036	-0.723
HETATM	29	H	UNK	0001	-1.000	-3.003	-1.604
HETATM	30	C	UNK	0001	-3.203	2.841	-0.401
HETATM	31	H	UNK	0001	-3.680	2.995	0.577
HETATM	32	H	UNK	0001	-4.012	2.842	-1.145
HETATM	33	H	UNK	0001	-2.556	3.701	-0.599
HETATM	34	H	UNK	0001	1.219	-1.455	1.543
HETATM	35	H	UNK	0001	3.973	0.111	-1.226
HETATM	36	O	UNK	0001	2.989	1.733	0.440
HETATM	37	C	UNK	0001	3.458	2.798	1.276
HETATM	38	H	UNK	0001	4.545	2.792	1.173
HETATM	39	H	UNK	0001	3.170	2.633	2.318
HETATM	40	H	UNK	0001	3.048	3.757	0.949
CONNECT	1	2	3	7			
CONNECT	2	1	12	36			
CONNECT	3	1	4	11			
CONNECT	4	5	6	3	35		



```

CONNECT 5 4
CONNECT 6 4
CONNECT 7 1 8 22 20
CONNECT 8 9 7 10 13
CONNECT 9 8
CONNECT 10 8 11 23 26
CONNECT 11 10 3
CONNECT 12 2
CONNECT 13 14 15 8 16
CONNECT 14 13
CONNECT 15 13
CONNECT 16 17 18 13 19
CONNECT 17 16
CONNECT 18 16
CONNECT 19 16 20 30
CONNECT 20 21 19 7
CONNECT 21 20
CONNECT 22 7
CONNECT 23 24 25 10 34
CONNECT 24 23
CONNECT 25 23
CONNECT 26 27 28 29 10
CONNECT 27 26
CONNECT 28 26
CONNECT 29 26
CONNECT 30 31 32 33 19
CONNECT 31 30
CONNECT 32 30
CONNECT 33 30
CONNECT 34 23
CONNECT 35 4
CONNECT 36 2 37
CONNECT 37 38 39 40 36
CONNECT 38 37
CONNECT 39 37
CONNECT 40 37
END

```

TS CBC<sub>est</sub> (+19.31 kcal/mol)  
Energy= -508572.900 kcal/mol

HEADER

REMARK Spartan `06 exported M001

HETATM	1	O	UNK	0001	0.068	-1.548	0.586
HETATM	2	C	UNK	0001	1.262	-1.708	0.956
HETATM	3	C	UNK	0001	-0.743	0.333	1.115
HETATM	4	C	UNK	0001	0.435	1.099	1.058
HETATM	5	H	UNK	0001	0.424	2.026	0.487
HETATM	6	C	UNK	0001	1.650	0.645	1.551
HETATM	7	H	UNK	0001	2.466	1.352	1.688
HETATM	8	C	UNK	0001	1.999	-0.714	1.706

HETATM	9	C	UNK	0001	3.316	-0.946	2.335
HETATM	10	C	UNK	0001	1.921	-2.981	0.444
HETATM	11	H	UNK	0001	1.332	-3.341	-0.403
HETATM	12	H	UNK	0001	1.905	-3.743	1.232
HETATM	13	O	UNK	0001	4.056	-0.062	2.735
HETATM	14	C	UNK	0001	-1.203	-0.276	2.414
HETATM	15	H	UNK	0001	-1.898	0.435	2.888
HETATM	16	H	UNK	0001	-0.375	-0.447	3.104
HETATM	17	H	UNK	0001	-1.742	-1.212	2.248
HETATM	18	C	UNK	0001	-1.841	0.584	0.105
HETATM	19	H	UNK	0001	-2.299	1.556	0.348
HETATM	20	H	UNK	0001	-2.631	-0.163	0.243
HETATM	21	C	UNK	0001	-1.384	0.589	-1.370
HETATM	22	H	UNK	0001	-0.610	1.347	-1.515
HETATM	23	H	UNK	0001	-0.905	-0.380	-1.566
HETATM	24	C	UNK	0001	-2.537	0.791	-2.315
HETATM	25	H	UNK	0001	-3.284	-0.006	-2.288
HETATM	26	C	UNK	0001	-2.758	1.809	-3.162
HETATM	27	C	UNK	0001	-3.986	1.830	-4.042
HETATM	28	H	UNK	0001	-3.709	1.859	-5.106
HETATM	29	H	UNK	0001	-4.592	2.727	-3.856
HETATM	30	H	UNK	0001	-4.621	0.953	-3.882
HETATM	31	C	UNK	0001	-1.848	3.000	-3.338
HETATM	32	H	UNK	0001	-1.495	3.069	-4.376
HETATM	33	H	UNK	0001	-0.969	2.975	-2.689
HETATM	34	H	UNK	0001	-2.389	3.934	-3.132
HETATM	35	H	UNK	0001	2.963	-2.840	0.153
HETATM	36	O	UNK	0001	3.621	-2.262	2.504
HETATM	37	C	UNK	0001	4.870	-2.514	3.162
HETATM	38	H	UNK	0001	5.703	-2.089	2.595
HETATM	39	H	UNK	0001	4.957	-3.601	3.216
HETATM	40	H	UNK	0001	4.871	-2.080	4.166
CONNECT	1	2	3				
CONNECT	2	1	8	10			
CONNECT	3	1	4	14	18		
CONNECT	4	5	3	6			
CONNECT	5	4					
CONNECT	6	7	4	8			
CONNECT	7	6					
CONNECT	8	6	2	9			
CONNECT	9	8	13	36			
CONNECT	10	11	12	2	35		
CONNECT	11	10					
CONNECT	12	10					
CONNECT	13	9					
CONNECT	14	15	16	17	3		
CONNECT	15	14					
CONNECT	16	14					
CONNECT	17	14					
CONNECT	18	19	20	3	21		
CONNECT	19	18					
CONNECT	20	18					

CONECT 21 22 23 18 24  
 CONECT 22 21  
 CONECT 23 21  
 CONECT 24 25 21 26  
 CONECT 25 24  
 CONECT 26 24 27 31  
 CONECT 27 28 29 30 26  
 CONECT 28 27  
 CONECT 29 27  
 CONECT 30 27  
 CONECT 31 32 33 34 26  
 CONECT 32 31  
 CONECT 33 31  
 CONECT 34 31  
 CONECT 35 10  
 CONECT 36 9 37  
 CONECT 37 38 39 40 36  
 CONECT 38 37  
 CONECT 39 37  
 CONECT 40 37  
 END

TS *cis*- $\Delta^1$ -THC<sub>est</sub> (+30.94 kcal/mol)  
 Energy= -508561.268 kcal/mol

HEADER

REMARK Spartan `06 exported M001

HETATM	1	C	UNK	0001	-1.091	-2.443	0.254
HETATM	2	C	UNK	0001	-0.233	-1.303	0.574
HETATM	3	C	UNK	0001	1.187	-1.323	0.817
HETATM	4	C	UNK	0001	1.969	-2.574	1.184
HETATM	5	H	UNK	0001	2.978	-2.268	1.469
HETATM	6	H	UNK	0001	2.028	-3.267	0.337
HETATM	7	O	UNK	0001	-2.231	-2.354	-0.191
HETATM	8	C	UNK	0001	-0.840	-0.011	0.405
HETATM	9	H	UNK	0001	-1.912	-0.116	0.231
HETATM	10	C	UNK	0001	-0.543	0.742	-1.309
HETATM	11	H	UNK	0001	-1.032	-0.059	-1.866
HETATM	12	C	UNK	0001	0.851	0.773	-1.518
HETATM	13	O	UNK	0001	1.818	-0.249	0.678
HETATM	14	C	UNK	0001	1.694	1.970	-1.222
HETATM	15	H	UNK	0001	1.351	2.845	-1.793
HETATM	16	H	UNK	0001	2.745	1.790	-1.458
HETATM	17	H	UNK	0001	1.621	2.221	-0.157
HETATM	18	C	UNK	0001	1.461	-0.414	-2.192
HETATM	19	H	UNK	0001	1.014	-1.338	-1.796
HETATM	20	H	UNK	0001	2.545	-0.456	-2.071
HETATM	21	H	UNK	0001	1.226	-0.398	-3.267
HETATM	22	C	UNK	0001	-0.499	1.079	1.366
HETATM	23	H	UNK	0001	-0.080	0.740	2.310
HETATM	24	C	UNK	0001	-0.698	2.395	1.195

HETATM	25	C	UNK	0001	-1.147	2.996	-0.113
HETATM	26	H	UNK	0001	-2.054	3.598	0.050
HETATM	27	H	UNK	0001	-0.385	3.726	-0.425
HETATM	28	C	UNK	0001	-1.426	1.995	-1.249
HETATM	29	H	UNK	0001	-1.369	2.521	-2.212
HETATM	30	H	UNK	0001	-2.460	1.641	-1.163
HETATM	31	C	UNK	0001	-0.415	3.383	2.299
HETATM	32	H	UNK	0001	-0.050	2.884	3.203
HETATM	33	H	UNK	0001	-1.320	3.947	2.565
HETATM	34	H	UNK	0001	0.336	4.125	1.993
HETATM	35	H	UNK	0001	1.492	-3.121	2.002
HETATM	36	O	UNK	0001	-0.519	-3.661	0.488
HETATM	37	C	UNK	0001	-1.354	-4.787	0.196
HETATM	38	H	UNK	0001	-0.769	-5.665	0.477
HETATM	39	H	UNK	0001	-1.607	-4.821	-0.867
HETATM	40	H	UNK	0001	-2.282	-4.744	0.774
CONNECT	1	2	7	36			
CONNECT	2	1	3	8			
CONNECT	3	2	4	13			
CONNECT	4	5	6	3	35		
CONNECT	5	4					
CONNECT	6	4					
CONNECT	7	1					
CONNECT	8	9	2	10	22		
CONNECT	9	8					
CONNECT	10	11	8	12	28		
CONNECT	11	10					
CONNECT	12	10	13	14	18		
CONNECT	13	12	3				
CONNECT	14	15	16	17	12		
CONNECT	15	14					
CONNECT	16	14					
CONNECT	17	14					
CONNECT	18	19	20	21	12		
CONNECT	19	18					
CONNECT	20	18					
CONNECT	21	18					
CONNECT	22	23	8	24			
CONNECT	23	22					
CONNECT	24	22	25	31			
CONNECT	25	26	27	24	28		
CONNECT	26	25					
CONNECT	27	25					
CONNECT	28	29	30	25	10		
CONNECT	29	28					
CONNECT	30	28					
CONNECT	31	32	33	34	24		
CONNECT	32	31					
CONNECT	33	31					
CONNECT	34	31					
CONNECT	35	4					
CONNECT	36	1	37				

CONNECT 37 38 39 40 36  
CONNECT 38 37  
CONNECT 39 37  
CONNECT 40 37  
END

CBC<sub>ketv</sub> ( +10.85 kcal/mol)  
Energy= -508581.358 kcal/mol

HEADER

REMARK Spartan `06 exported M001

HETATM	1	C	UNK	0001	1.587	-1.304	-2.103
HETATM	2	C	UNK	0001	1.591	0.088	-0.055
HETATM	3	C	UNK	0001	0.533	-2.129	-0.115
HETATM	4	O	UNK	0001	0.618	-0.918	0.444
HETATM	5	C	UNK	0001	1.026	-2.430	-1.361
HETATM	6	C	UNK	0001	1.811	-0.113	-1.533
HETATM	7	H	UNK	0001	2.210	0.728	-2.093
HETATM	8	H	UNK	0001	1.797	-1.488	-3.151
HETATM	9	C	UNK	0001	0.961	-3.738	-2.040
HETATM	10	O	UNK	0001	1.372	-3.842	-3.195
HETATM	11	C	UNK	0001	2.887	-0.132	0.738
HETATM	12	H	UNK	0001	3.643	0.597	0.425
HETATM	13	H	UNK	0001	3.281	-1.134	0.543
HETATM	14	H	UNK	0001	2.714	-0.015	1.814
HETATM	15	C	UNK	0001	0.956	1.446	0.285
HETATM	16	H	UNK	0001	1.691	2.220	0.025
HETATM	17	H	UNK	0001	0.813	1.507	1.372
HETATM	18	C	UNK	0001	-0.378	1.733	-0.429
HETATM	19	H	UNK	0001	-1.099	0.956	-0.160
HETATM	20	H	UNK	0001	-0.221	1.641	-1.513
HETATM	21	C	UNK	0001	-0.901	3.109	-0.114
HETATM	22	H	UNK	0001	-0.242	3.923	-0.426
HETATM	23	C	UNK	0001	-2.047	3.451	0.495
HETATM	24	C	UNK	0001	-3.083	2.477	1.003
HETATM	25	H	UNK	0001	-3.271	2.638	2.074
HETATM	26	H	UNK	0001	-2.799	1.431	0.866
HETATM	27	H	UNK	0001	-4.044	2.632	0.494
HETATM	28	C	UNK	0001	-2.399	4.903	0.719
HETATM	29	H	UNK	0001	-3.347	5.161	0.226
HETATM	30	H	UNK	0001	-1.625	5.576	0.336
HETATM	31	H	UNK	0001	-2.538	5.117	1.788
HETATM	32	C	UNK	0001	0.402	-4.964	-1.334
HETATM	33	H	UNK	0001	-0.658	-4.832	-1.092
HETATM	34	H	UNK	0001	0.919	-5.156	-0.387
HETATM	35	H	UNK	0001	0.522	-5.819	-2.002
HETATM	36	O	UNK	0001	-0.150	-3.007	0.631
HETATM	37	C	UNK	0001	-0.551	-2.633	1.958
HETATM	38	H	UNK	0001	0.310	-2.331	2.560
HETATM	39	H	UNK	0001	-1.006	-3.532	2.374
HETATM	40	H	UNK	0001	-1.280	-1.819	1.933

```

CONNECT 1 8 5 6
CONNECT 2 4 6 11 15
CONNECT 3 5 4 36
CONNECT 4 2 3
CONNECT 5 1 3 9
CONNECT 6 1 2 7
CONNECT 7 6
CONNECT 8 1
CONNECT 9 5 10 32
CONNECT 10 9
CONNECT 11 12 13 14 2
CONNECT 12 11
CONNECT 13 11
CONNECT 14 11
CONNECT 15 16 17 2 18
CONNECT 16 15
CONNECT 17 15
CONNECT 18 19 20 15 21
CONNECT 19 18
CONNECT 20 18
CONNECT 21 22 18 23
CONNECT 22 21
CONNECT 23 21 24 28
CONNECT 24 25 26 27 23
CONNECT 25 24
CONNECT 26 24
CONNECT 27 24
CONNECT 28 29 30 31 23
CONNECT 29 28
CONNECT 30 28
CONNECT 31 28
CONNECT 32 33 34 35 9
CONNECT 33 32
CONNECT 34 32
CONNECT 35 32
CONNECT 36 3 37
CONNECT 37 38 39 40 36
CONNECT 38 37
CONNECT 39 37
CONNECT 40 37
END

```

*trans*- $\Delta^1$ -THC<sub>ket</sub> (+0.09 kcal/mol)  
Energy= -508592.119 kcal/mol

HEADER

REMARK Spartan `06 exported M001

HETATM	1	C	UNK	0001	2.447	-0.654	-1.670
HETATM	2	C	UNK	0001	1.338	1.630	-1.376
HETATM	3	C	UNK	0001	0.095	-0.459	-0.782
HETATM	4	C	UNK	0001	0.570	0.909	-0.260

HETATM	5	C	UNK	0001	1.316	-1.236	-1.251
HETATM	6	C	UNK	0001	2.626	0.851	-1.702
HETATM	7	H	UNK	0001	1.595	2.658	-1.093
HETATM	8	H	UNK	0001	1.225	-2.316	-1.276
HETATM	9	H	UNK	0001	3.008	1.158	-2.686
HETATM	10	H	UNK	0001	0.708	1.694	-2.273
HETATM	11	H	UNK	0001	-0.540	-0.296	-1.668
HETATM	12	H	UNK	0001	1.284	0.714	0.554
HETATM	13	H	UNK	0001	3.418	1.129	-0.987
HETATM	14	C	UNK	0001	-0.751	-1.181	0.266
HETATM	15	C	UNK	0001	-0.581	1.688	0.395
HETATM	16	O	UNK	0001	-1.045	0.860	1.523
HETATM	17	C	UNK	0001	-1.195	-0.464	1.342
HETATM	18	C	UNK	0001	3.634	-1.461	-2.134
HETATM	19	H	UNK	0001	4.528	-1.235	-1.535
HETATM	20	H	UNK	0001	3.892	-1.229	-3.177
HETATM	21	H	UNK	0001	3.441	-2.536	-2.064
HETATM	22	C	UNK	0001	-0.118	2.977	1.074
HETATM	23	H	UNK	0001	0.759	2.794	1.703
HETATM	24	H	UNK	0001	-0.919	3.376	1.705
HETATM	25	H	UNK	0001	0.136	3.736	0.329
HETATM	26	C	UNK	0001	-1.779	1.955	-0.523
HETATM	27	H	UNK	0001	-1.470	2.563	-1.380
HETATM	28	H	UNK	0001	-2.556	2.502	0.021
HETATM	29	H	UNK	0001	-2.213	1.025	-0.902
HETATM	30	C	UNK	0001	-1.197	-2.550	-0.048
HETATM	31	O	UNK	0001	-0.986	-3.010	-1.172
HETATM	32	O	UNK	0001	-1.848	-1.037	2.371
HETATM	33	C	UNK	0001	-2.512	-0.200	3.327
HETATM	34	H	UNK	0001	-3.234	0.463	2.841
HETATM	35	H	UNK	0001	-1.796	0.400	3.894
HETATM	36	H	UNK	0001	-3.029	-0.893	3.993
HETATM	37	C	UNK	0001	-1.925	-3.419	0.969
HETATM	38	H	UNK	0001	-2.902	-2.996	1.229
HETATM	39	H	UNK	0001	-1.363	-3.506	1.904
HETATM	40	H	UNK	0001	-2.064	-4.404	0.519
CONNECT	1	5	6	18			
CONNECT	2	7	10	4	6		
CONNECT	3	11	5	4	14		
CONNECT	4	2	3	12	15		
CONNECT	5	1	3	8			
CONNECT	6	1	2	9	13		
CONNECT	7	2					
CONNECT	8	5					
CONNECT	9	6					
CONNECT	10	2					
CONNECT	11	3					
CONNECT	12	4					
CONNECT	13	6					
CONNECT	14	3	17	30			
CONNECT	15	4	16	22	26		
CONNECT	16	15	17				

```

CONNECT 17 16 14 32
CONNECT 18 19 20 21 1
CONNECT 19 18
CONNECT 20 18
CONNECT 21 18
CONNECT 22 23 24 25 15
CONNECT 23 22
CONNECT 24 22
CONNECT 25 22
CONNECT 26 27 28 29 15
CONNECT 27 26
CONNECT 28 26
CONNECT 29 26
CONNECT 30 14 31 37
CONNECT 31 30
CONNECT 32 17 33
CONNECT 33 34 35 36 32
CONNECT 34 33
CONNECT 35 33
CONNECT 36 33
CONNECT 37 38 39 40 30
CONNECT 38 37
CONNECT 39 37
CONNECT 40 37
END

```

*cis*- $\Delta^1$ -THC<sub>ket</sub> (+0.13 kcal/mol)  
 Energy= -508592.074 kcal/mol

HEADER

REMARK Spartan `06 exported M001

HETATM	1	C	UNK	0001	2.499	-0.790	-0.801
HETATM	2	C	UNK	0001	2.245	1.201	0.768
HETATM	3	C	UNK	0001	0.579	-0.692	0.859
HETATM	4	C	UNK	0001	0.751	0.841	0.894
HETATM	5	C	UNK	0001	1.434	-1.349	-0.212
HETATM	6	C	UNK	0001	2.958	0.609	-0.458
HETATM	7	H	UNK	0001	2.729	0.801	1.668
HETATM	8	H	UNK	0001	0.943	-1.081	1.823
HETATM	9	H	UNK	0001	1.162	-2.371	-0.463
HETATM	10	H	UNK	0001	2.839	1.259	-1.340
HETATM	11	H	UNK	0001	2.391	2.287	0.805
HETATM	12	H	UNK	0001	0.431	1.178	1.890
HETATM	13	H	UNK	0001	4.042	0.600	-0.268
HETATM	14	C	UNK	0001	-0.889	-1.098	0.789
HETATM	15	C	UNK	0001	-0.224	1.566	-0.069
HETATM	16	O	UNK	0001	-1.585	1.159	0.324
HETATM	17	C	UNK	0001	-1.833	-0.134	0.582
HETATM	18	C	UNK	0001	-1.180	-2.508	1.096
HETATM	19	O	UNK	0001	-0.255	-3.254	1.426
HETATM	20	C	UNK	0001	-0.232	3.077	0.167



HETATM	21	H	UNK	0001	0.706	3.525	-0.174
HETATM	22	H	UNK	0001	-0.363	3.309	1.229
HETATM	23	H	UNK	0001	-1.053	3.542	-0.390
HETATM	24	C	UNK	0001	-0.105	1.263	-1.567
HETATM	25	H	UNK	0001	0.840	1.634	-1.970
HETATM	26	H	UNK	0001	-0.918	1.772	-2.096
HETATM	27	H	UNK	0001	-0.165	0.193	-1.777
HETATM	28	C	UNK	0001	3.309	-1.514	-1.846
HETATM	29	H	UNK	0001	4.355	-1.634	-1.530
HETATM	30	H	UNK	0001	3.333	-0.952	-2.792
HETATM	31	H	UNK	0001	2.902	-2.509	-2.054
HETATM	32	O	UNK	0001	-3.153	-0.388	0.670
HETATM	33	C	UNK	0001	-4.087	0.627	0.283
HETATM	34	H	UNK	0001	-4.001	1.511	0.919
HETATM	35	H	UNK	0001	-5.067	0.166	0.412
HETATM	36	H	UNK	0001	-3.946	0.918	-0.763
HETATM	37	C	UNK	0001	-2.587	-3.083	1.005
HETATM	38	H	UNK	0001	-3.237	-2.661	1.779
HETATM	39	H	UNK	0001	-2.512	-4.164	1.142
HETATM	40	H	UNK	0001	-3.057	-2.858	0.042
CONNECT	1	5	6	28			
CONNECT	2	7	11	4	6		
CONNECT	3	8	5	4	14		
CONNECT	4	2	3	12	15		
CONNECT	5	1	3	9			
CONNECT	6	1	2	10	13		
CONNECT	7	2					
CONNECT	8	3					
CONNECT	9	5					
CONNECT	10	6					
CONNECT	11	2					
CONNECT	12	4					
CONNECT	13	6					
CONNECT	14	3	17	18			
CONNECT	15	4	16	20	24		
CONNECT	16	15	17				
CONNECT	17	16	14	32			
CONNECT	18	14	19	37			
CONNECT	19	18					
CONNECT	20	21	22	23	15		
CONNECT	21	20					
CONNECT	22	20					
CONNECT	23	20					
CONNECT	24	25	26	27	15		
CONNECT	25	24					
CONNECT	26	24					
CONNECT	27	24					
CONNECT	28	29	30	31	1		
CONNECT	29	28					
CONNECT	30	28					
CONNECT	31	28					
CONNECT	32	17	33				

CONNECT 33 34 35 36 32  
CONNECT 34 33  
CONNECT 35 33  
CONNECT 36 33  
CONNECT 37 38 39 40 18  
CONNECT 38 37  
CONNECT 39 37  
CONNECT 40 37  
END

TS CBC<sub>ket</sub> (+25.59 kcal/mol)  
Energy= -508566.621 kcal/mol

HEADER

REMARK Spartan `06 exported M001

HETATM	1	O	UNK	0001	0.261	-1.397	0.791
HETATM	2	C	UNK	0001	1.447	-1.569	1.195
HETATM	3	C	UNK	0001	-0.486	0.389	1.300
HETATM	4	C	UNK	0001	0.677	1.206	1.275
HETATM	5	H	UNK	0001	0.631	2.155	0.745
HETATM	6	C	UNK	0001	1.893	0.756	1.742
HETATM	7	H	UNK	0001	2.713	1.457	1.881
HETATM	8	C	UNK	0001	2.251	-0.609	1.896
HETATM	9	C	UNK	0001	3.589	-0.866	2.484
HETATM	10	O	UNK	0001	4.255	0.075	2.912
HETATM	11	C	UNK	0001	-0.981	-0.151	2.620
HETATM	12	H	UNK	0001	-1.645	0.607	3.060
HETATM	13	H	UNK	0001	-0.162	-0.325	3.320
HETATM	14	H	UNK	0001	-1.559	-1.070	2.488
HETATM	15	C	UNK	0001	-1.566	0.616	0.265
HETATM	16	H	UNK	0001	-2.066	1.562	0.526
HETATM	17	H	UNK	0001	-2.328	-0.165	0.367
HETATM	18	C	UNK	0001	-1.077	0.680	-1.196
HETATM	19	H	UNK	0001	-0.322	1.465	-1.299
HETATM	20	H	UNK	0001	-0.564	-0.267	-1.412
HETATM	21	C	UNK	0001	-2.215	0.877	-2.161
HETATM	22	H	UNK	0001	-2.957	0.076	-2.149
HETATM	23	C	UNK	0001	-2.427	1.895	-3.010
HETATM	24	C	UNK	0001	-3.640	1.909	-3.910
HETATM	25	H	UNK	0001	-3.347	1.940	-4.969
HETATM	26	H	UNK	0001	-4.254	2.805	-3.734
HETATM	27	H	UNK	0001	-4.274	1.030	-3.760
HETATM	28	C	UNK	0001	-1.520	3.091	-3.170
HETATM	29	H	UNK	0001	-1.153	3.163	-4.203
HETATM	30	H	UNK	0001	-0.651	3.070	-2.509
HETATM	31	H	UNK	0001	-2.070	4.022	-2.972
HETATM	32	O	UNK	0001	2.051	-2.731	0.864
HETATM	33	C	UNK	0001	1.257	-3.699	0.166
HETATM	34	H	UNK	0001	0.339	-3.922	0.716
HETATM	35	H	UNK	0001	1.887	-4.588	0.095
HETATM	36	H	UNK	0001	0.997	-3.340	-0.834

```

HETATM 37 C UNK 0001 4.145 -2.276 2.622
HETATM 38 H UNK 0001 5.026 -2.224 3.266
HETATM 39 H UNK 0001 4.433 -2.678 1.645
HETATM 40 H UNK 0001 3.410 -2.968 3.046
CONNECT 1 2 3
CONNECT 2 1 8 32
CONNECT 3 1 4 11 15
CONNECT 4 5 3 6
CONNECT 5 4
CONNECT 6 7 4 8
CONNECT 7 6
CONNECT 8 6 2 9
CONNECT 9 8 10 37
CONNECT 10 9
CONNECT 11 12 13 14 3
CONNECT 12 11
CONNECT 13 11
CONNECT 14 11
CONNECT 15 16 17 3 18
CONNECT 16 15
CONNECT 17 15
CONNECT 18 19 20 15 21
CONNECT 19 18
CONNECT 20 18
CONNECT 21 22 18 23
CONNECT 22 21
CONNECT 23 21 24 28
CONNECT 24 25 26 27 23
CONNECT 25 24
CONNECT 26 24
CONNECT 27 24
CONNECT 28 29 30 31 23
CONNECT 29 28
CONNECT 30 28
CONNECT 31 28
CONNECT 32 2 33
CONNECT 33 34 35 36 32
CONNECT 34 33
CONNECT 35 33
CONNECT 36 33
CONNECT 37 38 39 40 9
CONNECT 38 37
CONNECT 39 37
CONNECT 40 37
END

```

TS *trans*- $\Delta^1$ -THC<sub>ket</sub> (+32.26 kcal/mol)  
Energy= -508559.948 kcal/mol

HEADER

REMARK Spartan `06 exported M001

HETATM	1	C	UNK	0001	1.145	0.700	-0.250
HETATM	2	C	UNK	0001	1.593	1.767	0.650
HETATM	3	C	UNK	0001	1.934	-0.403	-0.714
HETATM	4	C	UNK	0001	-0.263	0.547	-0.574
HETATM	5	C	UNK	0001	-1.135	-0.675	0.473
HETATM	6	H	UNK	0001	-1.059	-0.128	1.416
HETATM	7	C	UNK	0001	-0.406	-1.894	0.481
HETATM	8	O	UNK	0001	1.405	-1.447	-1.146
HETATM	9	O	UNK	0001	0.769	2.432	1.288
HETATM	10	C	UNK	0001	-2.554	-0.688	-0.107
HETATM	11	H	UNK	0001	-3.143	-1.490	0.358
HETATM	12	H	UNK	0001	-2.511	-0.922	-1.179
HETATM	13	C	UNK	0001	-3.269	0.648	0.093
HETATM	14	H	UNK	0001	-4.214	0.640	-0.470
HETATM	15	H	UNK	0001	-3.565	0.761	1.149
HETATM	16	C	UNK	0001	-2.445	1.846	-0.310
HETATM	17	C	UNK	0001	-1.130	1.773	-0.551
HETATM	18	H	UNK	0001	-0.598	2.697	-0.764
HETATM	19	H	UNK	0001	-0.365	-0.016	-1.505
HETATM	20	C	UNK	0001	0.625	-2.079	1.540
HETATM	21	H	UNK	0001	1.280	-2.934	1.352
HETATM	22	H	UNK	0001	0.143	-2.212	2.520
HETATM	23	C	UNK	0001	-0.788	-3.041	-0.396
HETATM	24	H	UNK	0001	-1.672	-3.550	0.022
HETATM	25	H	UNK	0001	0.020	-3.771	-0.479
HETATM	26	H	UNK	0001	-1.057	-2.704	-1.401
HETATM	27	C	UNK	0001	-3.181	3.160	-0.349
HETATM	28	H	UNK	0001	-3.632	3.389	0.627
HETATM	29	H	UNK	0001	-4.006	3.135	-1.076
HETATM	30	H	UNK	0001	-2.518	3.989	-0.613
HETATM	31	H	UNK	0001	1.232	-1.164	1.629
HETATM	32	C	UNK	0001	3.073	2.096	0.810
HETATM	33	H	UNK	0001	3.606	1.288	1.324
HETATM	34	H	UNK	0001	3.147	3.012	1.400
HETATM	35	H	UNK	0001	3.567	2.228	-0.158
HETATM	36	O	UNK	0001	3.289	-0.308	-0.610
HETATM	37	C	UNK	0001	4.022	-1.459	-1.041
HETATM	38	H	UNK	0001	5.075	-1.184	-0.950
HETATM	39	H	UNK	0001	3.782	-1.712	-2.077
HETATM	40	H	UNK	0001	3.803	-2.326	-0.409
CONNECT	1	2	3	4			
CONNECT	2	1	9	32			
CONNECT	3	1	8	36			
CONNECT	4	1	5	19	17		
CONNECT	5	6	4	7	10		
CONNECT	6	5					
CONNECT	7	5	8	20	23		
CONNECT	8	7	3				
CONNECT	9	2					
CONNECT	10	11	12	5	13		

```

CONNECT 11 10
CONNECT 12 10
CONNECT 13 14 15 10 16
CONNECT 14 13
CONNECT 15 13
CONNECT 16 13 17 27
CONNECT 17 18 16 4
CONNECT 18 17
CONNECT 19 4
CONNECT 20 21 22 7 31
CONNECT 21 20
CONNECT 22 20
CONNECT 23 24 25 26 7
CONNECT 24 23
CONNECT 25 23
CONNECT 26 23
CONNECT 27 28 29 30 16
CONNECT 28 27
CONNECT 29 27
CONNECT 30 27
CONNECT 31 20
CONNECT 32 33 34 35 2
CONNECT 33 32
CONNECT 34 32
CONNECT 35 32
CONNECT 36 3 37
CONNECT 37 38 39 40 36
CONNECT 38 37
CONNECT 39 37
CONNECT 40 37
END

```

TS *cis*- $\Delta^1$ -THC<sub>ket</sub> (+33.17 kcal/mol)  
Energy= -508559.040 kcal/mol

```

HEADER
REMARK Spartan`06 exported M001
HETATM 1 C UNK 0001 -1.330 -2.621 0.178
HETATM 2 C UNK 0001 -0.497 -1.455 0.478
HETATM 3 C UNK 0001 0.913 -1.427 0.720
HETATM 4 O UNK 0001 -2.480 -2.469 -0.259
HETATM 5 C UNK 0001 -1.117 -0.149 0.301
HETATM 6 H UNK 0001 -2.194 -0.310 0.193
HETATM 7 C UNK 0001 -0.872 0.562 -1.293
HETATM 8 H UNK 0001 -1.370 -0.207 -1.889
HETATM 9 C UNK 0001 0.528 0.605 -1.591
HETATM 10 O UNK 0001 1.582 -0.389 0.558
HETATM 11 C UNK 0001 1.378 1.799 -1.333
HETATM 12 H UNK 0001 1.016 2.666 -1.906

```

HETATM	13	H	UNK	0001	2.423	1.617	-1.596
HETATM	14	H	UNK	0001	1.327	2.065	-0.271
HETATM	15	C	UNK	0001	1.084	-0.586	-2.285
HETATM	16	H	UNK	0001	0.711	-1.496	-1.783
HETATM	17	H	UNK	0001	2.175	-0.599	-2.313
HETATM	18	H	UNK	0001	0.697	-0.642	-3.314
HETATM	19	C	UNK	0001	-0.806	0.916	1.313
HETATM	20	H	UNK	0001	-0.431	0.549	2.266
HETATM	21	C	UNK	0001	-0.987	2.236	1.162
HETATM	22	C	UNK	0001	-1.421	2.851	-0.145
HETATM	23	H	UNK	0001	-2.317	3.469	0.020
HETATM	24	H	UNK	0001	-0.648	3.567	-0.462
HETATM	25	C	UNK	0001	-1.725	1.844	-1.268
HETATM	26	H	UNK	0001	-1.656	2.348	-2.241
HETATM	27	H	UNK	0001	-2.765	1.513	-1.174
HETATM	28	C	UNK	0001	-0.726	3.206	2.286
HETATM	29	H	UNK	0001	-0.376	2.694	3.188
HETATM	30	H	UNK	0001	-1.636	3.766	2.545
HETATM	31	H	UNK	0001	0.030	3.954	2.006
HETATM	32	C	UNK	0001	-0.812	-4.037	0.389
HETATM	33	H	UNK	0001	0.067	-4.240	-0.233
HETATM	34	H	UNK	0001	-1.614	-4.731	0.130
HETATM	35	H	UNK	0001	-0.500	-4.195	1.426
HETATM	36	O	UNK	0001	1.520	-2.595	1.082
HETATM	37	C	UNK	0001	2.939	-2.522	1.245
HETATM	38	H	UNK	0001	3.249	-3.522	1.556
HETATM	39	H	UNK	0001	3.209	-1.786	2.008
HETATM	40	H	UNK	0001	3.432	-2.248	0.306
CONNECT	1	2	4	32			
CONNECT	2	1	3	5			
CONNECT	3	2	10	36			
CONNECT	4	1					
CONNECT	5	6	2	7	19		
CONNECT	6	5					
CONNECT	7	8	5	9	25		
CONNECT	8	7					
CONNECT	9	7	10	11	15		
CONNECT	10	9	3				
CONNECT	11	12	13	14	9		
CONNECT	12	11					
CONNECT	13	11					
CONNECT	14	11					
CONNECT	15	16	17	18	9		
CONNECT	16	15					
CONNECT	17	15					
CONNECT	18	15					
CONNECT	19	20	5	21			
CONNECT	20	19					
CONNECT	21	19	22	28			
CONNECT	22	23	24	21	25		
CONNECT	23	22					
CONNECT	24	22					

```
CONNECT 25 26 27 22 7
CONNECT 26 25
CONNECT 27 25
CONNECT 28 29 30 31 21
CONNECT 29 28
CONNECT 30 28
CONNECT 31 28
CONNECT 32 33 34 35 1
CONNECT 33 32
CONNECT 34 32
CONNECT 35 32
CONNECT 36 3 37
CONNECT 37 38 39 40 36
CONNECT 38 37
CONNECT 39 37
CONNECT 40 37
END
```

## Appendix D:

### Proteins and Ligands used in UBANTR approach

**DOCKING:** Open Eye Software used for conformer generation (Omega) and for docking (FRED) all conformers using default parameters, including a Chemgauss3 scoring method. Electrostatic charges were applied to all FDA-approved drug conformers before docking using Spartan '08.

#### PROTEINS:

**PDB: 1A27** (17-beta-Hydroxysteroid-Dehydrogenase)

Mazza, C., Human Type I 17Beta-Hydroxysteroid Dehydrogenase: Site Directed Mutagenesis and X-Ray Crystallography Structure-Function Analysis, Thesis, Universite Joseph Fourier, 1997.

**PDB: 1B59** (Methionine Aminopeptidase)

Liu, S.; Widom, J.; Kemp, C.W.; Crews, C.M.; Clardy, J., *Science*, **1998**, 282, 1324-1327.

**PDB: 1CX2** (Cyclooxygenase-2)

Kurumbail, R.G.; Stevens, A.M.; Gierse, J.K.; McDonald, J.J.; Stegeman, R.A.; Pak, J.Y.; Gildehaus, D.; Miyashiro, J.M.; Penning, T.D.; Seibert, K.; Isakson, P.C.; Stallings, W.C., *Nature*, **1996**, 384, 644-648.

**PDB: 1HWK** (HMG-CoA Reductase)

Istvan, E.S.; Deisenhofer, J.; *Science*, **2001**, 292, 1160-1164.

**PDB: 1R9O** (Cytochrome P450 2C9)

Wester, M.R.; Yano, J.K.; Schoch, G.A.; Yang, C.; Griffin, K.J.; Stout, C.D.; Johnson, E.F.; *J.Biol.Chem.*, **2004**, 279, 35630-35637.

**PDB: 1TGM** (Phospholipase A2)

Singh, N.; Jabeen, T.; Sharma, S.; Bhushan, A.; Singh, T.P., Crystal structure of a complex formed between group II phospholipase A2 and aspirin at 1.86 Å resolution.



**PDB: 1UZE** (Angiotensin Converting Enzyme)

Natesh, R.; Schwager, S.L.U.; Evans, H.R.; Sturrock, E.D.; Acharya, K.R., *Biochemistry*, **2004**, 43, 8718.

**PDB: 1VRT** (HIV-1 Reverse Transcriptase)

Ren, J.; Esnouf, R.; Garman, E.; Somers, D.; Ross, C.; Kirby, I.; Keeling, J.; Darby, G.; Jones, Y.; Stuart, D., *Nat.Struct.Biol.*, **1995**, 2, 293-302.

**PDB: 1X70** (Dipeptidyl peptidase IV)

Kim, D.; Wang, L.; Beconi, M.; Eiermann, G.J.; Fisher, M.H.; He, H.; Hickey, G.J.; Kowalchick, J.E.; Leiting, B.; Lyons, K.; Marsilio, F.; McCann, M.E.; Patel, R.A.; Petrov, A.; Scapin, G.; Patel, S.B.; Roy, R.S.; Wu, J.K.; Wyvratt, M.J.; Zhang, B.B.; Zhu, L.; Thornberry, N.A.; Weber, A.E.; *J.Med.Chem.*, **2005**, 48, 141-151.

**PDB: 2F16** (Yeast 20S proteasome)

Groll, M.; Berkers, C.R.; Ploegh, H.L.; Ovaas, H., *Structure*, **2006**, 14, 451-456.

**PDB: 2HT8** (Neuraminidase)

Russell, R.J.; Haire, L.F.; Stevens, D.J.; Collins, P.J.; Lin, Y.P.; Blackburn, G.M.; Hay, A.J.; Gamblin, S.J.; Skehel, J.J.; *Nature*, **2006**, 443, 45-49.

**PDB: 2JEY** (Acetylcholinesterase)

Ekstrom, F.J.; Astot, C.; Pang, Y., *Clin.Pharmacol.Ther.*, **2007**, 82, 282.

**PDB: 2VT4** (Beta-1 Adrenergic receptor)

Warne, A.; Serrano-Vega, M.J.; Baker, J.G.; Moukhametzianov, R.; Edwards, P.C.; Henderson, R.; Leslie, A.G.W.; Tate, C.G.; Schertler, G.F.X., *Nature*, **2008**, 454, 486.

**PDB: 3G45** (cAMP-specific 3',5'-cyclic phosphodiesterase 4B)

Burgin, A.B.; Magnusson, O.T.; Singh, J.; Witte, P.; Staker, B.L.; Bjornsson, J.M.; Thorsteinsdottir, M.; Hrafnisdottir, S.; Hagen, T.; Kiselyov, A.S.; Stewart, L.J.; Gurney, M.E., *Nat.Biotechnol.*, **2010**, 28, 63-70.

**PDB: 3MHJ** (Tankyrase-2 (catalytic PARP domain))

Wahlberg, E.; Karlberg, T.; Kouznetsova, E.; Markova, N.; Macchiarulo, A.; Thorsell, A.G.; Pol, E.; Frostell, A.; Ekblad, T.; Oncu, D.; Kull, B.; Robertson, G.M.; Pellicciari, R.; Schuler, H.; Weigelt, J., *Nat.Biotechnol.*, **2012**, 30, 283-8.

**DRUGS:**

**analgesic:** Salicylamide, Trolamine, Ethenzamide, Phenazopyridine\_Z, Phenazopyridine\_E, Hydromorphone, Ethoheptazine\_R, Ethoheptazine\_S, Tramadol, Hydrocodone, Methotrimeprazine

**analgesic; anti inflammatory:** Diflunisal, Emorfazone, Relafen, Flufenamic acid, Fenoprofen\_R, Fenoprofen\_S, Ketorolac\_R, Ketorolac\_S, Benoxaprofen\_R, Benoxaprofen\_S, Bextra, Rofecoxib, Vioxx, Azapropazone dihydrate\_R, Azapropazone dihydrate\_S

**anti inflammatory:** Mofebutazone\_R, Mofebutazone\_S, Pirprofen\_S, Pirprofen\_R, Niflumic acid, Pranoprofen\_S, Pranoprofen\_R, Tiaprofenic acid\_S, Tiaprofenic acid\_R, Mefenamic acid, Metiazinic acid, Fenbufen, Diclofenac, Bucloxic acid, Proquazone, Fentiazac, Phenylbutazone, Ibuprofen piconol\_S, Ibuprofen piconol\_R, Budesonide, Feprazone, Sulindac\_E\_R, Sulindac\_Z\_R, Sulindac\_E\_S, Sulindac\_Z\_S

**anorexic:** Clortermine, Chlorphentermine, Phendimetrazine\_RR, Phendimetrazine\_SR, Phendimetrazine\_RS, Phendimetrazine\_SS, Fenfluramine\_R, Fenfluramine\_S, Mazindol\_R, Mazindol\_S, Benzphetamine, Sibutramine\_S, Sibutramine\_R

**anthelmintic:** Arecoline, Levamisole, Pyrantel\_Z, Pyrantel\_E, Diethylcarbamazine, Dichlorophen, Albendazole, Oxamniquine\_R, Oxamniquine\_S, Flubendazole, Bephenium, Bephenium hydroxynaphthoate

**antiarrhythmic:** Adenosine, Alinidine, Procainamide, Adenosine-5-phosphate, Cifenline\_S, Cifenline\_R, Esmolol\_R, Esmolol\_S, Flecainide\_R, Flecainide\_S, Aprindine, Encainide\_R, Encainide\_S

**anticholinergic:** Etomidate\_R, Etomidate\_S, Homatropine\_R, dl methylbromide, Homatropine\_S, dl methylbromide, Atropine N-oxide\_R, Atropine N-oxide\_S, Diphemanil, Anisotropine methylbromide, Pentapiperide\_SS, Pentapiperide\_RS, Pentapiperide\_SR, Pentapiperide\_RR, Timepidium\_R bromide, Timepidium\_S bromide, Adiphenine, Proglumide\_S, Proglumide\_R, Dicyclomine, Glycopyrrolate\_SS, Glycopyrrolate\_SR, Glycopyrrolate\_RS, Glycopyrrolate\_RR, Hexocyclium\_R, Hexocyclium\_S, Oxyphencyclimine\_R, Oxyphencyclimine\_S, Mepenzolate\_S, Mepenzolate\_R, Clidinium bromide\_S, Clidinium bromide\_R, Tridihexethyl\_S, Tridihexethyl\_R, Pipenzolate bromide\_RR, Pipenzolate bromide\_SR, Pipenzolate

bromide\_RS, Pipenzolate bromide\_SS, Oxybutynin\_S, Oxybutynin\_R, Propantheline bromide,

**anticonvulsant:** Trimethadione, Ethosuximide\_R, Ethosuximide\_S, Paramethadione\_R, Paramethadione\_S, Levetiracetam, Phenacemide, Gabapentin, Phensuximide\_S, Phensuximide\_R, Metharbital, Ethotoin\_R, Ethotoin\_S, Lamotrigine, Methsuximide\_S, Methsuximide\_R, Albutoin\_R, Albutoin\_S, Primidone, Mephenytoin\_R, Mephenytoin\_S, Aminoglutethimide\_R, Aminoglutethimide\_S, Clonazepam

**antidepressant:** Fenpentadiol\_S, Fenpentadiol\_R, Isocarboxazid, Bupropion\_R, Bupropion\_S, Nomifensine\_R, Nomifensine\_S, Amoxapine, Desipramine, Protriptyline, Fluoxetine\_R, Fluoxetine\_S, Nialamide, Doxepin\_E, Doxepin\_Z, Venlafaxine\_R, Venlafaxine\_S Cymbalta, Dibenzepin, Amitriptyline, Dothiepin\_Z, Dothiepin\_E, Clomipramine, Trimipramine\_S, Trimipramine\_R, Dimetacrine, Citalopram\_R, Citalopram\_S, Butriptyline\_R, Butriptyline\_S, Sultopride\_S, Sultopride\_R

**antidiabetic:** Chlorpropamide, Glybuzole, Glycodiazine, Tolazamide, Acetohexamide, Gliclazide\_RR, Gliclazide\_RS, Gliclazide\_SR, Gliclazide\_SS, Rosiglitazone maleate\_R, Rosiglitazone maleate\_S

**antihistaminic:** Tripelennamine, Chlorpheniramine\_R, Phenindamine\_R, Phenindamine\_S, Chlorpheniramine\_S, Antazoline, Phenyltoloxamine, Dexbrompheniramine, Brompheniramine\_R, Brompheniramine\_S, Carbinoxamine\_R, Carbinoxamine\_S, Bromodiphenhydramine\_S, Bromodiphenhydramine\_R, Triprolidine\_E, Triprolidine\_Z, Diphenylpyraline, Pyrilamine, Mequitazine\_R, Mequitazine\_S, Dimethindene\_S, Dimethindene\_R, Oxomemazine\_R, Oxomemazine\_S, Pyrrobutamine\_E, Pyrrobutamine\_Z, Clemastine, Acrivastine\_ZZ, Acrivastine\_ZE, Acrivastine\_EE, Acrivastine\_EZ, Cetirizine\_S, Cetirizine\_R

**antihyperlipoproteinemic:** Clofibrate, Ciprofibrate\_R, Ciprofibrate\_S, Gemfibrozil, Clofibril, fluvastatin, lovastatin, pravastatin, simvastatin, rosuvastatin

**antihypertensive:** Hydralazine, Guancydine\_S, Guancydine\_R, Diazoxide, Pargyline, Clonidine, Bethanidine\_Z, Bethanidine\_E, Methyldopa, Lofexidine\_R, Lofexidine\_S, Mebutamate\_S, Mebutamate\_R, Cyclopenthiazide\_R, Cyclopenthiazide\_S, Phenoxybenzamine\_R, Phenoxybenzamine\_S, Labetalol\_RR, Labetalol\_SR, Labetalol\_RS, Labetalol\_SS, Nitrendipine\_R, Nitrendipine\_S, Terazosin\_R, Terazosin\_S, Bunazosin, Enalapril, Moveltipril, Bopindolol\_S, Bopindolol\_R, Losartan, Eprosartan\_Z, Eprosartan\_E, Candesartan, Ramipril, Irbesartan, Trandolapril, Valsartan

**antihypertensive; antianginal:** Nadolol\_S, Nadolol\_R, Felodipine\_R, Felodipine\_S, Isradipine\_R, Isradipine\_S, Nisoldipine\_R, Nisoldipine\_S, Celiprolol\_R, Celiprolol\_S, Carvedilol\_S, Carvedilol\_R

**antineoplastic:** Thioguanine, Mechlorethamine, Nitrogen mustard oxide, Dacarbazine, Tegafur-Uracil\_R, Tegafur-Uracil\_S, Thio-TEPA, Dibromodulcitol, Dibromomannitol, Azacytidine, 5- Busulfan, Lomustine, Altretamine, Streptozocin, Cladribine, Procarbazine, ICRF-159\_S, ICRF-159\_R, Pipobroman, Chlorozotocin, Mannomustine, Fludarabine phosphate, Melphalan, Letrozole, Testolactone, Exemestane, Dromostanolone, Calusterone, Trimetrexate, AMSA, M-, Dromostanolone propionate, Mycophenolate mofetil\_Z, Mycophenolate, mofetil\_E, Proreside, Carminomycin

**antipsychotic:** Molindone\_S, Molindone\_R, Promazine, Chlorprothixene\_Z, Chlorprothixene\_E, Clozapine, Clothiapine, Triflupromazine, Bromperidol, Thioridazine\_R, Thioridazine\_S, Quetiapine, Mesoridazine\_SS, Mesoridazine\_RS, Mesoridazine\_RR, Mesoridazine\_SR, Spiclomazine, Acetophenazine, Piperacetazine, Butaperazine, Carphenazine

**anxiolytic:** Oxazepam\_R, Oxazepam\_S, Lorazepam\_R, Lorazepam\_S, Chlordiazepoxide, Alprazolam, Tybamate\_R, Tybamate\_S, Clotiazepam, Pinazepam, Halazepam, Loxapine, Prazepam

**bronchodilator:** Theophylline, Ephedrine, Methoxyphenamine\_S, Methoxyphenamine\_R, Isoproterenol\_R, Isoproterenol\_S, Dyphylline\_S, Dyphylline\_R, Doxofylline, Oxitropium bromide, Tretoquinol, Reproterol\_S, Reproterol\_R, Etofylline, clofibrate, Bamifylline

**diuretic; antihypertensive:** Trichlormethiazide\_S, Trichlormethiazide\_R, Furosemide, Chlorthalidone\_R, Chlorthalidone\_S, Buthiazide\_R, Buthiazide\_S, Xipamide, Bendroflumethiazide\_R, Bendroflumethiazide\_S, Benzthiazide

**glucocorticoid:** Prednisolone acetate, Cortisone, Prednisolone, Meprednisone, Methylprednisolone, Paramethasone, Prednisolone sodium succinate, Cortisone acetate, Methylprednisolone acetate, Paramethasone acetate

**narcotic analgesic:** Dezocine, Meperidine, Levorphanol, Alphaprodine, Tilidine, Oxycodone, Propiram\_R, Propiram\_S, Pentazocine, Butorphanol, Methadone\_S, Methadone\_R, Fentanyl, Anileridine, Propoxyphene, Sufentanil, Dextromoramide, Alfentanil

**sedative; hypnotic:** Paraldehyde, Triclofos, Barbital, Ethinamate, Carbromal, Methyprylon\_R, Methyprylon\_S, Dichloralphenazone, Aprobarbital, Butabarbital\_S, Butabarbital\_R, Butalbital, Vinbarbital\_Z, Vinbarbital\_E, Glutethimide\_R, Glutethimide\_S, Chloralose-alpha, Cyclobarbital, Thalidomide\_R, Thalidomide\_S,

Secobarbital\_RS, Secobarbital\_SS, Secobarbital\_RR, Secobarbital\_SR, Methaqualone, Estazolam, Temazepam\_R, Temazepam\_S, Brotizolam, Zaleplon, Doxefazepam\_R, Doxefazepam\_S, Propiomazine\_S, Propiomazine\_R

**skeletal muscle relaxant:** Mephenesin\_R, Mephenesin\_S, Tizanidine, Metaxalone\_R, Metaxalone\_S, Methocarbamol\_R, Methocarbamol\_S, Afloqualone, Dantrolene\_Z, Dantrolene\_E, Tolperisone\_R, Tolperisone\_S, Succinylcholine, Decamethonium bromide